Geostatistical Approaches to Characterizing the Hydrogeology of Glacial Drift

A DISSERTATION
SUBMITTED TO THE FACULTY OF THE GRADUATE SCHOOL
OF THE UNIVERSITY OF MINNESOTA
BY

John James Quinn

IN PARTIAL FULFILLMENT OF THE REQUIREMENTS
FOR THE DEGREE OF
DOCTOR OF PHILOSOPHY

Dr. Howard D. Mooers, Adviser

December 2009

Acknowledgements

My committee included my advisor, Howard Mooers, and Randal Barnes, John Swenson, Harvey Thorleifson, and Olaf Pfannkuch, who, along with Howard, co-advised my M.S. quite awhile ago. They are really a dream team for a dissertation like this, as each one brings a different, important perspective to the discussion. I thank them all for their well-put questions and sharing of ideas at different stages of this project. I thank Howard especially for his efforts over many, many years to get me to this point. He has been excellent in the combined role of professor, advisor, and funding finder in two phases of my life. At some point after the UMD project at Camp Ripley got underway, Howard brought up the idea of a possible dissertation. "You could be done in, what, a year? Maybe two?" he said at the time. I looked into it, and sure enough, I had taken so many classes for my M.S. that I was only two geology courses shy of PhD requirements. So, I signed on, not fully realizing what was in store. The path was not easy, but I thank Howard for once again contributing to my development.

Quite a few other people have factored into this project reaching its completion. Their assistance ranged from the practical to the financial, from the computational to the graphical… to just plain encouragement.

From Argonne, in no particular order, these include Dave LePoire, Swati Wagh, Bob Johnson, Lisa Durham, Tony Dvorak, Terri Patton, Dave Gartman, Jim Kuiper, Andy Huttenga, Brian Cantwell, Bobby Herrera, Tom Sydelko, and Kathy Eggers. Dave Miller (1957-2009) was keenly interested in the scope of this project. He was my

supervisor at its onset, and enjoyed “geologizing” (his word) with me about a research project that included his interests in glacial geology and groundwater. Dave had such a positive effect on me (and, from my perspective, on everyone else around him) with his gifted combination of enthusiasm, clear thinking, and humor.

I wish to thank former UMD students/staff Ben Bertsch, Matt Whitehill, Dave Stark, and Andrea Grygo for discussions and the sharing of data; Major Jon Kolstad and John Ebert of Camp Ripley for their support; Cary Talbot of the Waterways Experiment Station for responding to my countless GMS questions over the years; Bob Tipping of the MGS for his help in acquiring the CWI data and for sharing mutual grad student encouragement for the second time in our lives; Bob Ritzi of Wright State for guidance; Jim Landmeyer of the USGS for encouragement; and Tim Eaton of Queens College for a tip at a GSA meeting about something new - transition probability geostats.

My parents have always stressed education, so perhaps it’s not too big of a surprise that I eventually returned to graduate school. I’m grateful for them and their influence on me. My wife, Jill, and kids Erin, Rob, and Daniel have been supportive and very patient even during the periods of heavy involvement with this project. I thank Jill for her support over the course of this dissertation; it would not have happened without her.

Dedication

To my dad,

who happened to train at Camp Ripley with the Illinois National Guard

Dad wasn't a geologist, but he loved model train layouts with realistic-looking mountains and outcrops. He wasn't an academic, but his sustained, detailed research on the family tree was impressive. He would be glad about this milestone.

Abstract

Subsurface correlation of aquifer and aquitard materials can be challenging, especially in glaciated terrain, because of complexity in the thickness and lateral extent of the depositional units and a general scarcity of data. Geostatistical methods provide a means for exploring that correlation structure, allowing comparisons of results from different geomorphological settings and approaches to populating the hydraulic conductivity arrays of numerical groundwater flow models.

In this study, indicator geostatistics and transition probability geostatistics are applied to nearly 300 km of drilling data derived mainly from over 11,000 private well drilling logs. Analyses are focused on a nearly 12,000-km^2 region in central Minnesota comprised of four counties plus a portion of a fifth, in a setting dominated by the Rainy, Superior, and Wadena lobes of late-Wisconsinan glaciation. The area of interest surrounds Camp Ripley, a 210-km^2 Minnesota National Guard training facility. Data for Camp Ripley include 208 monitoring wells with detailed logging information obtained through split spoon sampling and nine even higher quality rotasonic boreholes. These data provide a basis for comparison of high-quality data to the abundant water well logs in the surrounding counties.

The drilling data are categorized according to the logged sediment descriptions. In one scheme, the materials are separated according to presumed high or low hydraulic conductivity (K) for use in binary indicator geostatistical and transition probability geostatistical analyses. In another, the number of categories is expanded to five on the

basis of combined K and depositional setting information for use in a separate transition probability geostatistical analysis.

The drilling data are separated into different geomorphological settings associated with various depositional environments of several ice advances. Vertical variograms are very well supported in all geomorphological areas, while lateral variograms vary from well supported to indecipherable scatter. The ratio of vertical to lateral range varies but has an average value of ten. Results for the numerous geomorphological settings indicate overlapping geostatistical parameters in terms of ranges, sills, and vertical lens thicknesses. A lack of stationarity was observed, consistent with a fundamental complexity of glacial depositional and erosional processes. Correlation generally varied as much between geographically distinct zones of like geomorphology as it did between zones of different geomorphology. High-resolution data associated with monitoring well installation typically deviated from the private well data; this is attributed to site-specific geology and detailed logging of thin units.

Indicator variography and kriging, as well as binary and 5-category transition probability geostatistical simulation, were applied to a drilling data set in the Camp Ripley vicinity to evaluate their relative capability for 3-D numerical modeling of regional groundwater flow in the glacial drift. For the kriging approach, the flow model relied on the kriging results by grading the K values between high and low values on the basis of the indicator output. Calibration was performed by systematic testing of various plausible end members of the K range. The transition probability runs were calibrated by

stochastic inverse modeling. A baseline single-K analysis was also calibrated through inverse modeling. Resulting K values from all four approaches were comparable, with the indicator kriging providing a slight edge in terms of the calculated errors at calibration targets. The modeling suggests that in complex glaciated terrain, in which lateral correlation of hydrostratigraphic units is small relative to grid spacing and drilling data spacing, a single-K model provides a suitable approach to determining regional groundwater flow, despite the large contrasts in K prevalent in glacial drift materials.

Table of Contents

List of Tables x

List of Figures xii

List of Abbreviations xvi

INTRODUCTION 1

Significance of Problem 1

Glacial Sedimentary Processes Related to Hydrogeology 2

Geostatistical Methods for Assessing the Subsurface Framework 5

Indicator Geostatistical Approach 6

Transition Probability Geostatistical Approach 14

Relation between Variogram and Transition Probability 19

Groundwater Flow Modeling in Glacial Drift 21

Purpose 24

Study Area 26

Location, Climate, Physiography 26

Glacial History and Geology 33

Subsurface Data Sources 43

GEOSTATISTICAL ANALYSES OF GLACIAL DRIFT 57

Methodology 57

Data Preparation 57

Indicator Variography 59

Transition Probability Geostatistics 60
Results 61
Basic Statistics 61
Indicator Variography 61
Transition Probability 69
Discussion 73
Conclusions 94
GEOSTATISTICAL APPROACHES TO GROUNDWATER MODELING IN GLACIAL DRIFT 99
Approach 99
Study Area 100
Location 100
Surface Water 100
Aquifer Recharge 102
Hydraulic Conductivity 106
Pumping Stresses 107
Groundwater Levels 108
Methodology 110
Numerical Flow Model 110
Conceptual Flow Model 110
Model Selection 111

Grid Design and Boundary Conditions 112

Input Parameters 119

Geostatistical Modeling of the Subsurface 120

Indicator Kriging Approach 121

Transition Probability Approach 122

Calibration and Parameter Estimation 124

Results 125

Discussion and Conclusions 145

REFERENCES 148

Appendix A: Locations of Geomorphologically Grouped Data Sets 164

List of Tables

Table 1. Borehole Data Density at Geostatistically Investigated Glaciated Sites in the Literature 11

Table 2. Counties in Study Area 29

Table 3. Data Set Groupings and their Basic Statistics 53

Table 4. Converting from Drillers' Descriptions to Material Types 60

Table 5. Binary TPROGS Results 70

Table 6. Five-Category TPROGS Results 70

Table 7. Summary of Geostatistical Findings 74

Table 8. Ratios of Lateral:Vertical Range for Cases of Fair to Good Quality Lateral Variograms 90

Table 9. Mapping Units of Mooers (1996) in the Camp Ripley Study Area 104

Table 10. Calibrated Recharge Values of St. George (1994) for Units Relevant to Camp Ripley and Estimated Recharge Values 104

Table 11. Geometric Mean Hydraulic Conductivities from UMD Grain Size Analyses 107

Table 12. Pumping in the Study Area 108

Table 13. Calibration Targets for Relevant Monitoring Wells 109

Table 14. TPROGS Categories Based on EnDriP Interpretations 123

Table 15. Summary of Hydraulic Conductivity Results and Associated Error Measurements 126

Table 16. Root Mean Squared Errors (m) from Indicator Kriging Output and Various K_{high} and K_{low} Values 132

Table 17. Binary T-PROGS Summary 136

Table 18. Estimated Hydraulic Conductivity Values from 17 Realizations of the Binary T-PROGS Model 138

Table 19. Five-Category T-PROGS Summary 142

Table 20. Estimated Hydraulic Conductivity Values from 14 Realizations of the 5-Category T-PROGS Model 145

List of Figures

Figure 1. Location of Study Area 27

Figure 2. The Multi-County Study Area and the Camp Ripley Location..... 28

Figure 3. View from St. Croix Moraine down to Tamarack Lake, Camp Ripley 30

Figure 4. Topographic Elevation in Multi-County Study Area 31

Figure 5. Lakes, Rivers, Wetlands, and Streams in the Multi-County Study Area 32

Figure 6. Late-Wisconsin Ice Lobes in Minnesota (modified from Knaeble 2006)..... 34

Figure 7. Key Glacial Features on Shaded Relief Map 35

Figure 8. Late-Wisconsin Ice Advances in Study Area (modified from Schneider 1961) 37

Figure 9. EnDriP (Rotosonic) Locations at Camp Ripley 40

Figure 10. Oblique View of EnDriP Borehole Stratigraphy and Approximate Color Contacts within the Drift (Y direction is due north; X direction is due east) 41

Figure 11. Rotosonic Drilling. A. Rig. B. Core Boxes. C. 4-inch Core 47

Figure 12. Distribution of Drilling Data in Multi-County Study Area 49

Figure 13. Distribution of Monitoring Wells and Rotosonic Boreholes at Camp Ripley 50

Figure 14. Ice-Lobe Origins of Surficial Deposits..... 51

Figure 15. Surficial Sediment Types 52

Figure 16. Well Markers According to Geomorphological Terrain 55

Figure 17. Oblique View of Binary Data in Multi-County Study Area, from Southeast (V.E. = 100x) 63

Figure 18. Vertical Variogram for All Data and for All Monitoring Well and Rotosonic Data 64

Figure 19. Lateral Vvariogram for All Data and for All Monitoring Well and Rotosonic Data 66

Figure 20. Vertical Correlations Lengths for All Data Sets and for All Methods 68

Figure 21. Binary T-PROGS Analysis for the Complete Multi-County Data Set 69

Figure 22. Oblique View of 5-Category Data in Multi-County Study Area, from Southeast (V.E. = 100x) 71

Figure 23. Five-Category T-PROGS Aanalysis for the Complete Multi-County Data Set. 72

Figure 24. Vertical Variogram Results for Rainy Lacustrine Geomorphological Zone, based on Private Well Log Data and Monitoring Well Data 78

Figure 25. Vertical Variogram Results for Wadena Till Plain Geomorphological Zone, based on Private Well Log Data 79

Figure 26. Vertical Variogram Results for Rainy Supraglacial Geomorphological Zone, based on Private Well Log Data, Monitoring Well Data, and Rotosonic Data 80

Figure 27. Vertical Variogram Comparison among Data from Monitoring Wells (3 = Des Moines Outwash, 13 = Rainy Lacustrine, 14 = Rainy Outwash, 15 = Rainy Supraglacial, 21 = Superior Lacustrine) 81

Figure 28. Vertical Variogram Results for Rainy, Superior, and Wadena Till Plain Geomorphological Zone, based on Private Well Log Data 82

Figure 29. Lateral Variogram Results for Rainy, Superior, and Wadena Till Plain Geomorphological Zone, based on Private Well Log Data 83

Figure 30. Vertical Variogram Comparison among Data from Supraglacial Geomorphological Zones (15 = Rainy, 23 = Superior, 27 = Wadena) based on Private Well Log Data Only 84

Figure 31. Vertical Range vs. Mean Thickness for All Data Sets 88

Figure 32. Oblique View of Binary Data in Camp Ripley Landfarm Vicinity (V.E.=10x. Lateral tick spacing 100 m; Vertical tick spacing 10 m) 93

Figure 33. Hydrologic Features in the Flow Modeling Domain 101

Figure 34. Water Levels at Six Lakes near Camp Ripley (data from MDNR 2006) 102

Figure 35. Geomorphological Zones used as Recharge Zones 105

Figure 36. External and Internal Boundary Conditions 114

Figure 37. Model Grid and Borehole Locations 115

Figure 38. View of Model Grid and Drilling Data from the East 116

Figure 39. Oblique View of Model Grid and Drilling Data from the Southwest 116

Figure 40. Bedrock Surface Elevation in Model Domain 117

Figure 41. Topographic Surface Modeled with 60-m DEM Data 118

Figure 42. Heads Resulting from Single-K Approach 128

Figure 43. Vertical Indicator Variogram for Camp Ripley Vicinity 129

Figure 44. Lateral Indicator Variogram for Camp Ripley Vicinity 130

Figure 45. Example of Indicator Kriging Results for Model Layer 5 131

Figure 46. Hydraulic Conductivity Values Assigned to Layer 5 133

Figure 47. Heads Resulting from Optimal Klow and Khigh Values 134

Figure 48. Binary T-PROGS Results 136

Figure 49. Example of Binary T-PROGS Results for Layer 1 137

Figure 50. Heads Resulting from Binary T-PROGS Approach 139

Figure 51. Five-Category T-PROGS Results 141

Figure 52. Example of 5-Category T-PROGS Simulation 143

Figure 53. Heads Resulting from 5-Category T-PROGS Approach 144

List of Abbreviations

c_v	coefficient of variation
CWI	County Well Index (state database of well log information)
d	day
DEM	Digital Elevation Model
EnDriP	Environmental Drilling Program (see UMD Department of Geological Sciences 2002)
GMS	Groundwater Modeling System
K	hydraulic conductivity
m	meter
m/d	meter/day
MDH	Minnesota Department of Health
MGS	Minnesota Geological Survey
ME	mean error
MAE	mean absolute error
MSL	Mean Sea Level
MW	monitoring well
MDNR	Minnesota Department of Natural Resources
PES	a parameter estimation tool contained in MODFLOW 2000 (Hill et al. 2000)
RMSE	root mean squared error

T-PROGS	transition probability geostatistics
UMD	University of Minnesota – Duluth
V.E.	vertical exaggeration

INTRODUCTION

Significance of Problem

Glaciated terrain covers much of North America and other parts of the world. The depositional and erosional processes associated with glaciation produce a wide variety of sediment types and landforms. These materials have irregular geometry and represent a tremendous range of hydraulic conductivity values. The resulting complexity in the hydrogeologic framework complicates assessment for water resources or contaminant transport.

Geostatistical techniques incorporate spatial correlation to estimate the three-dimensional distribution of a material or a property of interest. Drilling data from water well installation, monitoring well installation, or exploratory boreholes provide dense material type data for vertical correlation studies, and, if of sufficient areal density, may support lateral correlation assessment also. The three-dimensional hydrogeologic framework of glacial drift has not been studied significantly. Questions addressed by this study include

- Does glacial drift have a correlation structure?
- Does the glacial hydrogeologic framework differ geostatistically in different geomorphological terrain?
- Does the data quality affect the calculated geostatistical parameters?
- How do different geostatistical methods compare?

- How well do geostatistical methods produce an accurate and therefore useful numerical groundwater flow model?

As described below, this study is focused on a multi-county area in central Minnesota. Nearly 300 km of drilling logs (mostly private well logs) were evaluated using binary indicator geostatistical and transition probability geostatistical approaches to evaluate the correlation structure of various geomorphological regions. The results from these glacial terrains may be useful in predicting the geostatistical structure elsewhere and have application in water resources or contaminant transport studies.

Glacial Sedimentary Processes Related to Hydrogeology

Glacial depositional and erosional processes typically result in a complex framework of materials with dramatically different hydraulic conductivities. The complexities arise because of the varied depositional environments associated with glaciation. Subglacial, supraglacial, englacial, ice-contact, morainal, glaciolacustrine, and glaciofluvial settings each have a variety of different associated facies, and these facies vary in their geotechnical properties. The deposits are further complicated by ice readvances and by soil formation processes between advances. Possible fracturing of fine-grained materials adds another level of complexity to hydrogeologic assessment in glacial terrain.

Stanford and Ashley (1998) summarize aspects of glacial sedimentology as follows:

- they deposit over irregular topography, rather than only in sedimentary basins controlled by base level
- they entrain, transport, and deposit all grain sizes
- they generate large volumes of meltwater with spatially and temporally varying discharge
- they continually encounter and create new topography
- ice can form depositional basins, creating inverted topography after melting.

For these reasons, glacial sediments create a hydrogeologic framework characterized by properties varying widely across short separation distances, complex geometry and bounding surfaces, and an irregular bedrock contact surface.

A facies model serves as a framework for interpreting and predicting the geology of a given sedimentary environment (Walker 1984). Glacial geologic facies models are useful in determining large-scale trends and distributions of different glaciogenic units (Eyles and Miall 1984). A glacial facies model is a generalized assemblage of sediments that are representative of a certain glaciological depositional environment. By understanding the surficial and buried sedimentological units in terms of their glacial genesis, one develops the ability to predict the distribution of aquifers and aquitards. These sorts of studies are usually concerned with large-scale facies because of the difficulties in evaluating small-scale heterogeneities (Anderson 1989, Fraser and Bleuer 1987).

Glacial terrain models are comprised of map units defined by sequences of sediments and regionally extensive landforms (Fleming 1998a, 1998b). They are

analogous to the glacial landsystems of Eyles (1983) and can be referred to as landform sediment assemblages. They are constructed by relying on field mapping, subsurface drilling, geophysics, and hydrological data and are used to establish a sedimentological framework for hydrogeological studies at local or regional scale.

The value in understanding glacial sedimentary processes for use in creating or improving hydrogeological conceptual models of glaciated study areas has been recognized for some time (e.g. Anderson 1989) and has lead to collaboration among sedimentologists and hydrogeologists (e.g. Dominic et al. 1998, Ritzi et al. 2000). The growing importance has lead to several collections of papers (Fraser and Davis 1998) and a continuing series entitled "Three-Dimensional Geological Mapping for Groundwater Applications Workshops", sponsored jointly by the Illinois State Geological Survey, the Geological Survey of Canada, and the Minnesota Geological Survey. Portions of the papers and presentations deal with various types of glacial settings.

Dominic et al. (1998) propose building quantitative facies models from data-rich sites. These models would include proportions, correlation, and ideas about origins and geometry of the various facies and would provide a means for interpreting other sites with more limited data.

Stanford and Ashley (1998) stress a simple, straightforward approach to handling hydrogeological modeling in glacial terrain. They note that the permeability within glacial aquifer or aquitard units varies less than the permeability between various units; conceptual information can therefore be input to a flow model without information on small-scale details in the permeability structure. This approach is of course scale

dependent; the authors suggest following it at a scale of approximately 1:24,000, but using these results only as a starting point for site-specific studies.

Koltermann and Gorelick (1996) wrote a treatise on heterogeneity in sedimentary deposits. With a focus on creating images of heterogeneity, they note three categories of methods for using geologic, hydrogeologic, and geophysical data. The structure-imitating category includes methods of statistical pattern imitation, focused on spatial correlation, or sedimentation pattern imitation, using rules from conceptual depositional models to predict evolution, grain sizes, and sedimentary structures. The process-imitating category includes geologic process modeling, relying on sediment transport simulation or aquifer model calibration. The descriptive category has methods focused on moving from geologic observations to facies relationships to divide an aquifer/aquitard system into appropriate units. Although this paper largely ignores glacial settings, the three categories of approaches may be applied in glacial terrain. The authors note that combinations of the methods are absent from the literature.

Geostatistical Methods for Assessing the Subsurface Framework

Two geostatistical approaches are evaluated in this study: indicator variography and transition probability. They were selected because they provide a means for quantifying the correlation structure of three-dimensional data. Other methods, such as plurigaussian simulation and multiple-point geostatistics, are also available (Yarus and

Chambers 2006). However, these methods require input in the form of lithologic rules and training images, either of which may be subjective and difficult to develop. This study therefore focuses on geostatistical methods that rely strictly on the available data.

Indicator Geostatistical Approach

The experimental variogram is the average squared difference of pairs of data points as a function of lag spacing. It represents a measure of the spatial structure of a data set and is calculated as

$$\gamma(\mathbf{h}) = \frac{1}{2N_h}\sum_{i=1}^{N_h}[Z(x_i+h)-Z(x_i)]^2 \qquad \textbf{Equation 1}$$

where $\gamma(h)$ = variogram value for separation distance (or lag) h,

h = separation distance between points (lag)

N_h = number of pairs of separation distance h,

$Z(x_i)$ = value of sample at location x, and

$Z(x_i+h)$ = value of sample at location x+h.

Modeling the variogram involves choosing a variogram type and determining the parameters the produce the best fit of the experimental variogram. These parameters generally include the nugget effect, the range, and the sill. The nugget represents the variogram value when h is zero; the range represents the lag up to which data are

correlated, and the sill represents the variance of the data past the range. Details are provided by Isaaks and Srivastava (1989).

Data may exhibit anisotropy in the range as a function of search direction. In a three-dimensional data set, the vertical range is generally much smaller than the lateral range, and directional variograms in lateral search directions may show differing ranges.

Variogram parameters are used as input to the kriging algorithm to calculate minimum-variance, linear, unbiased, estimates throughout a grid. The value of a grid cell is

$$\mathbf{Z^*(v)} = \sum_{i=1}^{n} \lambda_i Z(x_i) \qquad \textbf{Equation 2}$$

where $Z^*(v)$ = estimated value of cell v,

n = number of nearby samples (subject to user-specified search criteria)

$Z(x_i)$ = value of sample at χ_i, and

λ_i = kriging weight of sample *i*.

The literature has many examples of parametric kriging in hydrogeological studies, and at many scales of study. Many of these are focused on two-dimensional analyses of thickness, contact elevations, or permeability, while some are three-dimensional analyses of permeability or other parameters. Sudicky (1986) analyzed sub-meter scale hydraulic conductivity measurements in a sandy aquifer and found an exponential structure to the data. Davis et al. (1993) performed variogram analysis of air

permeameter measurements at approximately meter scale in architectural elements in alluvium, and found a correlation structure within each facies. A three-dimensional kriging study on glaciated Indiana terrain involved grouping materials into six categories, converting their hydraulic conductivity values into –log K values ranging from 1 to 6, and kriging using these values (Lampe and Olyphant 2003).

Indicator geostatistics is a non-parametric method in which the data are partitioned into categories and assigned indicator values on the basis of a cutoff value in the case of quantitative data, or assigned based on qualitative material type. Variography and kriging are performed using the indicator values. Binary indicator values of 0 and 1 are used as surrogates for the actual quantitative or qualitative data. Indicator variograms represent the spatial structure of the data, as converted into indicators, and indicator kriging provides results, ranging from 0 to 1, representing the spatially distributed probability of each category.

Journel (1983) initiated the use of indicators, and Journel and Alabert (1989) provided an early example of application to groundwater studies. Indicators are an attractive alternative in many cases because they allow an emphasis on facies occurrences rather than distribution of permeability values. Qualitative facies data that may be assigned to indicator categories are more abundant (and cheaper to acquire) than quantitative permeability measurements, and indicators provide a more robust variogram than parametric values.

Johnson and Dreiss (1989) and Johnson (1995) used three-dimensional indicators of an alluvial fan stratigraphic data set to represent low- or high-permeability materials.

They observed sensitivity in the variogram structure to search orientation and differences in variogram structure relative to the location of the data on the proximal/medial/distal portions of the fan. Tarboton et al. (1995) performed three-dimensional indicator kriging on San Joaquin Valley, California, sediments discretized into 3-m segments. Using the results, they assigned the highest measured K to the indicator results equal to approximately 1, assigned the lowest measured K to the indicator results at or near 0, and spread hydraulic conductivity values evenly in between, based on the calculated indicator.

Ritzi et al. (1994) performed 2-D indicator geostatistics of a valley-fill aquifer system comprised of sands and gravels with interbedded tills and clays. The analysis was aimed at matching facies boundaries of the dominant low-permeability interbed through indicator kriging and through stochastic conditional indicator simulation. They determined that rather than using a 0.5 cutoff to separate the low (1) and high (0) permeability zones, a 0.65 value provided a more accurate match. The analysis was expanded to three dimensions, including additional nearby study areas, by Ritzi et al. (1995), who determined geostatistical trends in aquitard units that match proportions and orientations expected in this depositional system. In one of the study areas with relatively high data density, Sminchak et al. (1996) performed indicator analyses for a series of subsurface layers to determine the interconnectedness of sands through a vertical thickness.

Ritzi et al. (2000) made detailed statistical comparisons of two data-rich Midwestern buried valley systems, and determined that they were similar in their overall

structure. A conclusion from this work is that relative consistency from similar depositional environments may allow statistical inferences to be made at other, data-poor sites. Indicator geostatistical studies have been used to explore and compare other Midwestern and Eastern valley fill settings (Damico et al. 2001, 2002; Patterson et al. 2001; Dominic et al. 2003).

Although these techniques have been applied to fluvial, alluvial fan, and buried valley systems, they have not been applied rigorously to morainal and ground morainal settings that dominate much of North America. Examples of indicator geostatistics applied to other glacial settings include 3D indicator variography analyses in a sandplain and ground moraine setting near Anoka, Minnesota (Quinn 1992, Quinn et al. 1992), and stacked 2D analyses in Stearns County, Minnesota (Meyer et al. 1995) and at the Buffalo aquifer, Minnesota (Harris et al. 1998). The Anoka investigation relied on water well records, while the other studies relied mainly on modified water well data, with the dominant sediment type assigned to 3-m borehole intervals.

Table 1 is a compilation of all known geostatistical studies in glaciated terrain. Representing a variety of scales, data density, glaciogenic terrains, and approaches, they suggest a wide variety of correlation distances in the vertical or lateral directions.

Table 1. Borehole Data Density at Geostatistically Investigated Glaciated Sites in the Literature

Location	Site	Source	Glacial setting	Approx. Areal Extent (km^2)	Number of bore-holes	Data density (bore-holes per km^2)	Data type	Method	Correlation information
Illinois	Sankoty-Mahomet Aquifer	Herzog et al. 2003	Till plain	2,784	2,306	0.8	Mostly water well records, some exploratory boreholes	3D imaging based on a series of variable-thickness layers	NA
Indiana	White River Valley	Ritzi et al. 2000	Glacio-fluvial valley fill	180	568	3.2	Water well records	Transition probability, statistical analyses, indicator variography	Vertical range of 3.5 m for muddy facies, c. 10 m for sandy facies. Vertical mean thickness from transition probability on the order of 10 m. Lateral effective range on the order of 1,000 m. Varying lateral mean length from transition probability on the order of 100 m.
Minnesota	Anoka County (portion)	Quinn 1992	Sand-plain atop mainly ground moraine	59	152	2.6	Water well records	Indicator variograms	Vertical range of 23 m, first lateral range of 370 m.

Location	Site	Source	Glacial setting	Approx. Areal Extent (km^2)	Number of bore-holes	Data density (bore-holes per km^2)	Data type	Method	Correlation information
Minnesota	the Buffalo aquifer	Harris et al. 1998	tunnel valley and fan	623	580	0.9	Water well records (dominant material in 3-m intervals); electrical resistivity data	Stacked 2D analyses of indicator kriging; cutoff of 40 ohm-meters used as sand indicator.	Variograms for resistivity data forced to be strongly anisotropic in north-south versus east-west direction to accommodate large spacing between resistivity lines.
Minnesota	Stearns County	Meyer et al. 1995	Outwash plain; buried outwash plain	387	302	0.8	Water well records (dominant material in 3-m intervals)	stacked 2D analyses of indicator kriging	Lateral range of 1 to 5 km for various 2D analyses; Lateral range of buried outwash plain of roughly 8 km.
North Dakota	Spiritwood Aquifer	Proce et al. 2004	Buried bedrock valley	6,400	c. 700	0.1	Water well records	Binary transition probability and variography	4 to 17 m thickness by transition probability, 12 to 18 m vertical range by variogram; 500 to 700 m lateral range by variogram.
Ohio	Miami Valley	Sminchak et. al 1996	Glacio-fluvial valley fill	18.6	800	43	Investigative boreholes and monitoring wells	3D kriging of binary (low- and high-K) material	Lateral range of 150 to 275 m, vertical range of 3.7 m

Location	Site	Source	Glacial setting	Approx. Areal Extent (km^2)	Number of bore-holes	Data density (bore-holes per km^2)	Data type	Method	Correlation information
Ohio	Northeast Ohio	Venteris 2007	End moraine, buried bedrock valley	130	c. 240	1.8	Water well records	Calculated proportions and mean thicknesses (variograms were poor)	Vertical range estimated from 1 to 5 m for till, 3 to 8 m for sand.
Ontario	Oak Ridges Moraine	Desbarats et al. 2001	Varied morainal deposits	4,000	10,370	2.6	Mainly water well records	Indicator kriging of a series of threshold thicknesses of a till unit	Nested variogram structures (isotropic 200 m, anisotropic 12 km, anisotropic 24 km
Ontario	Oro Moraine	Beckers and Frind 2001	Varied morainal deposits	696	619	0.9	Varied, mainly water well records	Kriging of contact elevations, kriging of ln K	Not available
Ontario	Waterloo Moraine	Martin and Frind 1998	Varied morainal deposits	750	2,044	2.7	Varied	Kriging of contact elevations, kriging of ln K	Not available
Quebec	St. Lawrence Lowlands	Ross et al. 2005	Clay plain and till plain	1,500	2,070	1.5	Surficial mapping, drilling, geophysics	Interpretation, data reliability weighting, and creation of numerous cross sections	Not available

Transition Probability Geostatistical Approach

More recent investigations of the three-dimensional hydrogeologic structure of various settings have begun shifting toward the use of transition probability geostatistics (T-PROGS). This approach combines geostatistics with Markov chain analysis on categorical variables. T-PROGS originated with a University of California-Davis group, and is documented by Carle (1999) and Carle and Fogg (1996, 1997).

The T-PROGS process includes calculation of transition probabilities, one- and three-dimensional Markov chain modeling of spatial structure, and conditional simulation to generate multiple realizations.

Transition probabilities address basic characteristics of a site's materials, based on

- volumetric proportions
- mean thicknesses and mean lens lengths
- juxtapositional tendencies among the units, and
- directional anisotropy.

A Markov chain is a sequence in which the state at one point is partially dependent on the preceding state (Davis 2002). Vertical stratigraphic sequences may be analyzed as Markov chains, and the relationships of the material types are cast in terms of transition probability matrices. A set of four material types would result in 16 graphs of transition probability vs. lag. Along the diagonal would be the four cases of auto-transition probabilities (i.e. from material j to material j); off-diagonal plots would relate

each type to the other types. The model curves' initial slopes, sills, and extrapolated x-intercepts relate to the transition rate, proportion, and mean lens thickness, respectively.

The following brief summary of mathematical basis of transition probability geostatistics is modified from Carle (1999) and other papers from the UC-Davis group.

Instead of the variogram as a measure of spatial structure of data, this technique relies on transition probability, t,

$$t_{jk}(h) = \Pr\{k \text{ occurs at } x + h \mid j \text{ occurs at } x\}$$

Equation 3

where j and k are material types, x is a location, and h is a lag distance. Material types in vertical boreholes can be analyzed to determine their transition probabilities as a function of h. The Markov chain model is calculated as

$$T(h_u) = \exp[R_u h_u]$$

Equation 4

where $T(h_u)$ is a matrix of transition probabilities, u is direction, and R_u is a matrix of transition rates

$$R_u = \begin{bmatrix} r_{11,u} & \cdots & r_{1,K,u} \\ \vdots & \ddots & \vdots \\ r_{K,1,u} & \cdots & r_{KK,u} \end{bmatrix}$$

Equation 5

with entries $r_{jk,u}$ representing the rate of change from category j to category k per unit length in direction u.

In addition to determining proportions and juxtapositional structure of the data, the T-PROGS analysis also provides a measure of the mean lens thickness:

$$r_{kk,u} = \frac{1}{\overline{L}_{k,u}} \qquad \textbf{Equation 6}$$

where $r_{kk,u}$ is the auto-transitional probability for material k, and $\overline{L}_{k,u}$ is the mean thickness or length.

After establishing the T-PROGS parameters, conditional simulation is performed, generating multiple equally probable simulations of the categorical variables (i.e. hydrogeologic units). Rather than a single stratigraphic model, the stochastic model runs create as many plausible models as the user specifies. The results of multiple model runs may be combined to determine the spatial distribution of the best estimate of each material type.

The TPROGS analysis determines the interrelationships of the modeled units through Markov chains, which are best in vertical directions because of abundant data relationships. They are inferred for horizontal directions, where data relationships are sparser, according to Walther's Law: any juxtapositional tendencies observed in the vertical direction will also hold true in the horizontal directions.

An option for evaluating the transition rate matrix is through embedded transition probability (Weissmann and Fogg 1999). In this case, the embedded Markov chain analysis considers the conditional probability of discrete occurrences of adjacent materials. The embedded transition probability $\pi_{jk,z}$ represents the following situation in the vertical (z) direction

$$\pi_{jk,z} = \Pr\{\text{k occurs above} \mid \text{j occurs below}\}$$

Equation 7

The embedded transition probability matrix then is

$$\Pi_u = \begin{bmatrix} \pi_{11,u} & \cdots & \pi_{1,K,u} \\ \vdots & \ddots & \vdots \\ \pi_{K,1,u} & \cdots & \pi_{KK,u} \end{bmatrix}$$

Equation 8

Because the embedded probabilities represent transitions between different material types, the diagonal terms of Π_u do not exist. However, with the knowledge of mean thickness or length $\overline{L}_{k,u}$, which is directly measurable at least for vertical borehole data, the entries of the matrix can be converted into entries in a transition rate matrix by

$$r_{jk,z} = \frac{\pi_{jk,z}}{\overline{L}_{j,z}}$$

Equation 9

and the transition rate matrix may then be determined.

T-PROGS originated in studies of California alluvial fan deposits (Carle et al. 1998, Weissmann et al. 1999) and alluvium (Fogg et al. 1998), where fining upward sequences are a critical component of the facies (and one not captured in a directionally insensitive indicator geostatistical approach). These fan deposits also provide researchers with distinct paleosols to divide the subsurface into sequences of similar properties, each of which is analyzed separately (Weissmann and Fogg 1999). This sequence-stratigraphic approach avoids non-stationarity issues among the various sequences, and allows a combination of modeled sequences into a single realization. The alluvial fan setting is also conducive to making use of published soil surveys to constrain the correlation of units in lateral Markov chains (Weissmann et al. 1999).

T-PROGS analysis of facies is superior to interpolation of parameter values such as hydraulic conductivity, because development of a proper facies model does not lead to unrealistic smoothing of the parameter field (Fogg et al. 1998).

T-PROGS has also been used to assess other alluvial fan settings (Burow et al. 2008), fractured media (Park et al. 2003), fluvial deposits (Maji et al. 2003), a localized glaciofluvial setting (Gödeke et al. 2008), alluvium (Sun et al. 2008), and glaciofluvial valley fill aquifer systems (Dominic et al. 1998, 2003; Proce et al. 2004).

Applications to studies of other types of glaciated terrain are scarce. Venteris (2007) analyzed an Ohio study area with binary indicators, with fine-grained facies dominating over sand. He found vertical variograms to be poor, and consequently determined the proportions, mean thicknesses, and coefficients of variation, then applied

an equation from Ritzi (2000) (discussed below) to calculate the ranges. Lateral correlation was not explored in detail.

Relation between Variogram and Transition Probability

Carle and Fogg (1996) provide a derivation for the relationship of the indicator cross-variogram to the transition probability

$$\gamma_{jk}(h) = p_j\{t_{jk}(0) - [t_{jk}(h) + t_{jk}(-h)]/2\}$$

Equation 10

and the relationship between the indicator cross-covariance C_{jk} and the transition probability

$$C_{jk}(h) = p_j[t_{jk}(h) - p_k]$$

Equation 11

They also showed that $\overline{L}$ is related to the slope of the tangent to $t_{kk}(h_u)$ and $\gamma(h_u)$ at zero lag, assuming stationary proportions, by

$$\overline{L} = -[\partial t_{kk}/\partial h|_{h=0}]^{-1} = p_k[\partial\gamma/\partial h|_{h=0}]^{-1}$$

Equation 12

For vertical (downhole) data, the mean length $\overline{L}$ of a material type can be directly calculated from the drilling logs.

In a study focused on binary indicators, Ritzi (2000) explored the relationships among autotransitional probability, indicator autovariance, and facies geometry. While $\overline{L}$ dictates the slope of $\partial t_{kk}/\partial h$ at h=0, the structural form and range are related to the variability in facies thickness or length, measured as the coefficient of variation (c_v, equal to the standard deviation of material thickness divided by mean thickness). As the c_v of the facies length or thickness approaches unity, the structure of the transition probability or variogram plot tends toward exponential, and periodicity in correlation structure disappears. Similarly, Ritzi and Allen-King (2007) evaluated the geostatistical aspects hydraulic conductivity (K) data from sandy sediments of two hierarchical groups, and determined that variogram parameters could be determined by knowing univariate statistics for the proportions, lengths, and K populations of units.

Ritzi (2000) also provided the general relationship between the structural range $a_{k,u}$ and the mean length $\overline{L}$

$$a_{k,u} = \phi (1-p_k)\ \overline{L}_{k,u}$$

Equation 13

with ϕ equal to 1.5 for spherical models and 3 for exponential models. Ritzi and Allen-King (2007) note that this equation is only valid if the two unit types occur in equal proportions.

Typically, $a_{k,u}$ and $\overline{L}_{k,u}$ will not be equal, as this is true only in the case of $\phi = (1-p_k)^{-1}$. The two parameters therefore are only equal if p_k is equal to 0.33 in the spherical case or 0.83 in the exponential case.

Groundwater Flow Modeling in Glacial Drift

Ultimately, the modeling of the subsurface sediment can serve as input to a groundwater flow model by dictating the distribution of K values. This section describes various approaches to creating the permeability structure of flow models in glaciated terrain.

Regional multiple aquifer studies focused on bedrock aquifers often categorize the drift as a single material. Schoenberg (1990) and Lindgren (1990) are examples of studies in the Twin Cities region in Minnesota. In these studies, coarse-resolution finite-difference models were built that consider the areally varying thickness of the drift, but assign to it a single hydraulic conductivity value. A more recent study of the Twin Cities region relies on data from thousands of wells to construct an analytic element model (Seaberg 2000). In this undertaking, the sand content of numerous glacial drift intervals were geostatistically interpolated to 20-m thick model layers, and the drift thickness was geostatistically interpolated into a coarse grid of approximately 1-mi^2 cells. While an advantage of this modeling technique is that site-scale data may be added to the model, clearly the difficulty of incorporating the details of the glacial drift promotes only a simple conceptualization of the bulk drift.

Similar work has been performed at a similar scale elsewhere in the Midwest by the Central Great Lakes Geologic Mapping Coalition (U.S.G.S. 1999). In this case, quadrangle-scale (approximately 130 km^2 or 50 $mi.^2$) three-dimensional maps are created of bedrock and drift (Abert et al. 2000) or of thick drift sequences (Soller et al. 1999). Interpolation from well log information is performed using EarthVision and the spline technique to model the geometry of large-scale lithologic units.

In the case of any regional bedrock model, it is possible that coarse-resolution input on the highly variable glacial drift may not create large mass balance errors in the simulated bedrock flow, but the purpose and accuracy must be considered in model design and construction.

Two-dimensional kriging analyses of contact surfaces or unit thicknesses may provide geological conceptualization of a glaciated study area (e.g. Meriano and Eyles 2003, Boyce and Eyles 2000). Meriano and Eyles used their results in a regional flow model.

Martin and Frind (1998) and Beckers and Frind (2001) developed a means of geostatistical modeling of complex morainal aquifer systems for use in detailed finite-element flow models. In their approach, numerous cross sections were constructed criss-crossing their study areas, and contact elevations between main aquifers and aquitards were determined. These contacts were kriged. Initial hydraulic conductivities were assigned to each vertical interval between contacts; these conductivities were kriged and modified during model calibration. While this approach may be reasonable for a regional scale analysis, a downfall is the numerous cross sections that require difficult, subjective

interpolation. In both studies, the distance between boreholes is roughly 1 km, which allows a great deal of uncertainty when correlating contacts, and no analysis was performed on the correlation of the data. Similarly, Ross et al. (2005) created a 3D geologic model by inspecting drilling data, assigning a reliability score to each well, and compiling many series of interpreted cross sections.

In general, three-dimensional analysis is favored over combining two-dimensional results, because interconnections are not properly accounted for in a two-dimensional model (Fogg 1986). Another potential problem with two-dimensional analysis is when a unit's kriging standard deviation is similar to the average unit thickness (e.g. Desbarats et al. 2001).

Sharpe et al. (1996, 2002) describe a geological approach to building a three-dimensional hydrostratigraphic model in glacial drift in Ontario, relying on borehole data, mapping, outcrop data, and shallow seismic surveys. Herzog et. al. (2003) use a similar approach to building a detailed three-dimensional hydrostratigraphic model of a glaciated portion of Illinois. The analysis made use of an extensive drilling database, a GIS, and three-dimensional geologic software. No rigorous analysis was made of correlation between units. The model was refined by multiple checks on the geometry of and relationships among the various modeled units by a team of experts, and ultimately was used to simulate groundwater flow in the study area (Wilson et al. 1998). However, Herzog et al. acknowledge that difficulties in the process included units that pinch out (a common factor in glacial settings) and data too sparse to map some of the sand units.

Purpose

Groundwater modeling studies rely on accurate input parameters, appropriate boundary conditions, and suitable calibration data. The inputs are generally spatially varying and in some cases temporally varying. Data on the spatial distribution of hydraulic conductivity (K) is a key component to any model. While fractured, karstified, and porous media are all complicated in various ways, among porous media scenarios, the glaciated setting is generally the most complex, having a variety of materials with a wide range of K values, irregular geometry, and generally short lateral extent and vertical thickness. Because the understanding of the structure of high- to low-permeability materials is limited by available data, and because of the large scale of many studies in glacial drift, the details of the complexities of glacial drift are typically ignored. However, these details may be critical in terms of defining the high-permeability zones for water resources assessments and contaminant transport investigations.

Various traditional approaches have been used to address the hydrogeologic framework of glacial drift settings for use in conceptual or numerical models. These include lumping the entire drift thickness into a single glacial drift "aquifer" for use in regional bedrock models, to outcrop studies, to constructing site-specific cross sections using borehole data, although the spacing between boreholes may lead to high uncertainty in the stratigraphic contacts in between.

A variety of methods for geologic analysis, including GIS systems of data and maps, geophysical surveys, and visualization, are being pursued to improve the modeling of hydrogeology in various geologic settings and scales of study (e.g. Fraser and Davis

1998, Berg and Thorleifson 2001, Thorleifson and Berg 2002a, Berg et al. 2004, Russell et al. 2006, Thorleifson et al. 2007). Few of these studies, however, rely on a careful, quantitative assessment of correlation when establishing the subsurface framework, and glaciated settings have not received much attention.

This dissertation aims to investigate the correlation structure of a glaciated setting in Minnesota, while addressing two hypotheses.

Hypothesis 1. Specific glacial drift settings each possess a characteristic correlation structure in terms of their aquifer/aquitard distribution

This hypothesis involves assessment of a complex glaciated setting, comprised of over four counties in central Minnesota, using two geostatistical methods that quantify the correlation of subsurface materials. Nearly 300 km of drilling logs are used as a basis for comparisons between different geomorphologic terrain and among geographically separate subunits of like geomorphologic origin (ice lobe and deposit type). Also, comparisons are made of results among three types of different data quality. Both vertical and lateral correlations are examined. If one or both of the tested geostatistical approaches shows a correlation structure, and their structure is unique in tested geomorphological zones, then this hypothesis will be supported.

Hypothesis 2. Geostatistical correlation of drift units provides an acceptable approach for populating K arrays in numerical groundwater flow models

This hypothesis builds on the results of the first step. It will be tested by comparison of numerical flow models developed using the geostatistical approaches for the suitability of each for three-dimensional flow modeling, and contrasted to other model approaches. The focus is a 460 km^2 modeling area located in the center of the multi-county study area.

Study Area

Location, Climate, Physiography

This study considers several scales focused on a portion of central Minnesota (Figure 1). The regional glacial geology is assessed and related to the geostatistical analysis study area comprised of four counties (Crow Wing, Morrison, Todd, and Wadena) and the southern portion of a fifth (Cass) (Table 2). Together, these counties roughly form a square with an area of nearly 12,000 km² (Figure 2), and is referred to in here as the "multi-county study area". The Camp Ripley training facility of the Minnesota National Guard is located in the center of the square, in northern Morrison County.

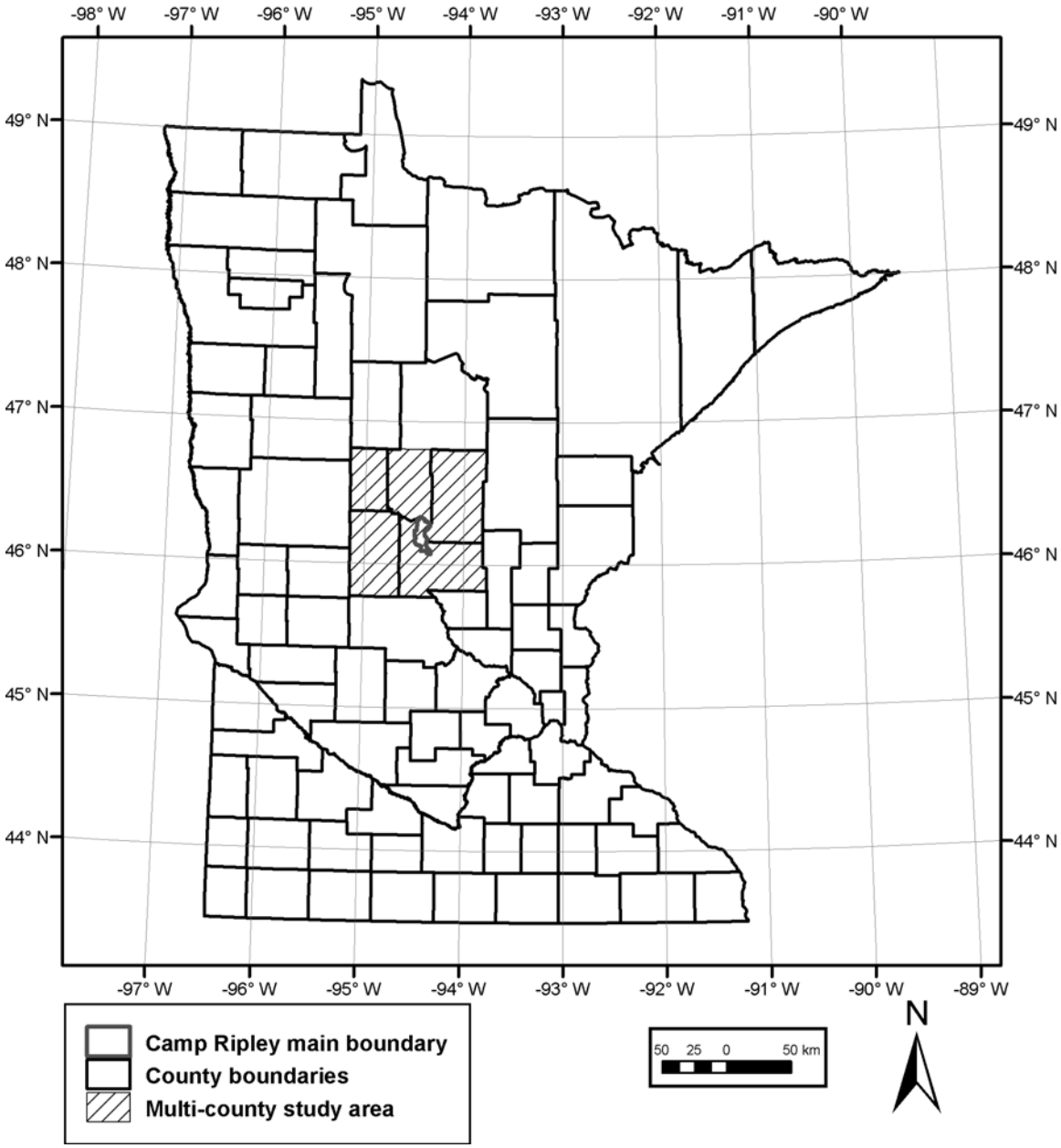

Figure 1. Location of Study Area

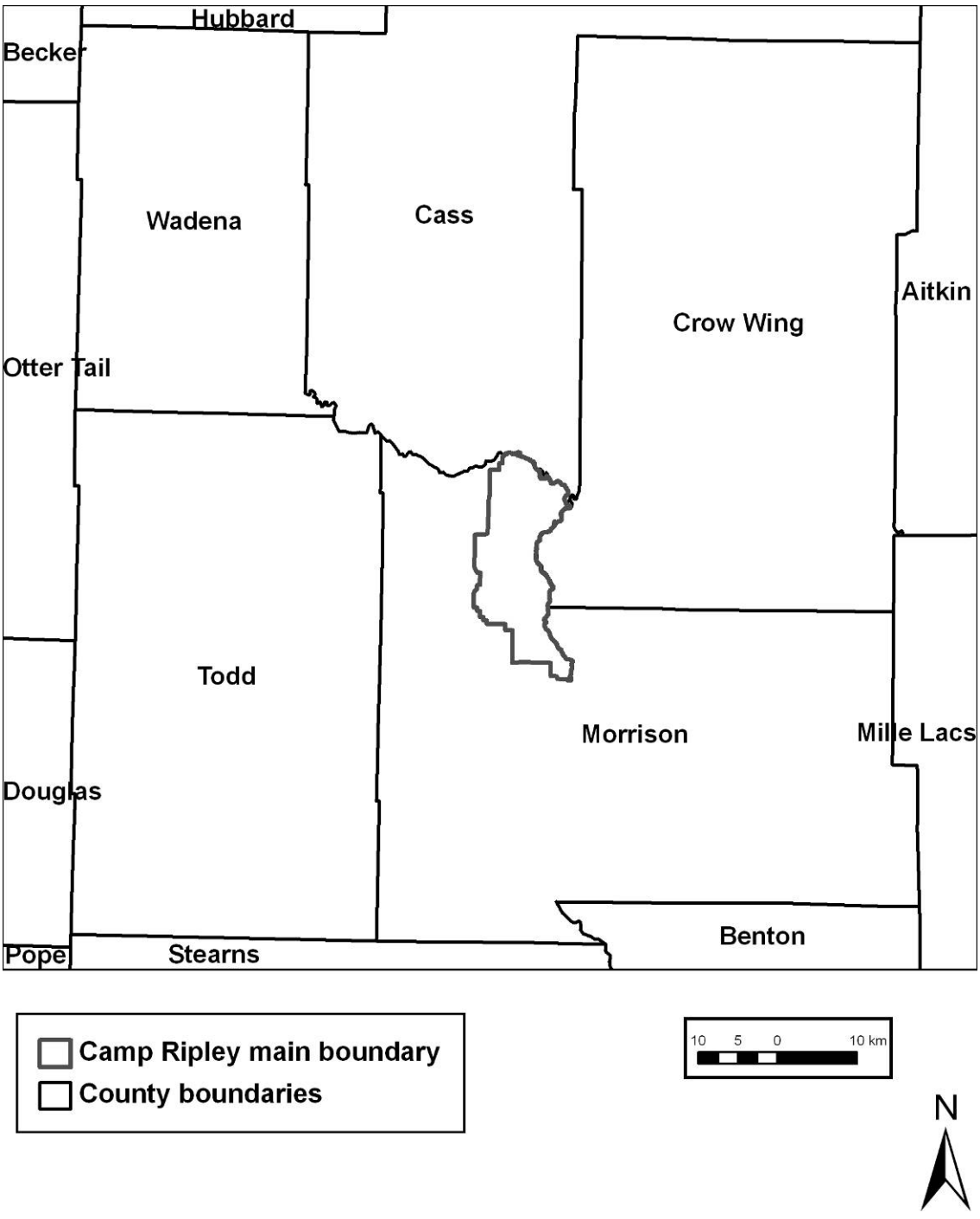

Figure 2. The Multi-County Study Area and the Camp Ripley Location

Table 2. Counties in Study Area

County	Area (km^2)	Area (mi^2)
Cass (southern only)	c. 2,024	c. 782
Crow Wing	2,995	1,157
Morrison	2,987	1,153
Todd	2,536	979
Wadena	1,406	543
Total	11,948	3,092

Central Minnesota is a region with a continental climate. Morrison County's annual precipitation is 66 cm (USDA 1994).

The regions greatest topographic relief is associated with the St. Croix moraine (Figure 3) and major drainages including the Mississippi River. In the multi-county study area, topographic highs are above 460 m MSL on the St. Croix Moraine in southern Cass County and on the Camp Ripley property in Morrison County (Figure 4). The topographic low is where the Mississippi discharges at the southern edge of the study area, where elevations are less than 310 m MSL.

Lakes and wetlands (Figure 5) are mapped from 1:100,000 scale hydrography derived from USGS digital line graph (DLG) data of the same scale, available from MDNR (2009). Streams in the figure are based on "blue-line" streams at 1:24,000-scale USGS topographic maps and are displayed only in the multi-county study area.

Figure 3. View from St. Croix Moraine down to Tamarack Lake, Camp Ripley

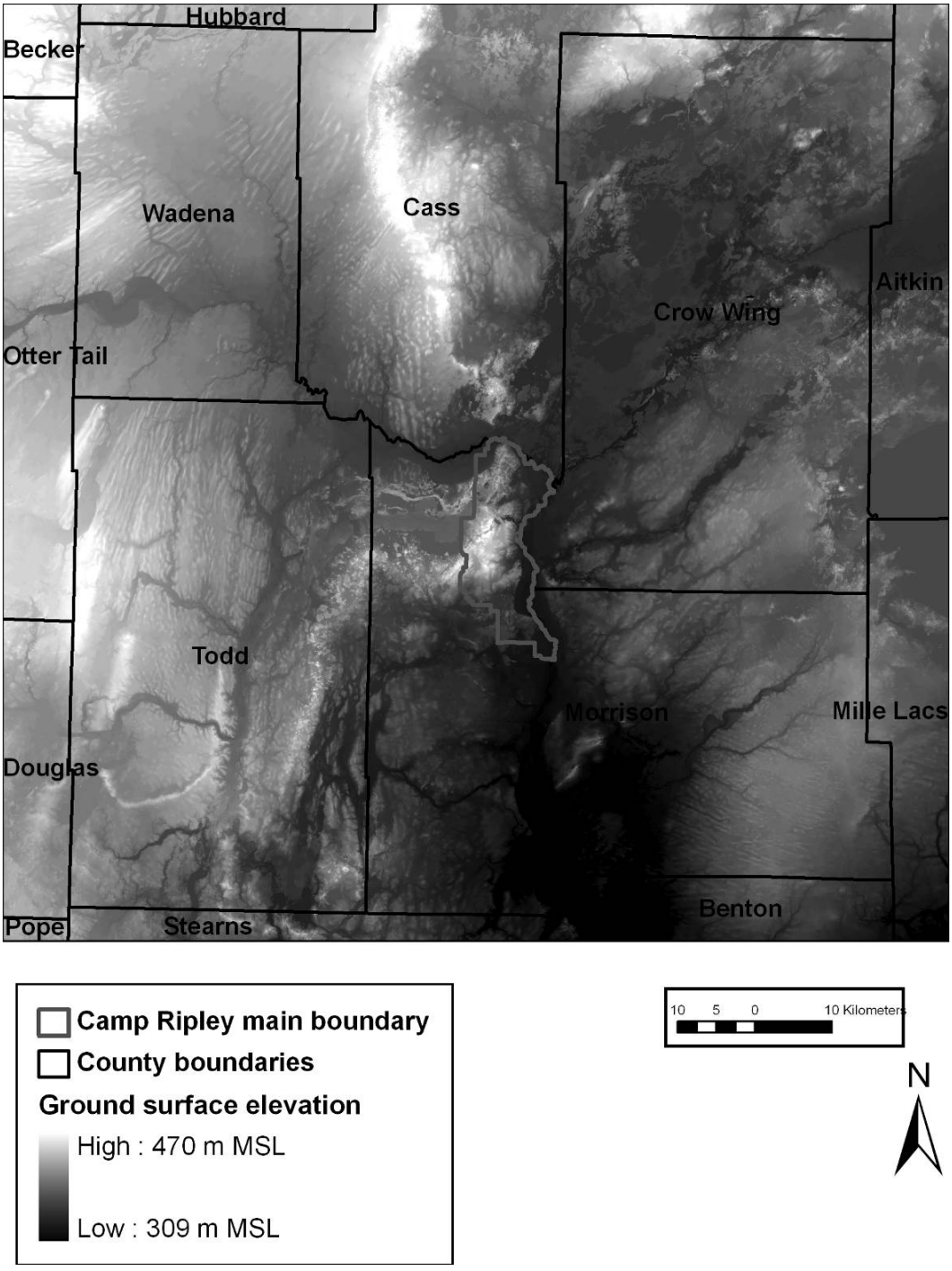

Figure 4. Topographic Elevation in Multi-County Study Area

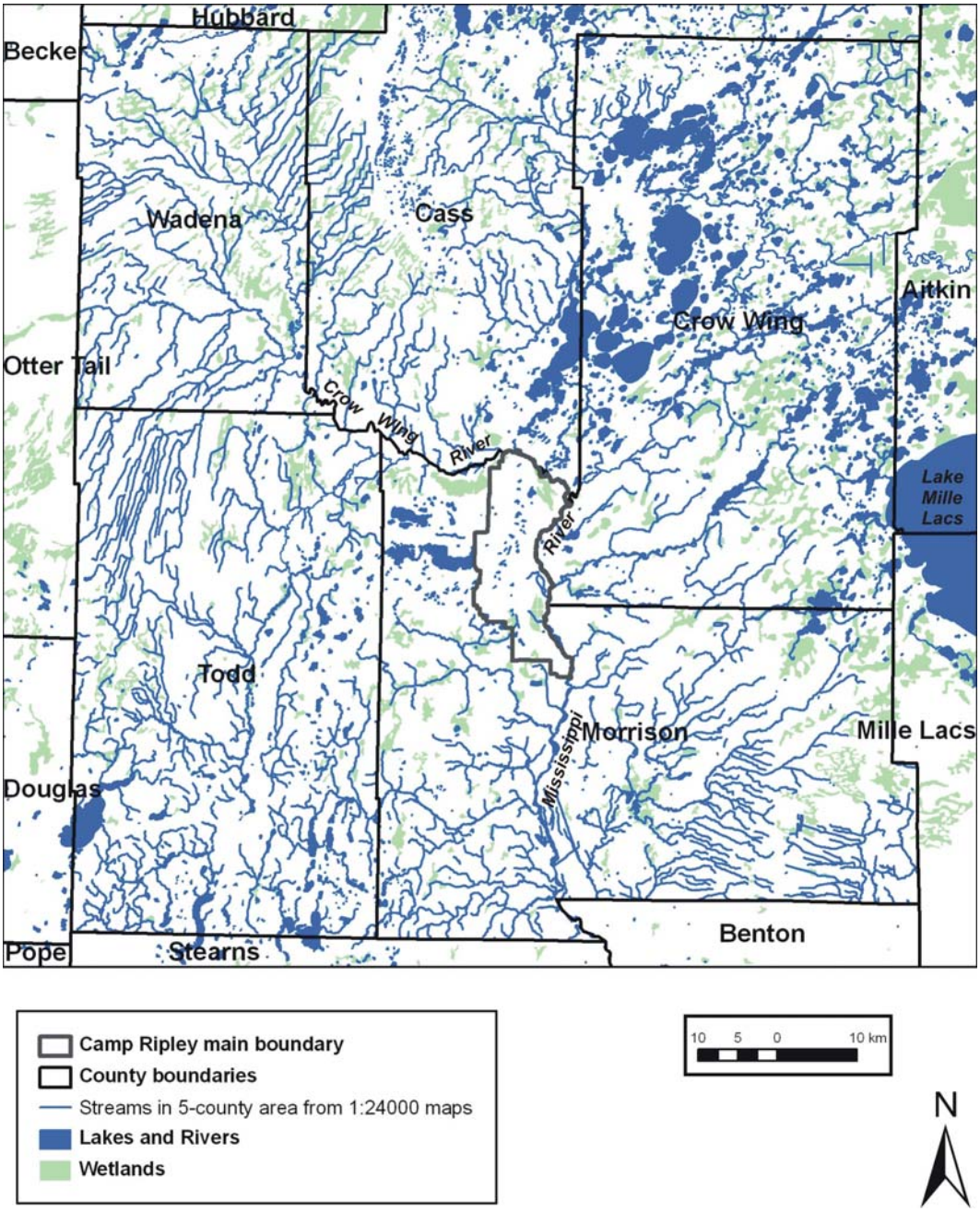

Figure 5. Lakes, Rivers, Wetlands, and Streams in the Multi-County Study Area

Glacial History and Geology

Central Minnesota has had a complex history of ice lobe advances and retreats. Buried pre-Wisconsinan sediments in the multi-county study area include northwest-source Browerville formation sediments and northeast-source Rainy lobe materials (Knaeble 2006).

In Late Wisconsinan time, central Minnesota was glaciated by the Hewitt phase of the Rainy lobe (Goldstein 1989), which advanced far south and west of the Camp Ripley region and formed the Wadena drumlin field and the Alexandria moraine, which is outside of the multi-county study area. Later in the late Wisconsinan stage, glacial lobes advanced into the Camp Ripley vicinity from three directions. These included the Wadena lobe from the north, the Rainy lobe from the northeast, and the Superior lobe from the east. Later advances of the Des Moines lobe and its St. Louis sublobe reached central Minnesota. The general arrangement and relative timing of these lobes is shown in Figure 6. The Wadena, Rainy, and Superior lobes have been identified as the key components of the Late Wisconsin glacial history of central Minnesota (Wright 1972; Schneider 1961). Their key landforms, which are described below, are illustrated on Figure 6.

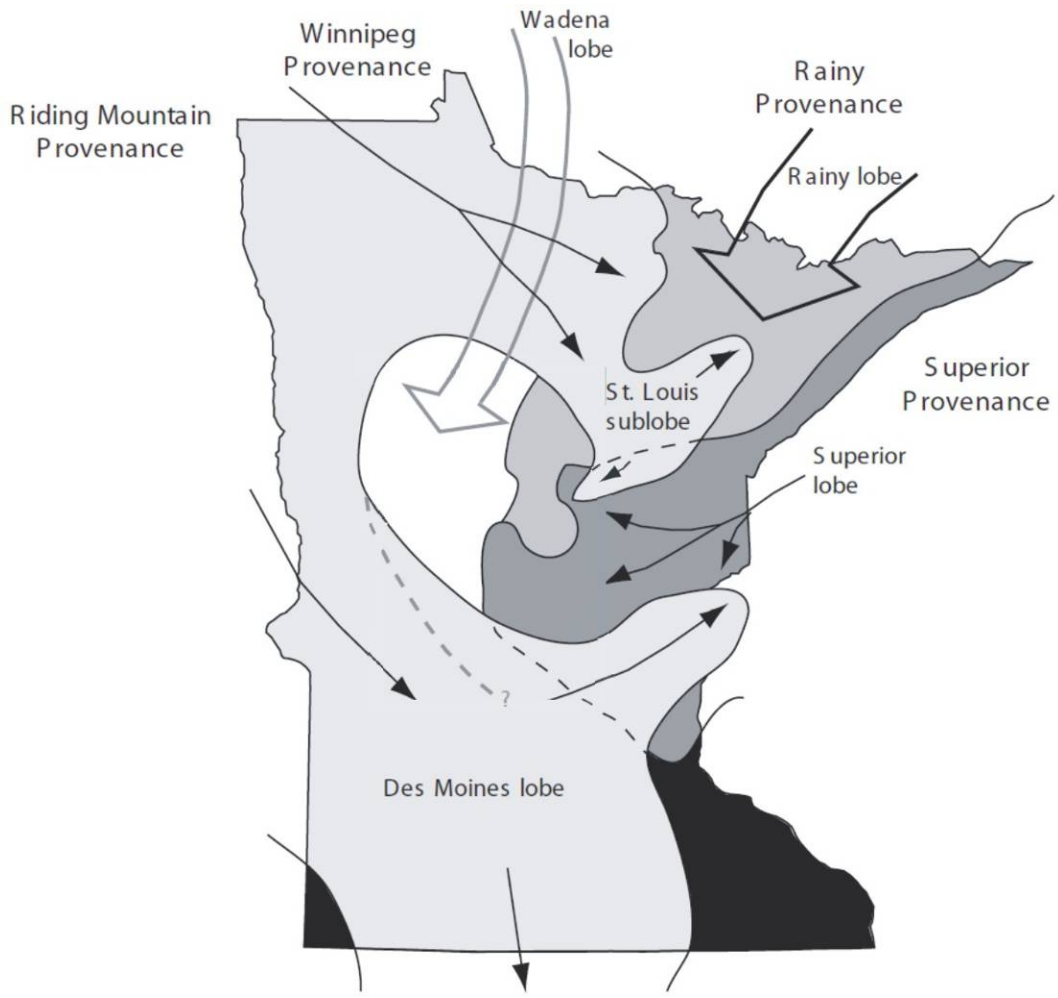

Figure 6. Late-Wisconsin Ice Lobes in Minnesota (modified from Knaeble 2006)

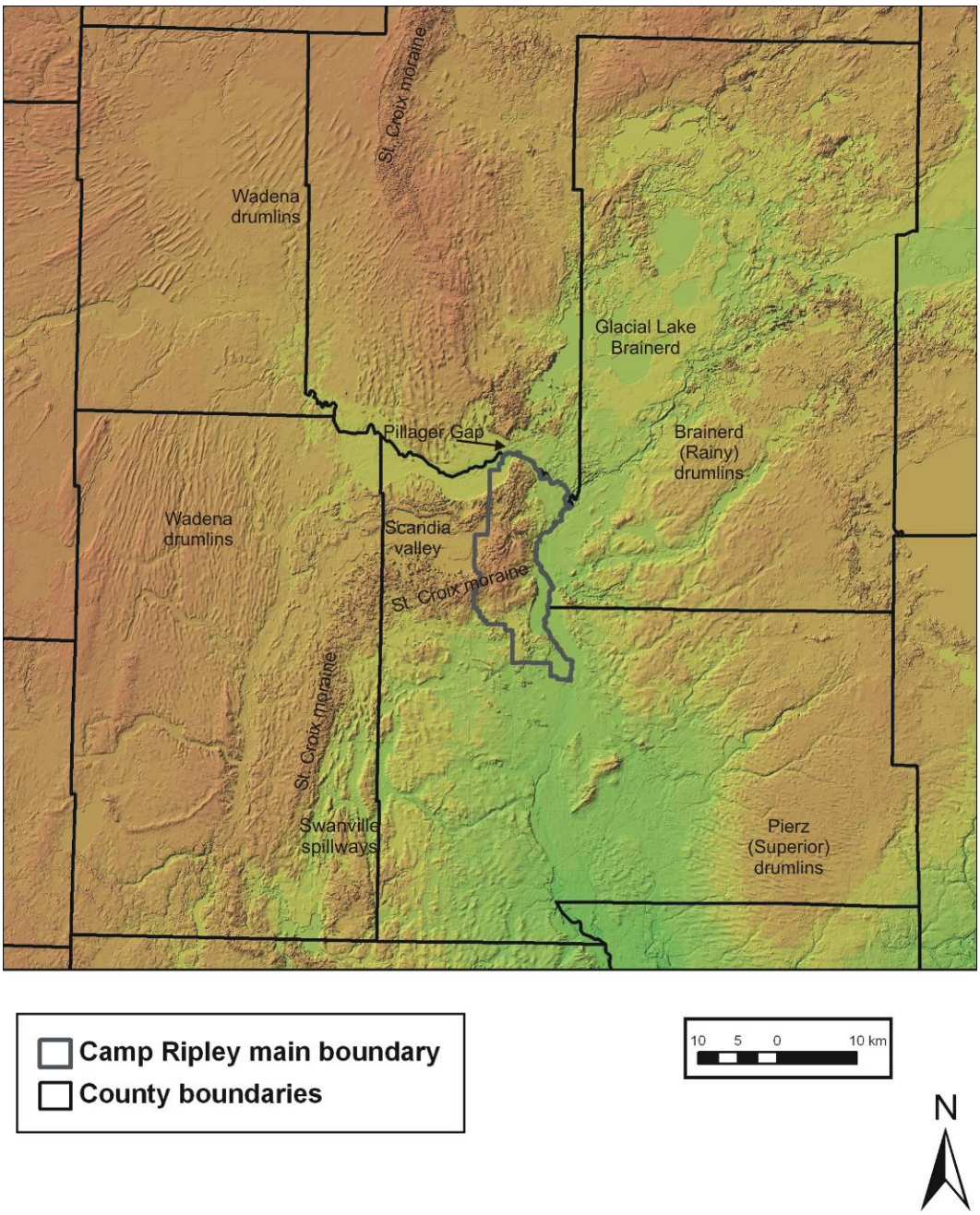

Figure 7. Key Glacial Features on Shaded Relief Map

The Wadena lobe emanated from the Labradorean spreading center in Canada, through the Hudson Bay region, and traveled across central Minnesota from the northeast (Goldstein 1989, 1998) (Figure 8). A fan-shaped pattern of drumlins indicates local flow directions in central Minnesota (Wright 1972). Its drift is gray if unoxidized, yellow-brown if oxidized, and calcareous. Its till is a sandy loam (Schneider 1961, Knaeble 2006). The character of the drift is the result of its Paleozoic carbonate source area.

The Rainy and Superior lobes also originated from the northeast, in the Labradorian spreading center, and both created drumlin fields (Schneider 1961; Wright 1972). Both deposited till that is a sandy loam in texture. The Rainy lobe traveled from the northeast over basalt and other northeastern lithologies, resulting in a drift that is brown and sandy. The Superior lobe flowed out of the Lake Superior basin alongside the Rainy lobe. Like the Rainy drift, the Superior drift is also coarse-grained, but it is red due to a prevalence of rhyolite and red sandstone. The Superior lobe fanned out in central Minnesota, with westward flow to the Camp Ripley vicinity. Together, the two lobes formed the St. Croix moraine in the multi-county study area - the Rainy north of the Pillager Gap and the Superior to the south. The surficial geology of three 1:24,000-scale quadrangles in western Crow Wing County have been mapped in detail, and the mapping shows several tunnel valleys associated with the Rainy lobe (Knaeble 2001, Hobbs 2001a, 2001b). The Rainy lobe was thinner than the adjacent Superior lobe; it therefore advanced slower and retreated faster than the Superior (Mooers 1990).

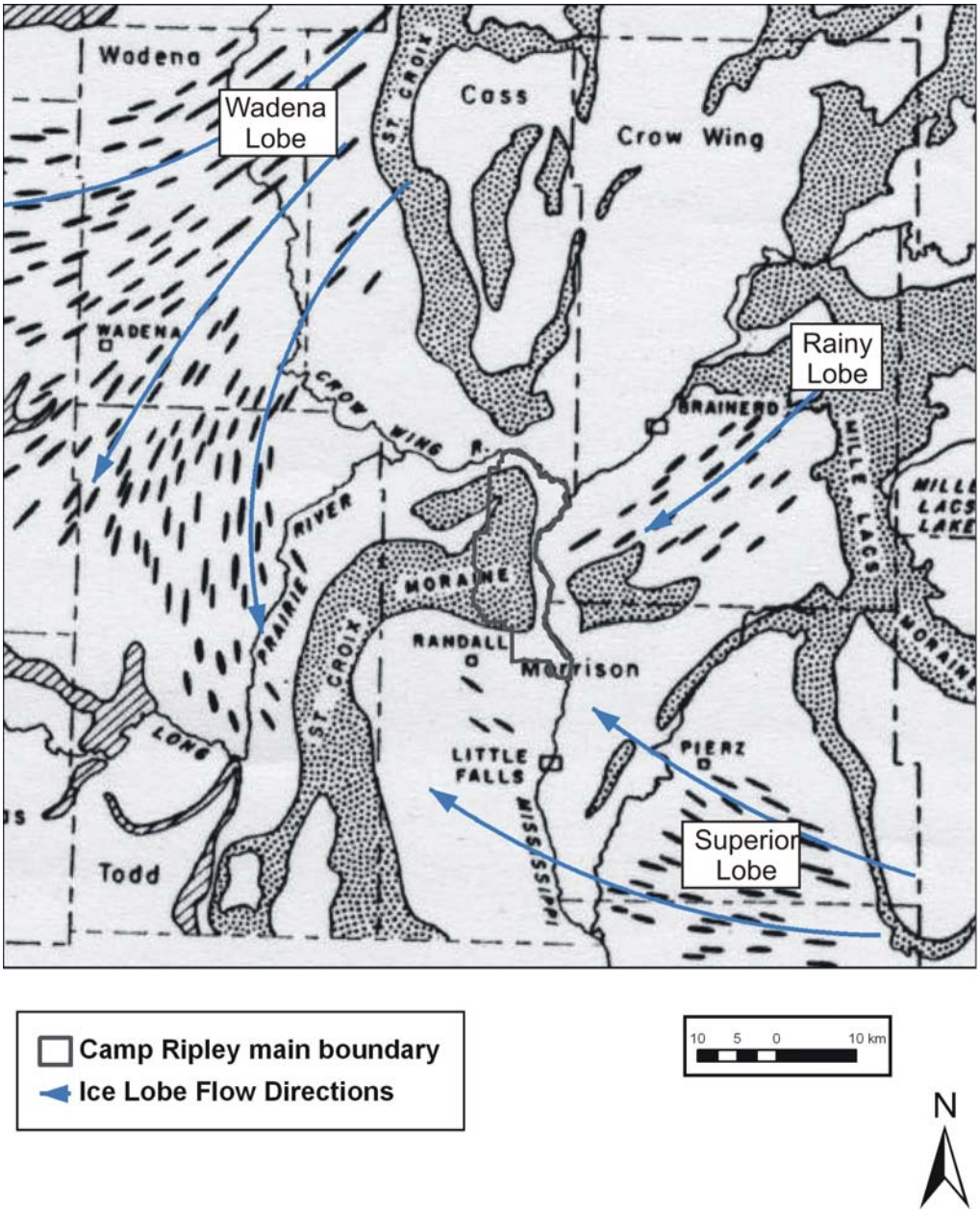

Figure 8. Late-Wisconsin Ice Advances in Study Area (modified from Schneider 1961)

Mooers (1990b) determined that hummocky stagnation moraines of the Rainy lobe were due in large part to thrusting of a frozen bed during surges. Surges have also been suggested for the Superior lobe (Wright 1973) and the Wadena lobe (Clayton et al. 1985). Landform analysis suggests that a frozen toe existed at the terminal moraine as well as at recessional moraines (Mooers 1990a).

Recessional moraines of the Superior lobe have associated systems of tunnel valleys, eskers, and terminal outwash fans (Wright 1973, Patterson 1994, Quinn 1998). Mooers (1989) attributed the formation of these tunnel valleys to meltwater at the ice surface flowing down crevasses and moulins to the bed, where erosion would take place. An analysis by Mooers (1990a) suggests that the glacier was subpolar while at its maximum limit at its terminal moraine, but became temperate during recessional phases, during which well-developed englacial and subglacial drainage evolved.

During retreat from the St. Croix moraine, the Superior lobe meltwater eroded a series of channels referred to as the Swanville spillways (Knaeble 2006). The Rainy's meltwater was, for a time, trapped behind the moraine, forming Glacial Lake Brainerd.

Des Moines lobe till is also present in the southwest corner of Todd County and referred to as New Ulm formation (Knaeble and Meyer 2007). Its glacial till is a loam to clay loam with clasts of Pierre Shale and a yellow-brown oxidized color. Outwash from the melting of the Des Moines lobe is present in low areas in much of Wadena and Todd counties and as valley train deposits along the Crow Wing River and along the Mississippi River downstream of its confluence with the Crow Wing.

Camp Ripley's 214-km^2 area is located primarily on an odd interruption in the otherwise smooth curve of the St. Croix moraine (Figure 7, Figure 8). The St. Croix moraine is generally considered to be built of till and ice-contact deposits of the Superior and Rainy lobes.

The UMD Department of Geological Sciences (2002) conducted the Environmental Drilling Program (EnDriP), a field investigation relying on rotosonic drilling (described below). Highly detailed subsurface information was logged at nine locations (Figure 9). Although not all of the nine borehole locations reach bedrock, in combination they provide a basis for understanding the site's glacial geologic framework (Figure 10).

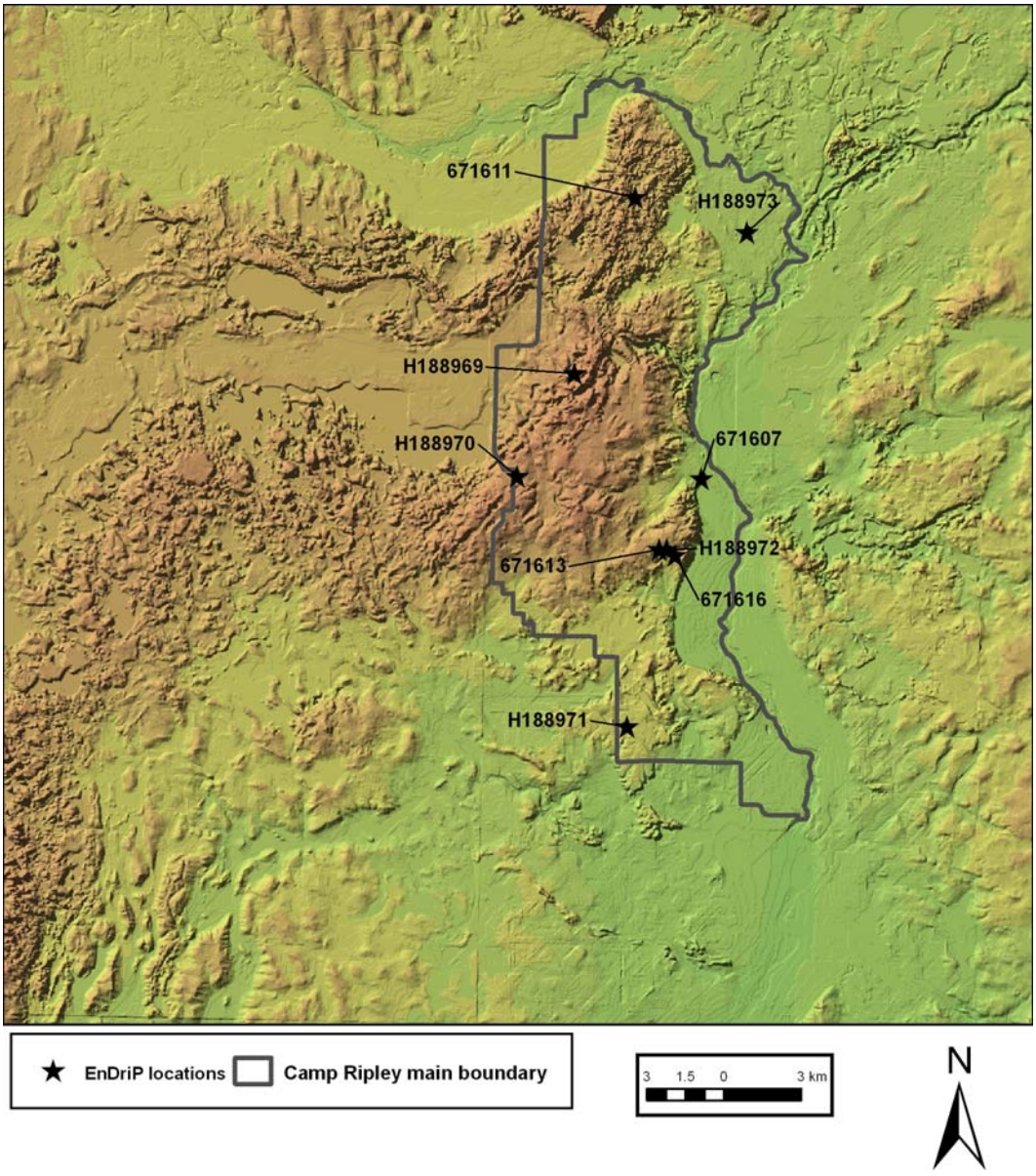

Figure 9. EnDriP (Rotosonic) Locations at Camp Ripley

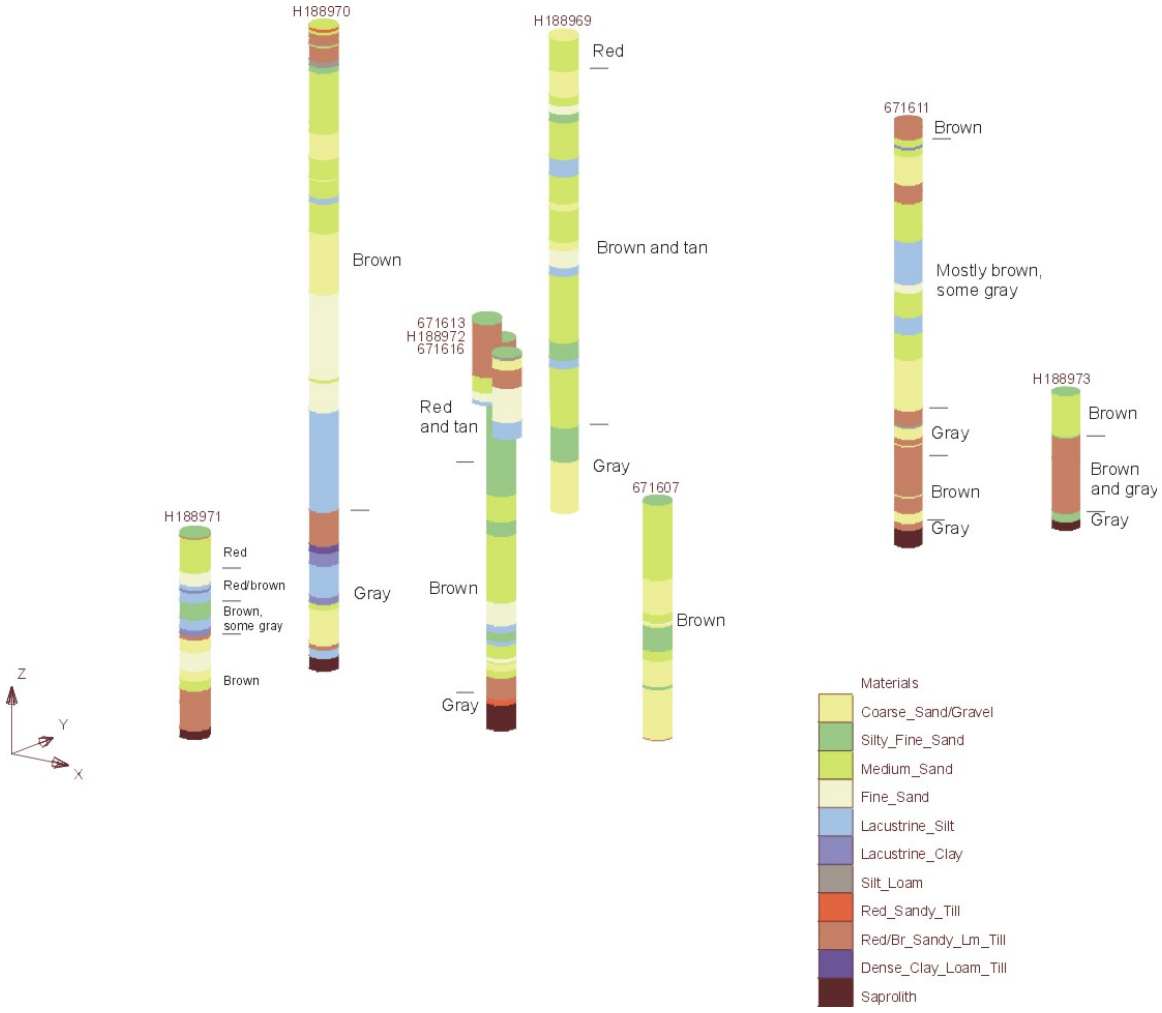

Figure 10. Oblique View of EnDriP Borehole Stratigraphy and Approximate Color Contacts within the Drift (Y direction is due north; X direction is due east)

The EnDriP data suggest that the bulk of the St. Croix moraine at Camp Ripley is sand rather than till. Most of these sands are interpreted to be lacustrine in origin, rather than glaciofluvial (outwash), on the basis of their grain size and sorting. The sands are mainly well-sorted medium sands, fine sands, and silty sands. The medium sands are locally interbedded with silts and clays. The drilling data also indicate a previously unrecognized possibility for this portion of the St. Croix moraine: that it is primarily

glaciolacustrine in origin. In order to create a large, thick lacustrine deposit, an ice-bounded basin must have been present. This basin would probably have had the Rainy lobe as its eastern boundary, and the Rainy lobe would have contributed most of the sediment load (on the basis of the sand color). The Superior lobe would have been present on the southern end of the basin. The Wadena lobe could have advanced to the current St. Croix moraine location in the Camp Ripley vicinity, possibly forming the western boundary of the basin. This idea is supported in part by interbedded gray and brown drift as described by UMD Department of Geological Sciences (2002) and Schneider (1961). The basin could have collected sediment for a time sufficient to create a thickness of roughly 60 m. Afterward, melting of all bounding ice would have resulted in the current inverted topography, with a topographic high composed of lacustrine deposits present at much of Camp Ripley. Note that while most of the St. Croix moraine's surface is pitted and irregular, much of its Camp Ripley portion is fairly smooth and can be attributed to glaciofluvial runoff (Figure 7).

Several past investigations (e.g., Goldstein 1998; Carney and Mooers 1998; Schneider 1961) have identified the Itasca, Rainy, and Superior lobes as contemporary at around 15,000 before present (B.P.). Until now, however, the location of the Itasca lobe was thought to have been further north than the Camp Ripley area at the time when the Rainy and Superior lobes were present there.

On the basis of the available data, the boundaries of the paleo lake basin are not fully defined; the masked glaciolacustrine deposits could be present north of the Pillager Gap, where the Crow Wing River now flows through the moraine. The St. Croix moraine

extends to the north from the Camp Ripley and Pillager Gap vicinity as a product of the Rainy lobe. South and east of Camp Ripley are morainal deposits of the Superior lobe, including the arcuate section connected to the south end of Camp Ripley and the continuation of the moraine to the south (Figure 7, Figure 8). Both the Rainy and Superior lobe portions of the adjacent portions of the St. Croix moraine are likely conventional till moraines, although exceptions may occur locally.

In summary, the geology and topography of the Camp Ripley property and its vicinity are the result of a complex glacial depositional history involving three ice lobes that deposited drifts of various characters and colors. These lobes were thought to have been concurrently active in central Minnesota; however, results from detailed geologic characterization of the site by the UMD Department of Geological Sciences (2002) may suggest new, previously unrecognized possibilities for the juxtapositioning of the ice lobes and for the nature of the St. Croix moraine at Camp Ripley. The lobes appear to have been present in the Camp Ripley vicinity concurrently, depositing well-sorted sands into an ice-bounded lacustrine basin. Occasional ice advances deposited discontinuous till units in the basin at various elevations, and glaciofluvial deposits mantle much of the surface.

Subsurface Data Sources

Data sources for subsurface characterization in glaciated terrain include drilling data, surface geophysics, and borehole geophysics. Drilling data are often the most prevalent data source, especially for studies of large areas for which logs from private and public water supply wells are plentiful and geophysical studies, if any, would provide

information on only very small portions of the region.

Drilling data are available in several forms, each of which varies in terms of their abundance, quality, and completeness. Water wells are commonly drilled with the mud rotary technique. Logging of the subsurface materials is the responsibility of the driller, who logs on the basis of rate of penetration, noise ("chatter") as the drill bit encounters larger clasts, and occasional inspection of the cuttings. This sort of log generally provides the overall lithologies (e.g. "sand" or "clay") with approximate contact depths, and occasional lithologic qualifiers (e.g. "gravelly sand") and color.

Hollow stem augers (HSAs) are the typical equipment of many geotechnical or groundwater contamination investigations. A split spoon sampler, usually of 2-inch diameter and 2-ft length, is hammered through the auger's hollow stem, providing measure of soil consistency. The lithologic sample provided by the sampler is usually logged by a geologist. The HSA approach can provide good quality drilling information, but may be limited by split spoons without 100% recovery. Also, the representativeness of the data may be limited if sampling is not done at continuous intervals throughout the depth of drilling.

Rotasonic drilling is a relatively new technology that provides full recovery of 4-inch diameter core. The sample, which is usually logged by a geologist, provides excellent details on the subsurface. The cost and newness of rotasonic, however, preclude the availability of this type of quality data from most studies.

The County Well Index (CWI) is a database of water wells developed by the Minnesota Geological Survey (MGS) and the Minnesota Department of Health (MDH)

for the storage, retrieval, and editing of water-well information (MDH 2006). The database contains basic information on well records (e.g. location, depth, static water level, well construction) for most private wells drilled in Minnesota since the 1970s. Importantly, the database also contains the subsurface information for most of the wells, as logged by the driller.

The CWI database for the area of interest contains a tremendous amount of information. Refinements during a data management step included deleting duplicates and deleting wells with incomplete information or obviously poor drilling logs. Because of obvious errors in ground surface elevations assigned to some of the CWI data, the 30-m digital elevation model (DEM) data from the MDNR Data Deli was used to assign ground surface elevations.

Crow Wing County initially had a much higher data density than the other counties, due in part to the development of an MGS atlas for that county. Because of the data density discrepancy and a software limitation for the amount of data to be managed, a random selection of 40% of available Crow Wing County boreholes were deleted.

Camp Ripley supplied stratigraphic logs for their onsite monitoring wells, production wells, and geotechnical borings. In combination they total 208 locations. These logs generally have good-quality logs based on split-spoon sampling. In addition, the EnDriP effort was conducted, relying on rotasonic drilling and sampling techniques to obtain continuous, high-quality, 4-in.-diameter cores of the Camp Ripley glacial sediments (UMD Department of Geological Sciences 2002) (Figure 11). Nine drilling locations (Figure 9) were selected across the Camp Ripley site to provide information on

various aspects of the subsurface, such as the depth to bedrock/saprolith, character of various portions of the St. Croix moraine, character of lowland areas, and various deep glacial drift units. Although not all of the nine EnDriP borehole locations reach bedrock, in combination they provide a detailed understanding of the site's glacial geologic framework (Figure 10). Eleven materials were noted in the EnDriP investigation: saprolith, coarse sand and gravel, silty fine sand, medium sand, fine sand, lacustrine silt, lacustrine clay, silt loam, red sandy till, red/brown sandy loam till, and dense clay loam till. Key attributes include red and brown drift in the south, grey drift above bedrock, interbedded drift examples, and an overall dominance by brown drift. The character of the uppermost sediment varies with location; examples include brown sand, brown till, and red sand.

A. 

B. 

C. 

Figure 11. Rotosonic Drilling. A. Rig. B. Core Boxes. C. 4-inch Core

Drillers' descriptions in the CWI data were interpreted with support from direct observations of EnDriP-derived materials. These additional well logs improved the stratigraphic data coverage over the study area.

Altogether, 11,388 holes in the multi-county study area were retained for analysis, including 11,172 CWI data locations, 210 monitoring or production wells from Camp Ripley, and 9 EnDriP monitoring wells or boreholes (Figure 12 and Figure 13). In combination, the data represent nearly 300,000 m of logged material. Summary statistical information according to individual geomorphological data sets is presented in Table 3. GIS tools were used to assign to the boreholes their geomorphological information from Mooers (1996). These assignments included lobe name (Figure 14) and sedimentological association (till plain, supraglacial drift complex, ice contact deposit, etc.) (Figure 15). While the geomorphologic groupings relate strongly to the surficial geology and near-surface hydrogeology, they do not necessarily have much bearing on the buried materials. Still, by analyzing the borehole data of specific groups, insights may be determined on the subsurface correlation structure of different geomorphological zones.

Table 3 also serves as a key to the code numbers for data sets and their corresponding geomorphological setting and data types.

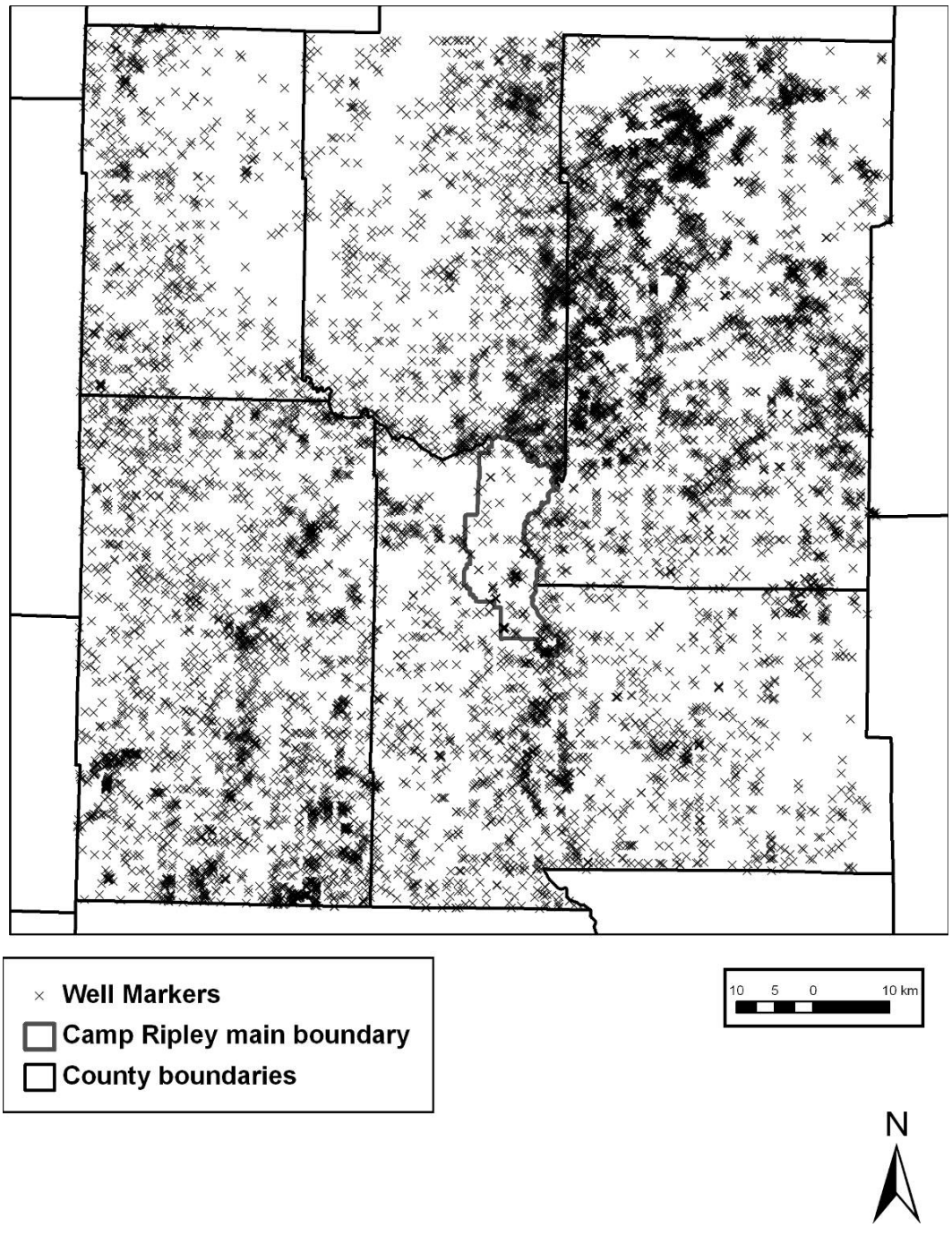

Figure 12. Distribution of Drilling Data in Multi-County Study Area

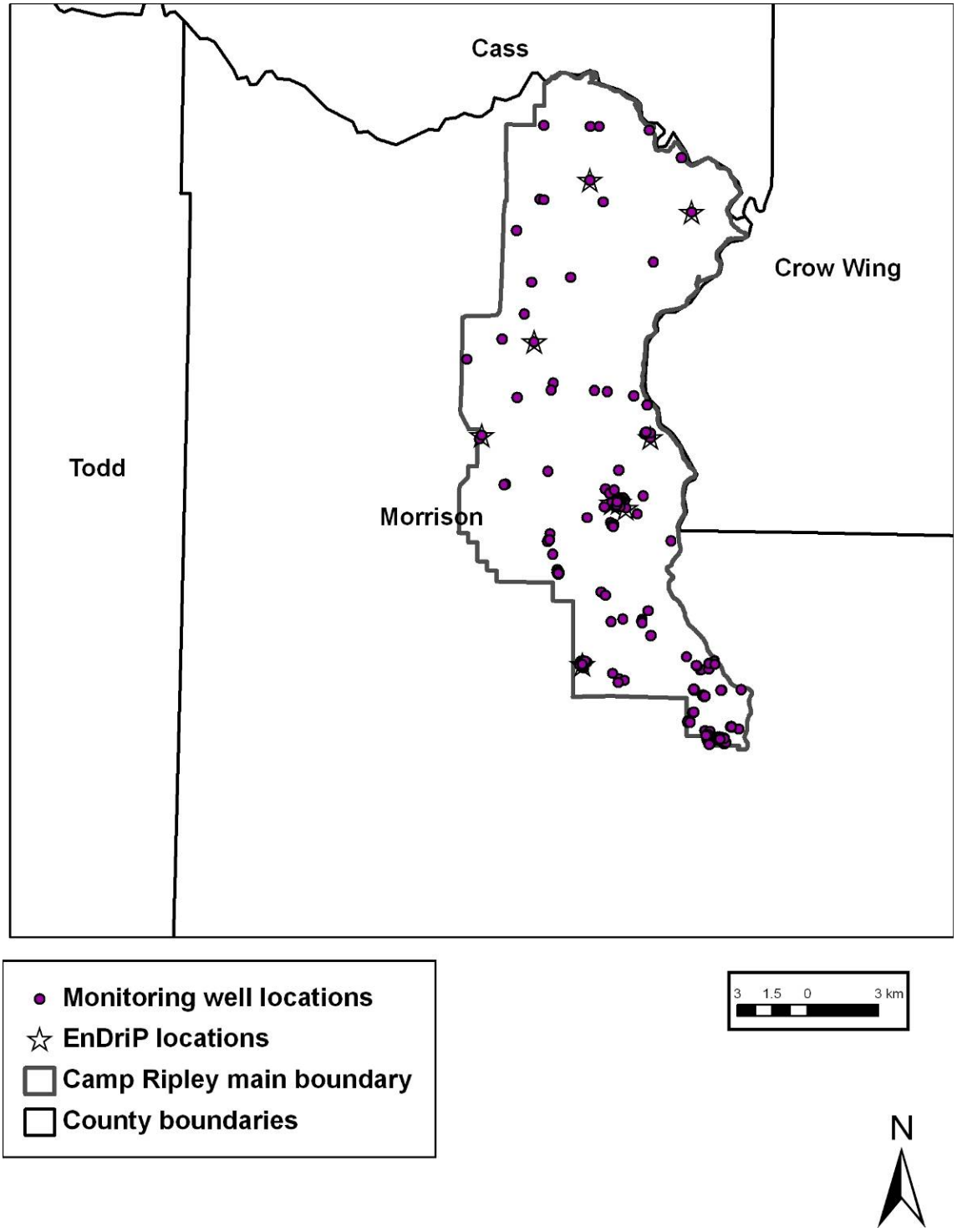

Figure 13. Distribution of Monitoring Wells and Rotosonic Boreholes at Camp Ripley

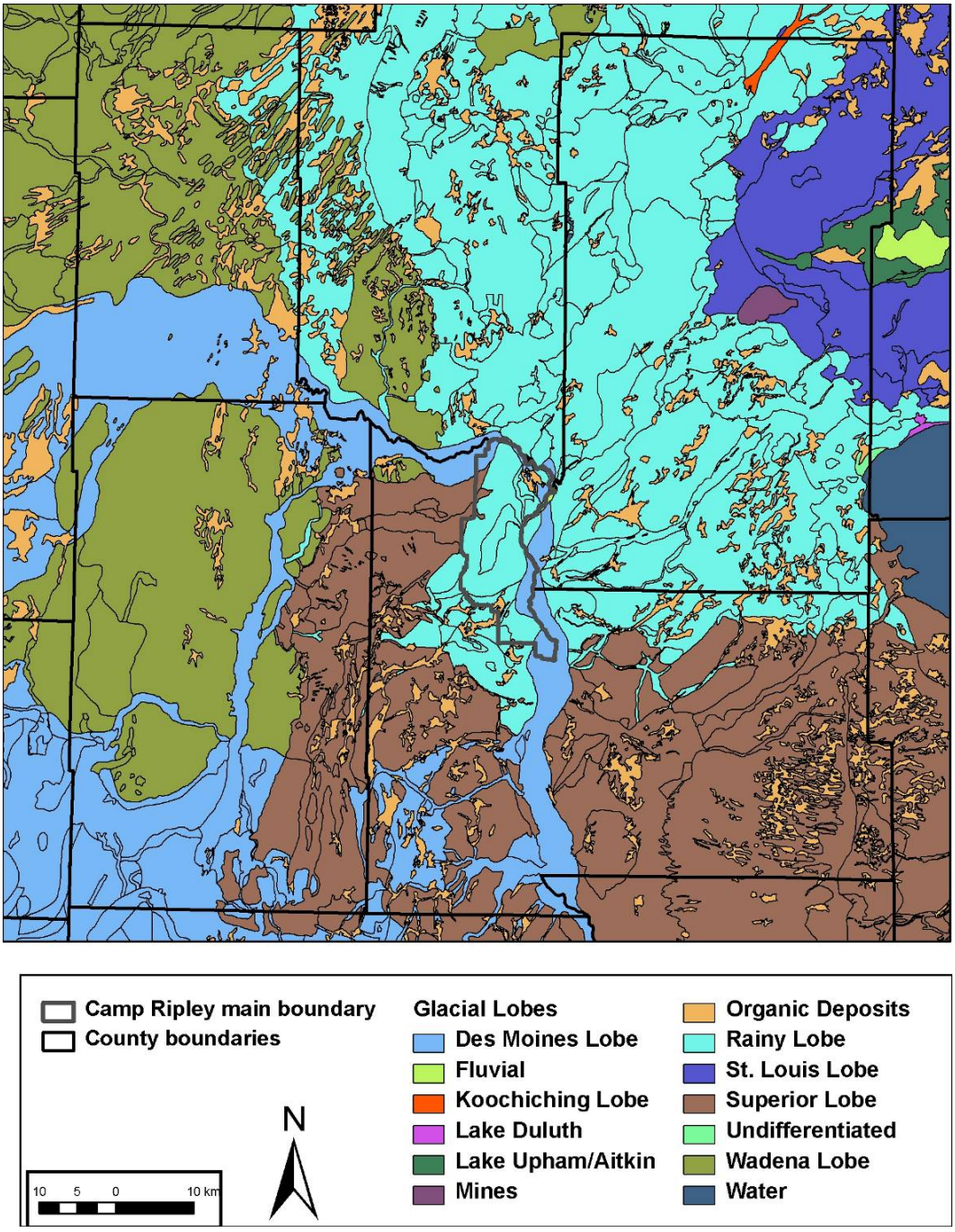

Figure 14. Ice-Lobe Origins of Surficial Deposits

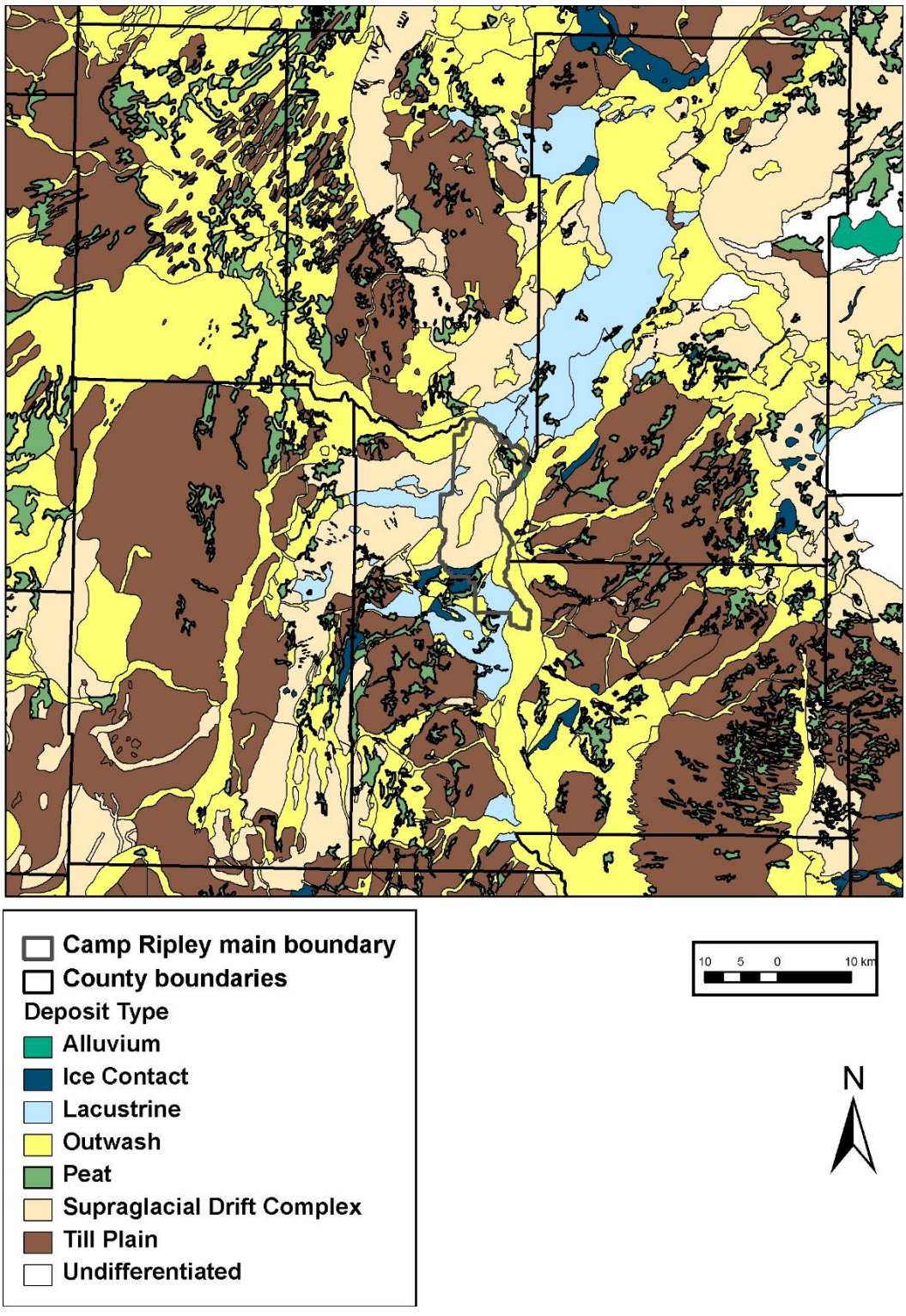

Figure 15. Surficial Sediment Types

Table 3. Data Set Groupings and their Basic Statistics

Data Sets	Geomorph Setting	Data Type(s)[1]	Number of Boreholes	Cumulative Length of Boreholes (m)	Average Borehole Length (m)	Approx. Range in Drift Thickness[2] (m)	Approx. Drift Thickness at Data Locations (m)	Approx. Average Percentage of Penetrated Drift
All data	all, including minor	CWI, MWs, EnDriP	11,388	297,677.9	26.1	0 to 160	55	48%
All MWs and EnDriP	several	MWs and EnDriP	219	3,187.2	14.6	20 to 110	39	37%
3 MWs	Des Moines outwash	MWs	109	1,432.7	13.1	18 to 25	20	66%
3	Des Moines outwash	CWI, MWs, EnDriP	1,420	29,405.9	20.7	10 to 160	45	46%
12cwi	Rainy ice contact	CWI	142	3,846.9	27.1	20 to 55	53	51%
13a	Rainy lacustrine	CWI	1,350	30,196.9	22.4	0 to 130	45	50%
13bCWI	Rainy lacustrine	CWI	72	1,158.2	16.1	10 to 70	24	67%
13 MWs	Rainy lacustrine	MWs	13	209.4	16.1	20 to 45	31	52%
14CWI	Rainy outwash	CWI	2,477	62,082.3	25.1	0 to 140	60	42%
14 EnDriP	Rainy outwash	EnDriP	1	35.1	35.1	35	35	100%
14 MWs	Rainy outwash	MWs	23	294.6	12.8	30 to 90	48	27%
15aCWI	Rainy supraglacial	CWI	388	11,366.9	29.3	30 to 140	60	49%
15b	Rainy supraglacial	CWI	320	7,654.6	23.9	15 to 120	48	50%
15a EnDriP	Rainy supraglacial	EnDriP	7	412.0	58.9	55 to 90	73	81%
15a MWs	Rainy supraglacial	MWs	51	617.3	12.1	60 to 100	65	19%
16a	Rainy till	CWI	393	11,182.5	28.5	15 to 65	40	71%
16b	Rainy till	CWI	242	7,538.9	31.2	50 to 140	83	38%
20	Superior ice contact	CWI	27	728.2	27.0	20 to 60	27	100%
21	Superior lacustrine	CWI	74	2,293.2	31.0	35 to 115	81	38%
21 MWs	Superior lacustrine	MWs	3	78.7	26.2	80 to 105	87	30%
22	Superior outwash	CWI	470	12,018.5	25.6	10 to 90	34	75%
23a	Superior supraglacial	CWI	76	2,631.3	34.6	20 to 70	45	77%
23b	Superior supraglacial	CWI	450	13,437.7	29.9	10 to 180	49	61%
23c	Superior supraglacial	CWI	18	354.2	19.7	20 to 70	45	44%
24a	Superior till	CWI	542	13,207.3	24.4	20 to 110	34	72%
24b	Superior till	CWI	270	7,086.6	26.2	10 to 70	28	94%
26	Wadena outwash	CWI	292	8,798.4	30.1	25 to 130	91	33%
27	Wadena supraglacial	CWI	77	2,621.5	34.0	30 to 120	82	42%

Data Sets	Geomorph Setting	Data Type(s)[1]	Number of Boreholes	Cumulative Length of Boreholes (m)	Average Borehole Length (m)	Approx. Range in Drift Thickness[2] (m)	Approx. Drift Thickness at Data Locations (m)	Approx. Average Percentage of Penetrated Drift
28a	Wadena till	CWI	185	6,648.6	35.9	45 to 120	80	45%
28b	Wadena till	CWI	107	3,296.4	30.8	20 to 120	73	42%
28c	Wadena till	CWI	803	25,428.0	31.7	10 to 160	73	43%

[1] CWI = County Well Index (private well logs), MWs = monitoring wells (split spoon sampling), EnDriP=Environmental Drilling Program (rotosonic drilling and sampling)
[2] The approximate total drift thickness was determined by comparing the ground surface elevation with the interpolated bedrock surface elevation.

Of the three key ice lobes (Rainy, Superior, Wadena), particular geomorphological zones were subdivided on the basis of geographical distribution (Table 3, Figure 16). These subunits were delineated to provide information on the stationarity of the geomorphological units' geostatistical character (i.e., whether the local mean is constant in different locations). For example, the Rainy supraglacial zone is divided into a western and eastern subunit. The western zone (ID 15a) is at or near the St. Croix moraine (and includes much of Camp Ripley), while the eastern zone (ID 15b) is at a recessional moraine. Ice contact and outwash geomorphological units were not subdivided because they generally represent localized, narrow deposits.

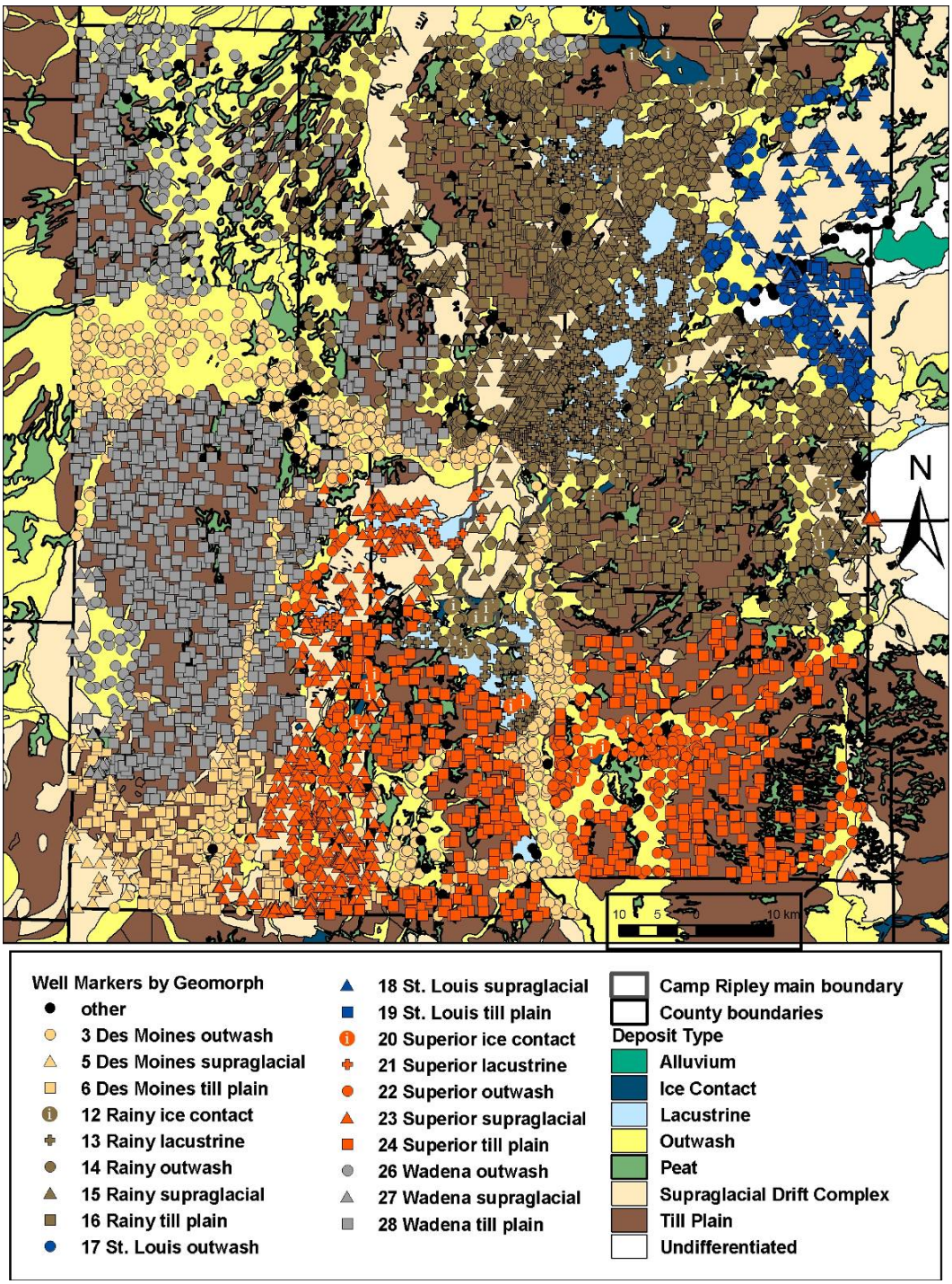

Figure 16. Well Markers According to Geomorphological Terrain

While other lobes' materials were present, they are not studied in detail beyond their contribution to the vertical and lateral variograms for the complete data set because they have a relatively minor distribution and are generally unimportant in the central area near Camp Ripley. Till of the St. Louis sublobe of the Des Moines lobe is only in the fringe area in the northeast corner of the study area, and the Des Moines lobe's till and supraglacial deposits are confined to the southwest corner. A very small amount of data from geomorphological units Lake Upham/Aitkin was ignored in the detailed analyses.

Also, monitoring well data and one EnDriP location that are in the Mississippi valley train, mapped in Figure 16 as Des Moines outwash, were not analyzed in detail because these data are typically shallow and heavily dominated by sand, therefore providing little information on statistical variability.

In addition to the one EnDriP sonic borehole in the valley train of Des Moines outwash in the northeast portion of Camp Ripley, seven EnDriP boreholes were located in the Rainy supraglacial setting and one in Rainy outwash along the southwest edge of Camp Ripley. These high-quality data sources, along with most of the Camp Ripley monitoring well data, were analyzed separately from the CWI water well data.

Of note is a comparison of the characterized portion of the glacial drift to the entire drift thickness is various geomorphological zones. The data (Table 3) indicate that a significant proportion of the subsurface is characterized by the available data.

GEOSTATISTICAL ANALYSES OF GLACIAL DRIFT

Methodology

Data Preparation

The initial step of the geostatistical evaluations is the assembly and evaluation of drilling data. The quality, which may vary throughout a set of available data, must be evaluated to determine which, if any, logs should be discarded. The quality may be ascertained by inspecting the descriptions of materials and by checking the contact depths for consistent round numbers, suggesting a lack of detailed observations.

The logged materials are then broken down into various categories on the basis of their lithologies. A spreadsheet is constructed of borehole data, including borehole name, easting, northing, material type, and contact elevations. The contact elevations are determined as accurately as possible, given the drilling method (e.g. split spoon recoveries <100% may require an estimate of a contact elevation). This information is brought into the Groundwater Modeling System (GMS) as a three-dimensional borehole stratigraphy dataset. The borehole data may then be inspected for its general geologic structure by manually spinning and zooming in on the data. The importance of this step is that it provides the researcher with a cognitive understanding of the three-dimensional

structure of the site with far more detail than can be conveyed with a set of static cross sections.

Both the indicator geostatistical approach and the transition probability approach rely on categorizing the lithologic data on the basis of their relative hydraulic conductivity values. The suitability of these methods is therefore dependent upon whether the available data can be reduced appropriately to two categories (for indicators or binary transition probability) or a reasonably small number of categories (for transition probability).

The analysis focuses on the Rainy, Superior, and Wadena deposits, as delineated by Mooers (1996) (see University of Minnesota-Duluth Department of Geological Sciences 1997). The DNR's geomorphological units imply some degree of information on the subsurface materials. The geomorphologic terrain units were used in a GIS to group the drilling data according to both their ice lobe and their surficial sediment type. In addition, some lobe-sediment zones were split into two or three zones on the basis of abundant data in geographically different areas. Finally, higher quality monitoring well data from Camp Ripley were split out from the private well logs from CWI, and very high quality logging at nine rotosonic EnDriP locations were analyzed separately. Comparisons could then be made among different drilling technologies for the same lobe-sediment zone, or among different geographical zones of the same geomorphological unit, or among data of the same terrain type but from different lobes.

Indicator Variography

To begin the indicator geostatistical analysis, the GMS borehole file is used as input to a utility that creates a three-dimensional set of data points with a format of x, y, z, and material type. This utility converts each vertical interval into a series of points with z values representing the midpoints of segments of a user-specified maximum length. A maximum spacing of 0.5 m was specified; fragments become additional data points at their exact midpoint elevation. From this data file, the material type is then converted in a numeric indicator of 0 or 1, with 0 representing relatively low K and 1 representing relatively high K (Table 4). The dataset is then of a format of x, y, z, indicator.

Basic statistics are then evaluated, including the mean and variance, for use in guiding variogram modeling. The stationarity of the data is also examined.

The variography of the indicator dataset is then performed. An initial variogram is constructed focused strictly on the vertical direction. In this step, the variogram search directions are restricted so that each data point is compared only to other data points within the same borehole; there is no cross-hole correlation. Lateral correlation is initially investigated by creating an omnidirectional lateral variogram, in which the angular tolerance and vertical bandwidth will be restricted so that a point in one borehole is compared only to points at a very similar elevation in other boreholes. Because of the relative sparseness of data for lateral searches, the lateral variograms may not show structure as clearly as the vertical variograms. The degree to which the experimental variogram supports a clear model will be determined in part by the lag distance, lag

tolerance, vertical angular tolerance, and vertical bandwidth settings. These are modified during the variography step to search for the best results. Directional lateral variograms will then be calculated to search for anisotropy in the lateral range. Whether anisotropy is detected will depend not only on whether it truly exists, but also on whether it can be detected with the available data. Variography is performed using tools contained in GMS, which are directly based on the GSLIB software (Deutsch and Journel 1992).

Table 4. Converting from Drillers' Descriptions to Material Types

Typical Drillers' Descriptions	Material Type (Binary)	Material Type (5 Categories)
Gravel, sand & gravel, coarse sand, coarse gravel, dirty gravel, fine gravel, gravel & rocks, gravel & water, sand & rocks	High-permeability (indicator=1)	1 Outwash
Sand, dirty sand, fine to medium sand, medium sand, water sand		2 Lacustrine Sand
Silt, very fine sand, fine sand & silt		3 Lacustrine Silt
Clay, blue clay, silty clay, sticky clay	Low-permeability (indicator=0)	4 Lacustrine Clay
Till, boulders, clay gravel, clay & rocks, clay sand, clay & rock, sandy clay		5 Tills

Transition Probability Geostatistics

The transition probability geostatistics were evaluated in two ways: a binary indicator approach and a 5-category approach. In the binary approach, the low-K and high-K borehole intervals were assigned values of 0 and 1, respectively, as they were in the indicator variogram analysis. In the 5-category approach, the myriad of drillers' descriptions were simplified into five categories, based on a combination of relative

permeability and depositional setting (Table 4). The embedded transition probability approach was followed in evaluating the Markov chains.

By performing T-PROGS analyses on both the binary and the 5-category data, the advantages and disadvantages of simpler vs. more complex data sets may be explored.

Results

Basic Statistics

This study incorporated 300 km of logged material in 11,388 boreholes in 4+ counties. Some of the material is in minor geomorphological units that are not studied in detail. Table 3 provides a comprehensive listing of each data set that was individually analyzed along with their corresponding basic statistics. Note that the data for geomorphologically different zones are subdivided into separate data sets (as appropriate) for cases of geographically distinct zones, and for cases of private well data (CWI), monitoring well data, and EnDriP rotosonic data. These data sets and their distribution are illustrated in Figure 16, and they are also shown in Appendix A.

Indicator Variography

Initially, the complete multi-county data set with over 297,000 m of logged materials was analyzed (Figure 17). These data were converted into the format of x, y, z, indicator. Because an attempt at 0.5 m spacing had caused the program to jam, the maximum spacing allowed in the vertical direction was extended to 1 m. At a 1-m maximum spacing, 320,933 points were available for calculating the variograms.

For the vertical variogram calculations, the variogram search was constrained to only compare data points in the same vertical borehole. For the complete data set, the data clearly indicate an exponential form, with a nugget of 0.05, a sill of 0.13, and a range of 18 m (Figure 18). Similar results were found for the combined monitoring well and rotosonic data (Figure 18).

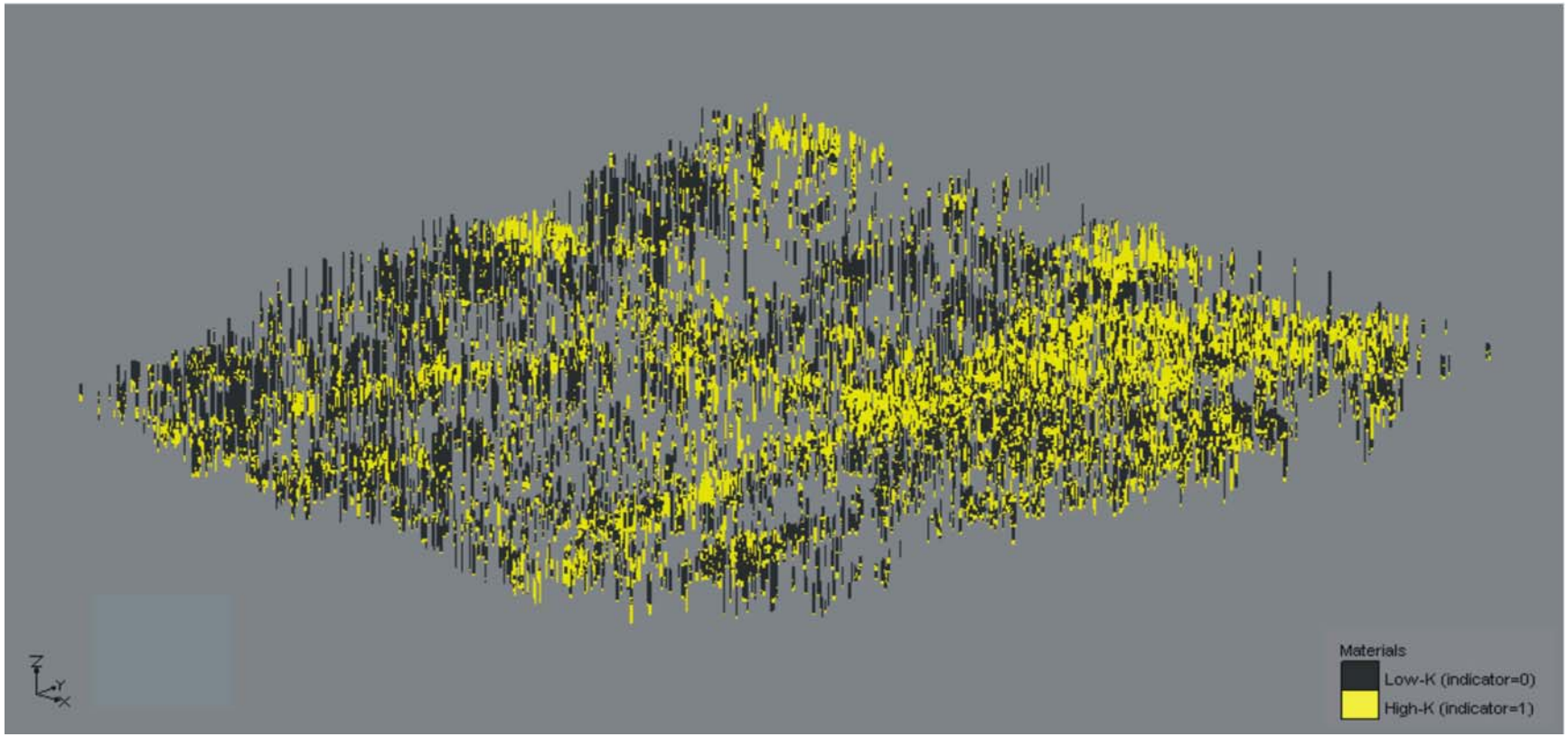

Figure 17. Oblique View of Binary Data in Multi-County Study Area, from Southeast (V.E. = 100x)

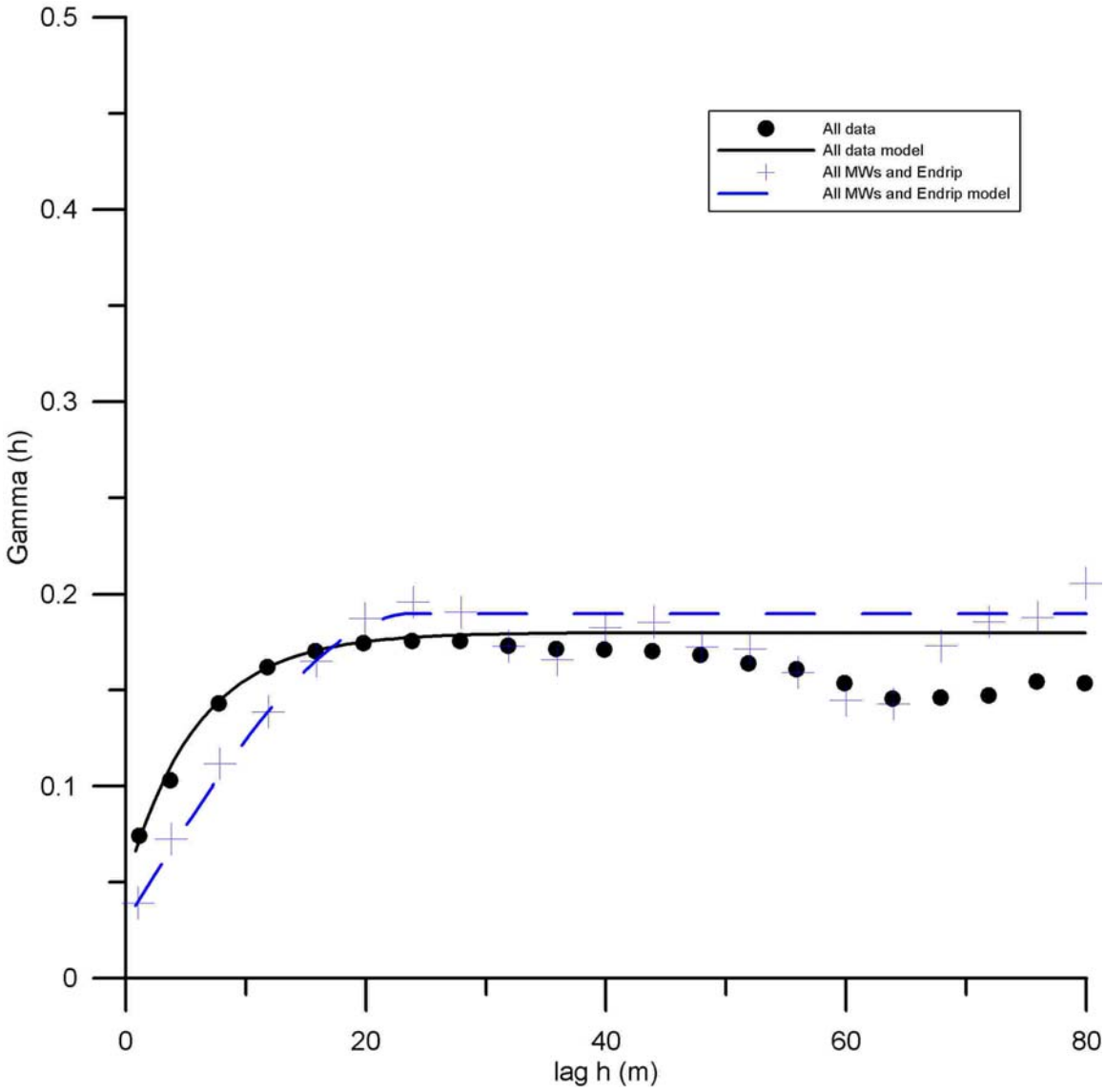

Figure 18. Vertical Variogram for All Data and for All Monitoring Well and Rotosonic Data

In contrast to vertical analysis, boreholes are generally too far apart to allow study of lateral correlation (e.g. Proce et al. 2004, Venteris 2007, Fogg et al. 1998). The lateral structure was initially assessed through a careful analysis of the full data set. For the omnidirectional lateral variogram, the variogram search was performed with a dip angle of 0.0 degrees, a half window dip tolerance of 10 to 20 degrees, and a dip bandwidth of 1 to 3 m. By experimenting with various dip tolerances and dip bandwidths, the sensitivity of these parameters was examined, though they produced insignificant differences in the calculated variogram. The resulting lateral variogram for the complete data set is shown in Figure 19. It was calculated with a dip tolerance of 10 degrees and a dip bandwidth of 2 m. The model is a nested structure of two exponential variograms. The first has a nugget of 0.02, a sill of 0.115, and a range of 60 m. The second variogram has a nugget of 0.0019, a sill of 0.038, and a range of 750 m. This second structure has a subtle effect on the model, but is needed to match up with the experimental variogram results at lags of several hundred meters. Taken together, the full three-dimensional data set has enough support to indicate a clear structure, even at a lag of less than 100 m.

The combined monitoring well and rotasonic borehole data have a much lower sill and a range of 120 m (Figure 19).

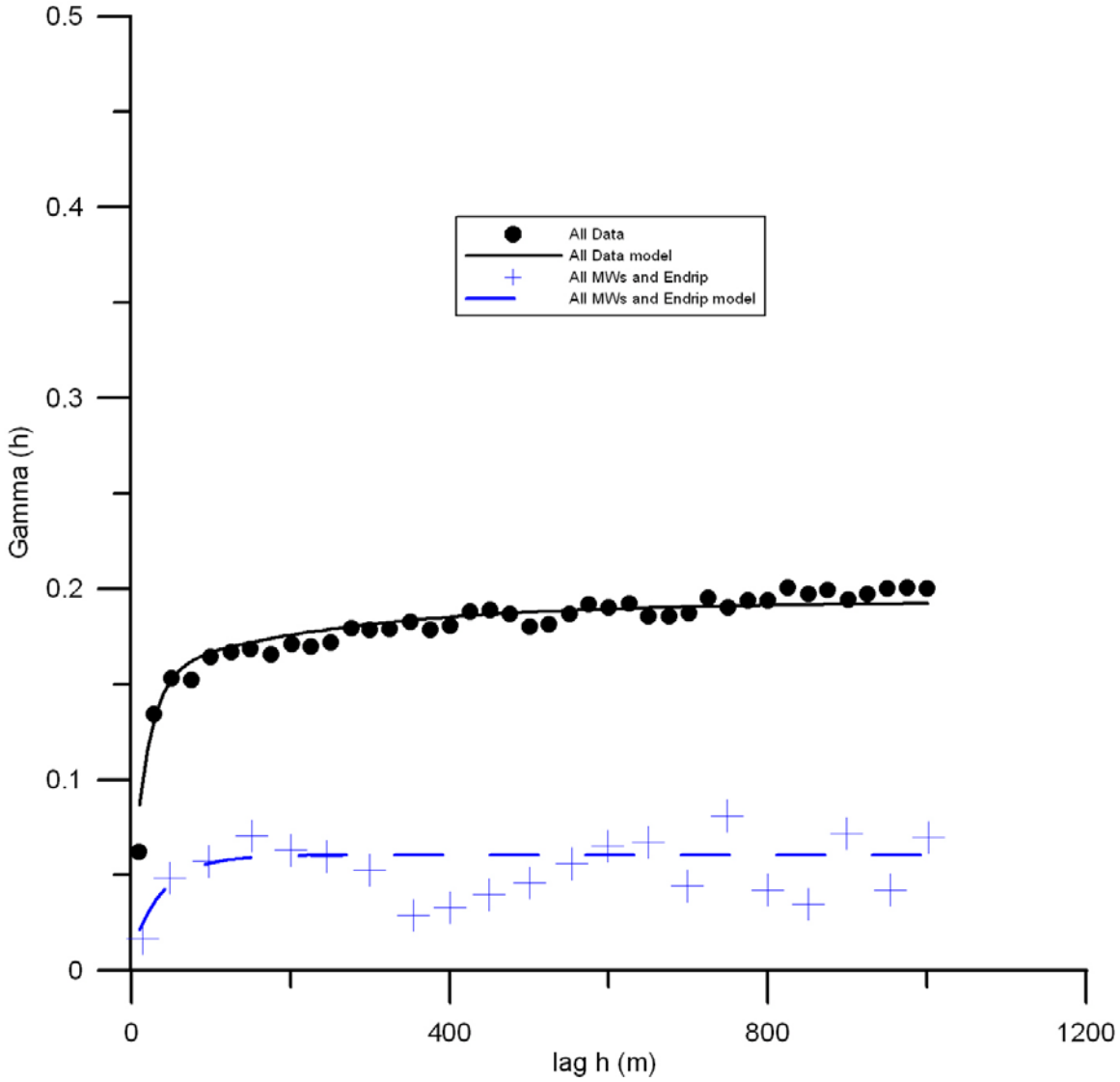

Figure 19. Lateral Vvariogram for All Data and for All Monitoring Well and Rotosonic Data

Vertical and lateral variography was also performed for each of the data sets that were divided by surficial geomorphology and by sampling technology (Table 3).

The vertical and omnidirectional lateral variograms were calculated for each zone of Table 3. Analyses included graphed comparisons of variograms from up to three geographically separate lobe and sediment groupings, of various technologies (e.g. Rainy supraglacial results from data sets 15a, 15b, 15a MWs, and 15a EnDriP), and from a single sediment type (e.g. all supraglacial zone data sets from the Rainy, Superior, and Wadena, which are 15a, 15b, 23a, 23b, 23c, 27). The ranges of all data sets are illustrated in Figure 20.

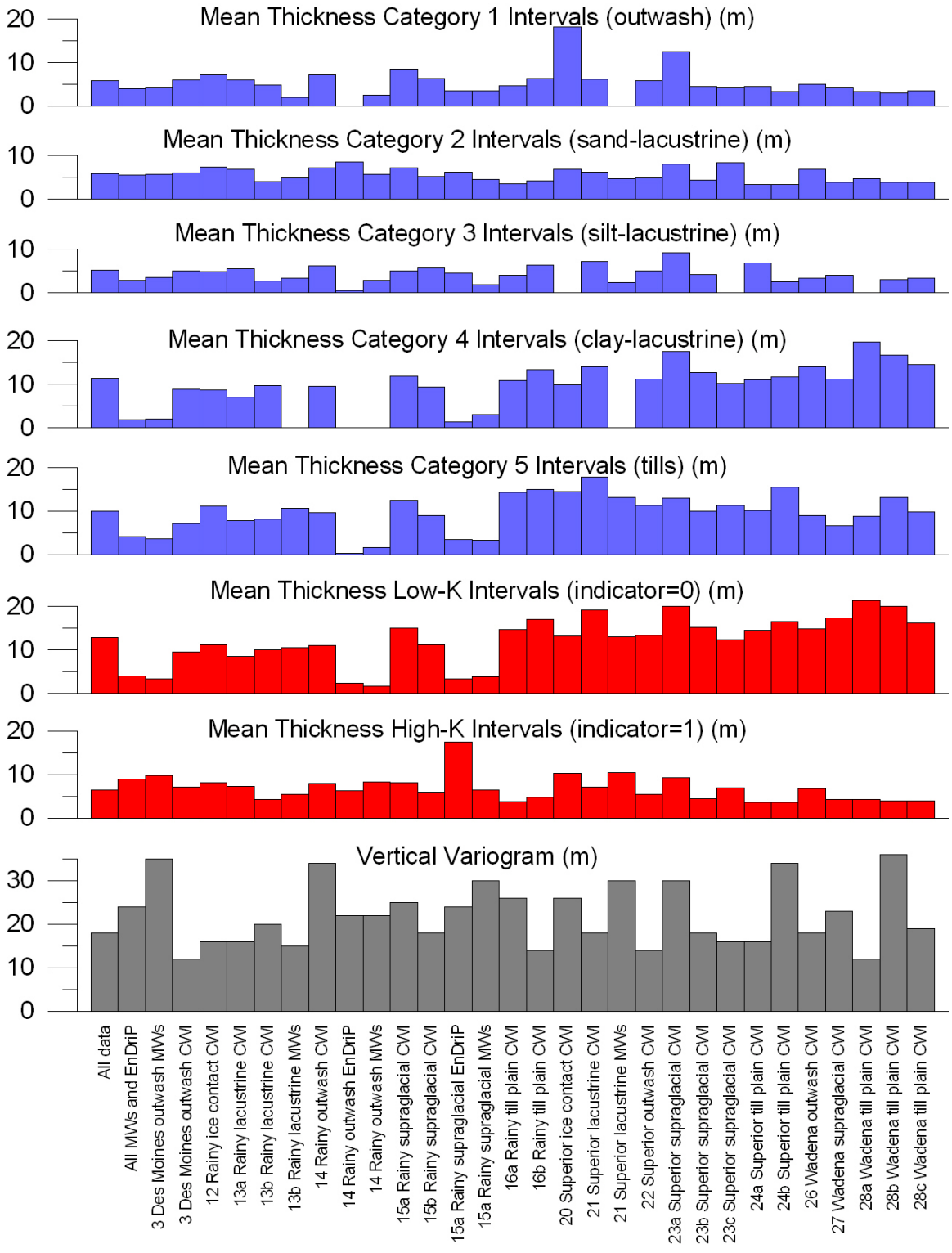

Figure 20. Vertical Correlations Lengths for All Data Sets and for All Methods

Transition Probability

Transition probability analyses were conducted on each data set with a binary approach (low vs. high permeability, as with indicators), and with a 5-category approach. Perspective views of the data are shown in Figure 17 and Figure 22. The T-PROGS capabilities for Markov chain analysis (GAMEAS) and simulation (TSIM) are included with GMS and rely on borehole-format data in GMS.

For the complete data set, the binary analysis (Figure 21) yielded proportions and mean thicknesses as shown in Table 5.

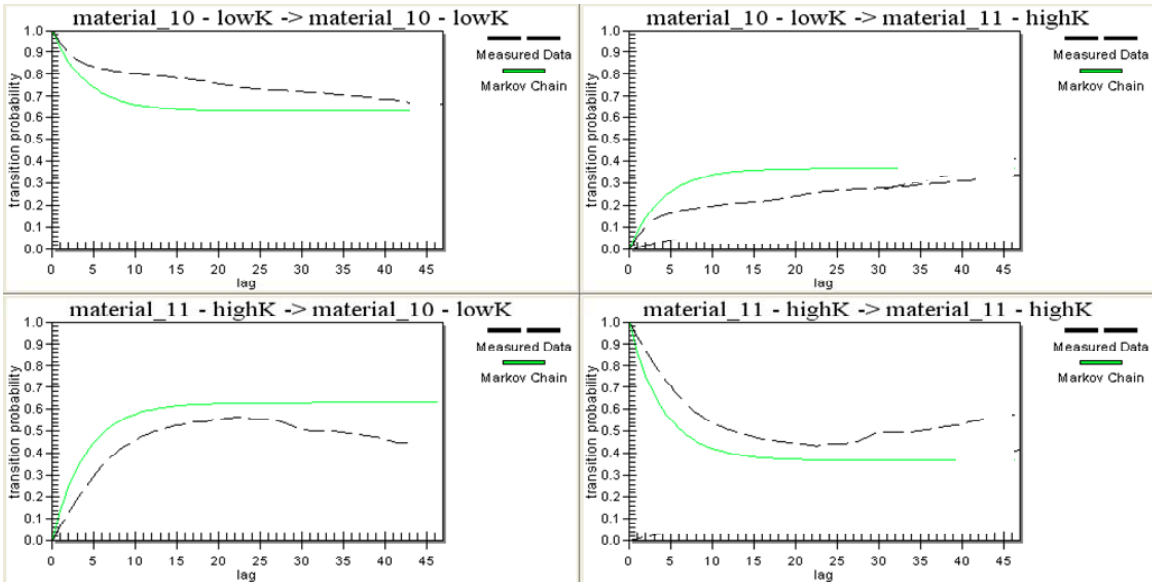

Figure 21. Binary T-PROGS Analysis for the Complete Multi-County Data Set

Table 5. Binary TPROGS Results

Material	Indicator	Proportion	$\bar{L}$ (m)
Low-K	0	0.60	12.9
High-K	1	0.40	6.4

The 5-category analysis (Figure 22 and Figure 23) yielded proportions and mean thicknesses as shown in Table 6. Mean thicknesses for the high-K units (outwash, lacustrine sand, lacustrine silt) are all below the 6.4 m determined in the binary analysis. This is due to adjacent materials being joined together to make high-K intervals for the binary analysis. Likewise, the low-K materials (lacustrine clay, till units) are each thinner than the mean thickness of the low-K material of the binary case. The results for all lens thickness measurements are illustrated in Figure 20.

Table 6. Five-Category TPROGS Results

Material	Indicator	Proportion	$\bar{L}$ (m)
Outwash	1	0.06	5.8
Lacustrine sand	2	0.29	5.9
Lacustrine silt	3	0.02	5.2
Lacustrine clay	4	0.40	8.5
Till units	5	0.23	10.0

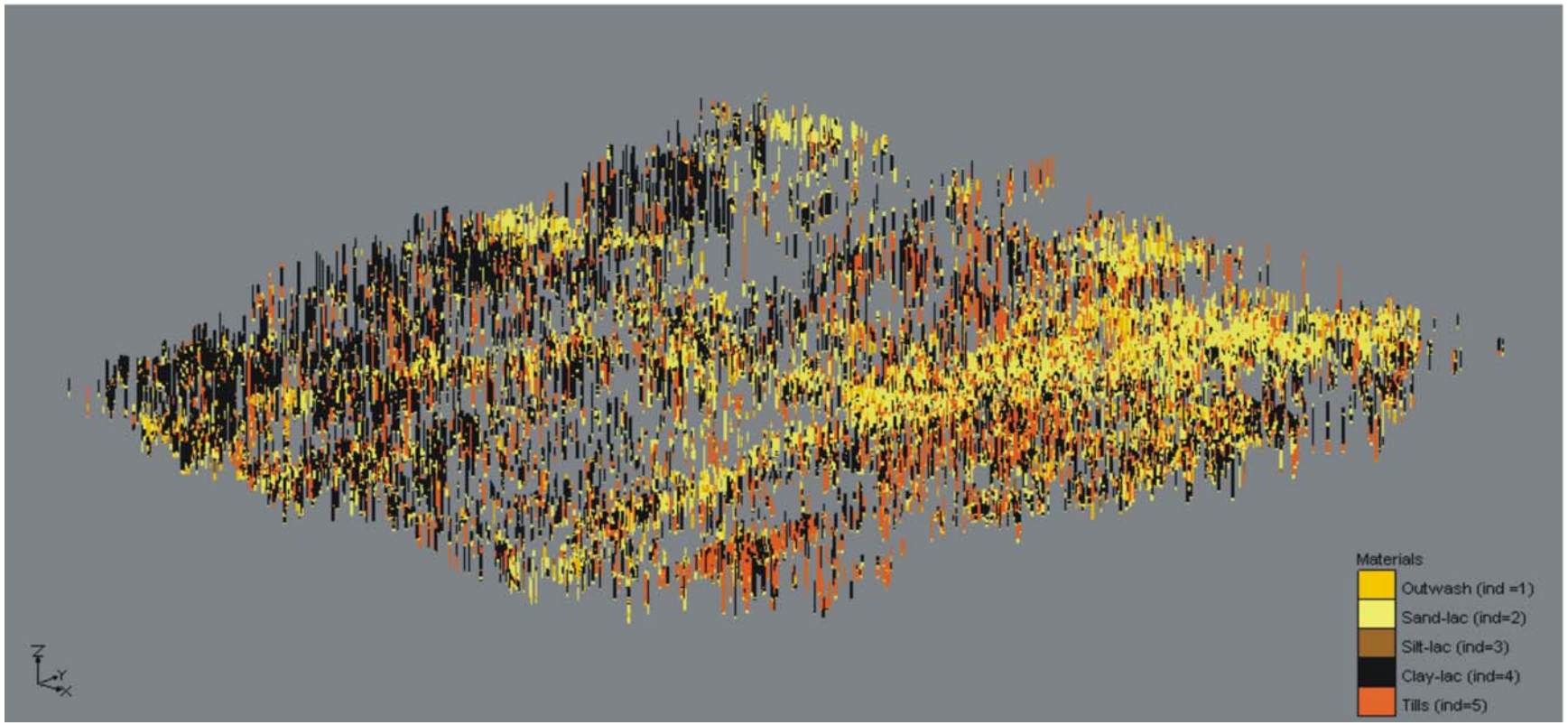

Figure 22. Oblique View of 5-Category Data in Multi-County Study Area, from Southeast (V.E. = 100x)

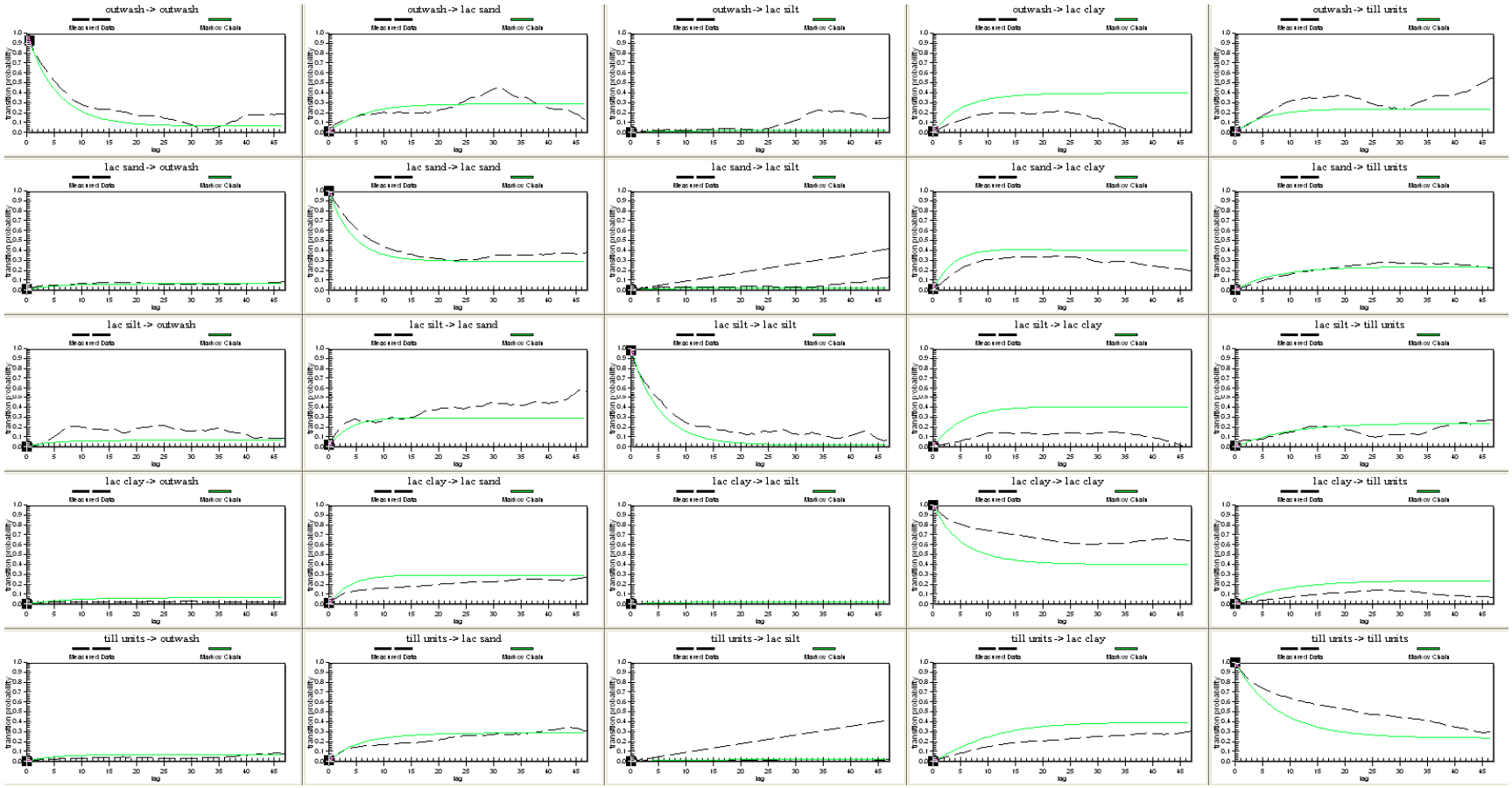

Figure 23. Five-Category T-PROGS Aanalysis for the Complete Multi-County Data Set.

Discussion

Figure 20 is a compilation of a key component of the geostatistical analyses: vertical correlation by the three methods. The figure demonstrates the variability in examined data sets. In this section, the results are discussed in terms of the relationships between lobes, locations, data quality, and glacial processes. A summary is provided in Table 7.

Table 7. Summary of Geostatistical Findings

Data Set*	Vertical Variogram Structure	Lateral Variogram Structure	Binary $\overline{L}$ for Low-K and High-K Materials**
All Data (CWI, MWs, EnDriP)	Clear exponential structure with range of 18 m	Nested exponential variograms with ranges of 60 m and 750 m	Low-K $\overline{L}$ 12.9 m High-K $\overline{L}$ 6.4 m
All MWs and EnDriP	Valley train sediments increase range compared to overall data set	Exponential range 120 m	Low-K $\overline{L}$ decreased compared to overall data due to drilling and sampling method
Geomorphologic subdivisions of MWs	Similar despite different landforms	Insufficient data	Different $\overline{L}$ and differences, and different from corresponding CWI results
Till plain comparisons (R/S/W)	Variety of sills and ranges. Level of variation among geographically subdivided areas is equal to that among different lobes.	Varying support	Similar $\overline{L}$, though Wadena has slightly higher Low-K $\overline{L}$
Lacustrine comparisons (R/S)	Similar ranges, but Rainy has higher sill	Lack of structure	Superior CWI has relatively large Low-K $\overline{L}$, otherwise fairly similar
Outwash comparisons (R/S/W/D)	Superior and Rainy have similar structure	Lack of structure	Fairly similar $\overline{L}$ from CWI data
Supraglacial comparisons (R/S/W)	Fairly similar ranges but different sills	Varying support	Fairly similar $\overline{L}$ from CWI data
Ice contact comparisons (R/S)	Superior range greater than Rainy's	Insufficient data	Fairly similar $\overline{L}$ from CWI data

* R = Rainy lobe, S = Superior lobe, W = Wadena lobe, D = Des Moines lobe

** $\overline{L}$ = mean thickness

A comparison between the CWI-dominated complete data set and the higher-quality monitoring well and rotosonic drilling suggests a similar sill for the vertical case though an unexpectedly longer range for the monitoring well data (Figure 18). This longer range may be explained by the concentration of monitoring wells in the Cantonment Area in the south end of Camp Ripley, which is located in sandy valley train sediments in part of the Des Moines outwash geomorphological zone. The weighting due to the sandy character of the monitoring wells is reflected in the data set's proportion of binary data with an indicator value of 1 (80%) compared to that of the overall data set (40%). The lateral case shows the Camp Ripley data as having a much smaller sill, indicating an expected smaller amount of variance in the data. The ratio of the lateral range:vertical range of the sparser monitoring well data (3.3) is similar to the complete data set's range (5).

The vertical variogram is very well supported in essentially every case, owing to the abundant data available for comparison within each borehole. The lateral variograms, however, vary from fairly well supported to poorly supported. In some cases, they suggest pure nugget effect, and a few cases had no viable variogram – only a shotgun pattern (13 MWs, 21 MWs). The set 14 EnDriP has only one hole and therefore has no lateral variogram. The set 12 MWs were all surficial sandy material without any low-permeability material, so they could not be analyzed vertically or laterally.

Only one geographically subdivided data set showed very similar vertical variogram structure in its subareas (e.g. Rainy lacustrine 13a/13b/13MWs) (Figure 24). Others showed a variety of ultimate sills and ranges (e.g. Rainy supraglacial

15a/15b/15aMWs/15aEnDriP, Superior supraglacial 23a/23b/23c, Superior till plain 24a/24b, and Wadena till plain 28a/28b/28c) (e.g. Figure 25).

The Rainy supraglacial 15a/15b/15aMWs/15aEnDriP analyses show similar vertical ranges but different sills (Figure 26). The set 15a is located on the St. Croix moraine. The set 15b is further east, along a recessional moraine. The 15b data show a higher variance. Yet the 15aMW monitoring well data closely match the 15b data, rather than their neighboring 15a data on the St. Croix. The seven EnDriP holes show a range similar to the range of the others, but at a significantly lower variance. In the lateral direction, the 15b set shows good structure, but the others do not.

Vertical analyses of monitoring well data in various geomorphologic units showed similar structure, suggesting that vertical correlation is independent of the landform sediment assemblage (Figure 27). Lateral variograms, which could only be supported for sets 14 MW and 15a MW, did not show clear structure. This can be attributed to insufficient data.

A comparison of the till plain data from all three lobes (Rainy, Superior, Wadena) shows a variety of sills and ranges for the vertical direction (Figure 28). Notably, the differences in these parameters are as significant among the two or three geographically divided subgroups of each lobe as they are among different lobes. In the lateral direction, the quality of the variograms ranges from good to poor; it is difficult to identify similarities or (Figure 29).

A comparison of lacustrine data for the Rainy and Superior lobes shows a similar vertical range, but the Rainy has a much higher sill. Lateral variograms are not well supported.

Outwash data from the Des Moines, Rainy, Superior, and Wadena lobes show a strong similarity between Superior and Wadena data in the vertical direction. Lateral variograms for each show shotgun patterns indicating a lack of structure.

Comparisons of the supraglacial zones of the three lobes indicate fairly similar ranges but different sills for the vertical direction (Figure 30). Interestingly, Rainy set 15a and Superior set 23b each form a portion of the St. Croix moraine north and southwest, respectively, of Camp Ripley. The Superior set shows a shorter range and a lower sill.

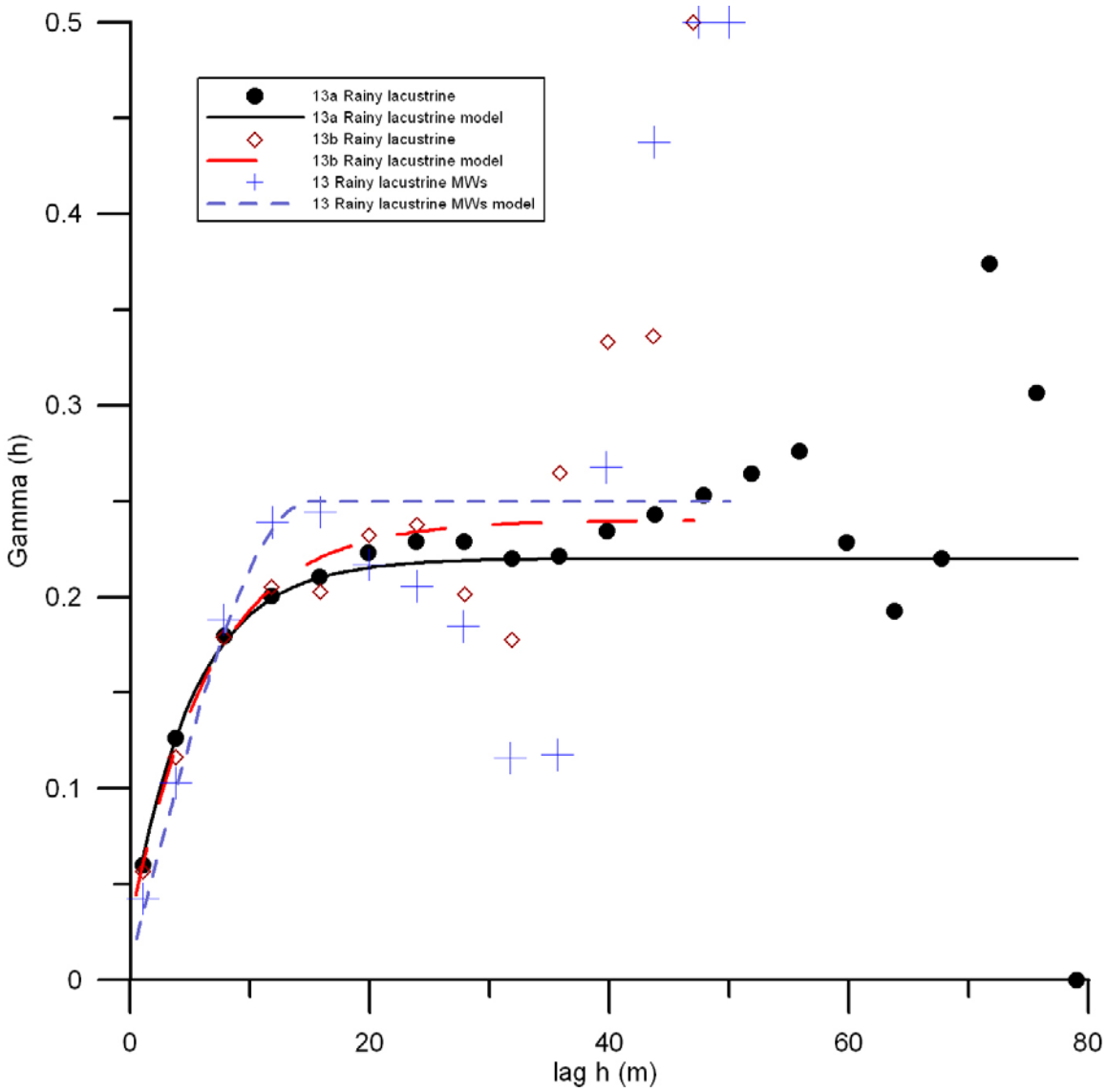

Figure 24. Vertical Variogram Results for Rainy Lacustrine Geomorphological Zone, based on Private Well Log Data and Monitoring Well Data

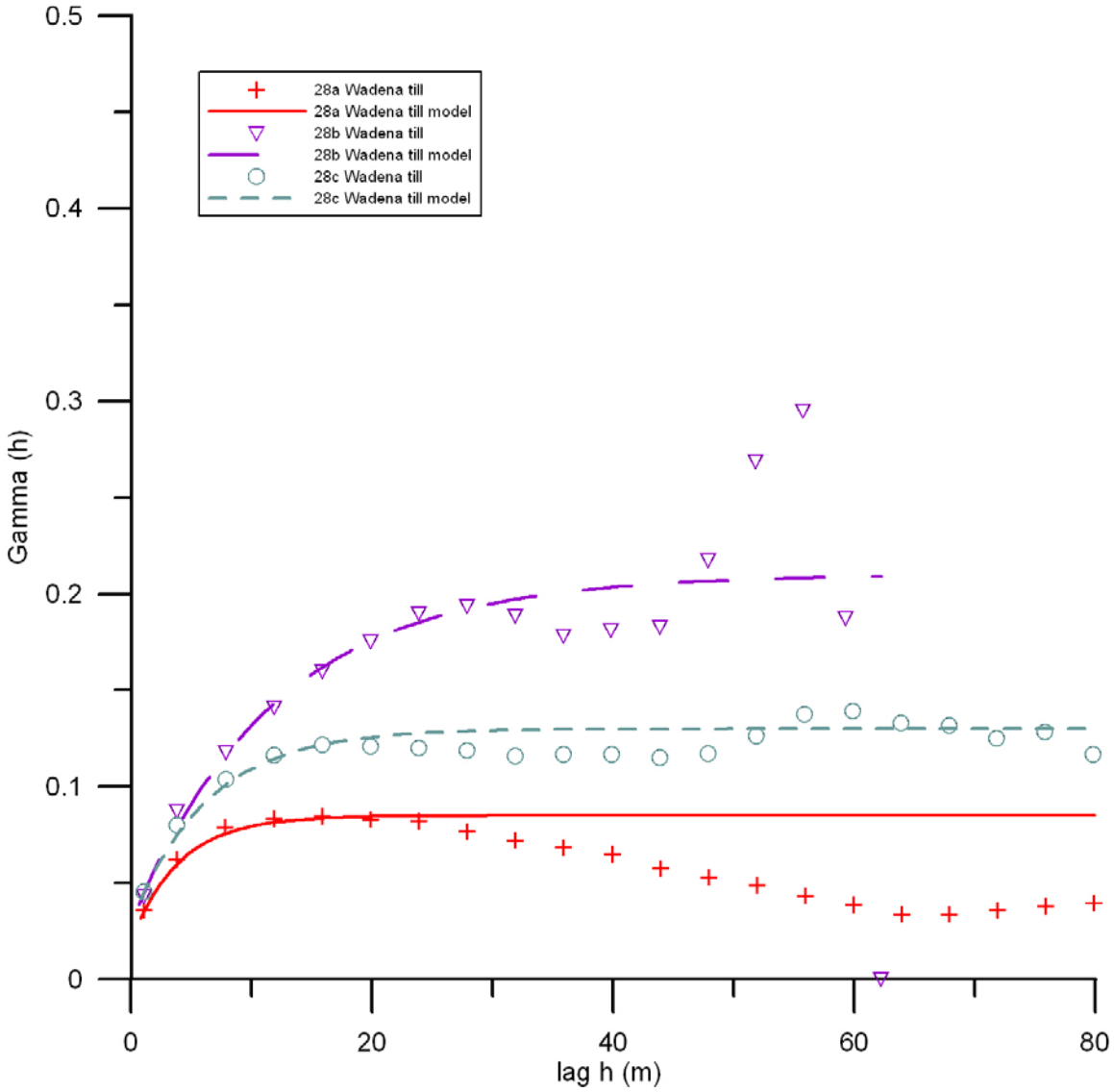

Figure 25. Vertical Variogram Results for Wadena Till Plain Geomorphological Zone, based on Private Well Log Data

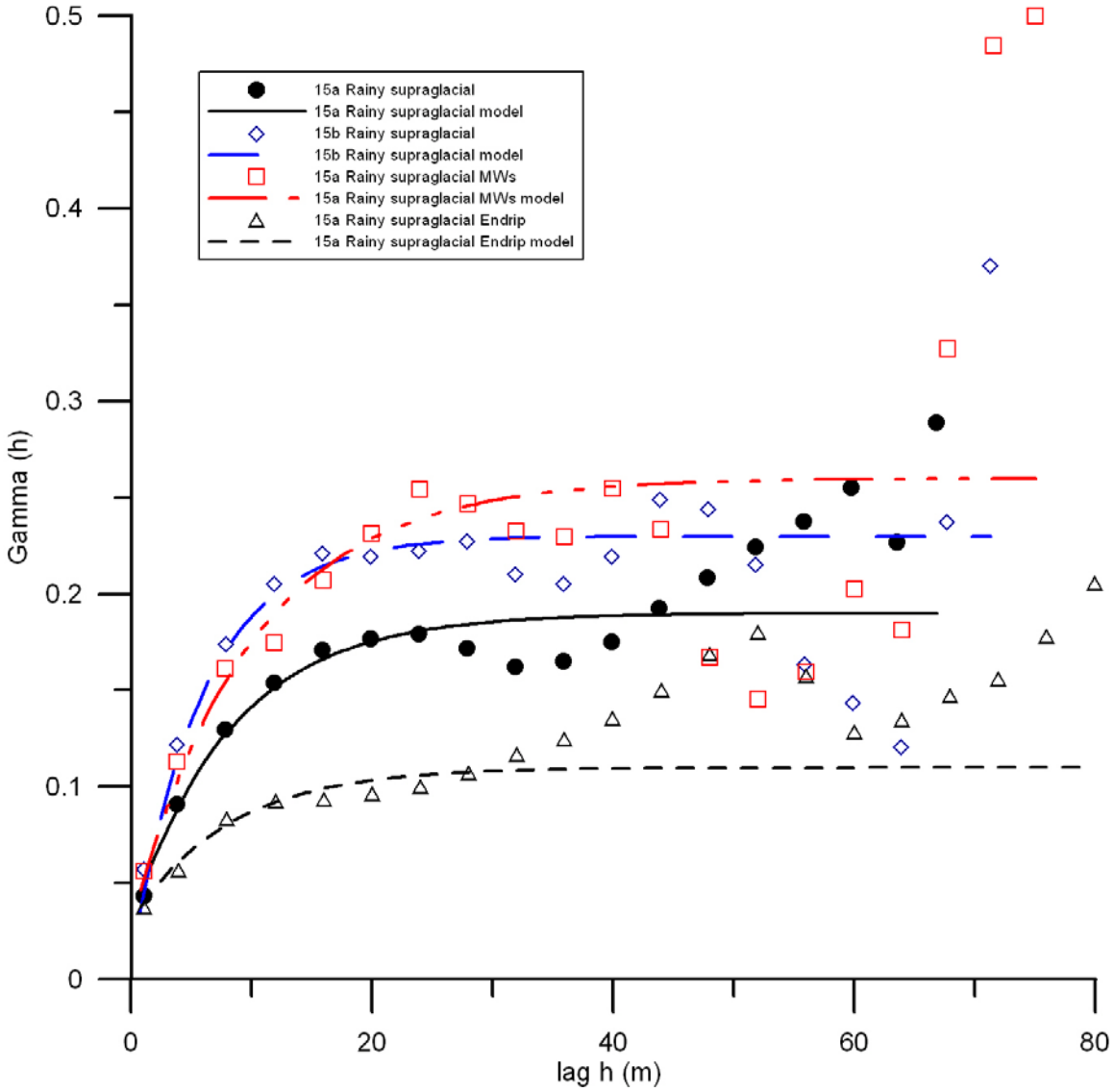

Figure 26. Vertical Variogram Results for Rainy Supraglacial Geomorphological Zone, based on Private Well Log Data, Monitoring Well Data, and Rotosonic Data

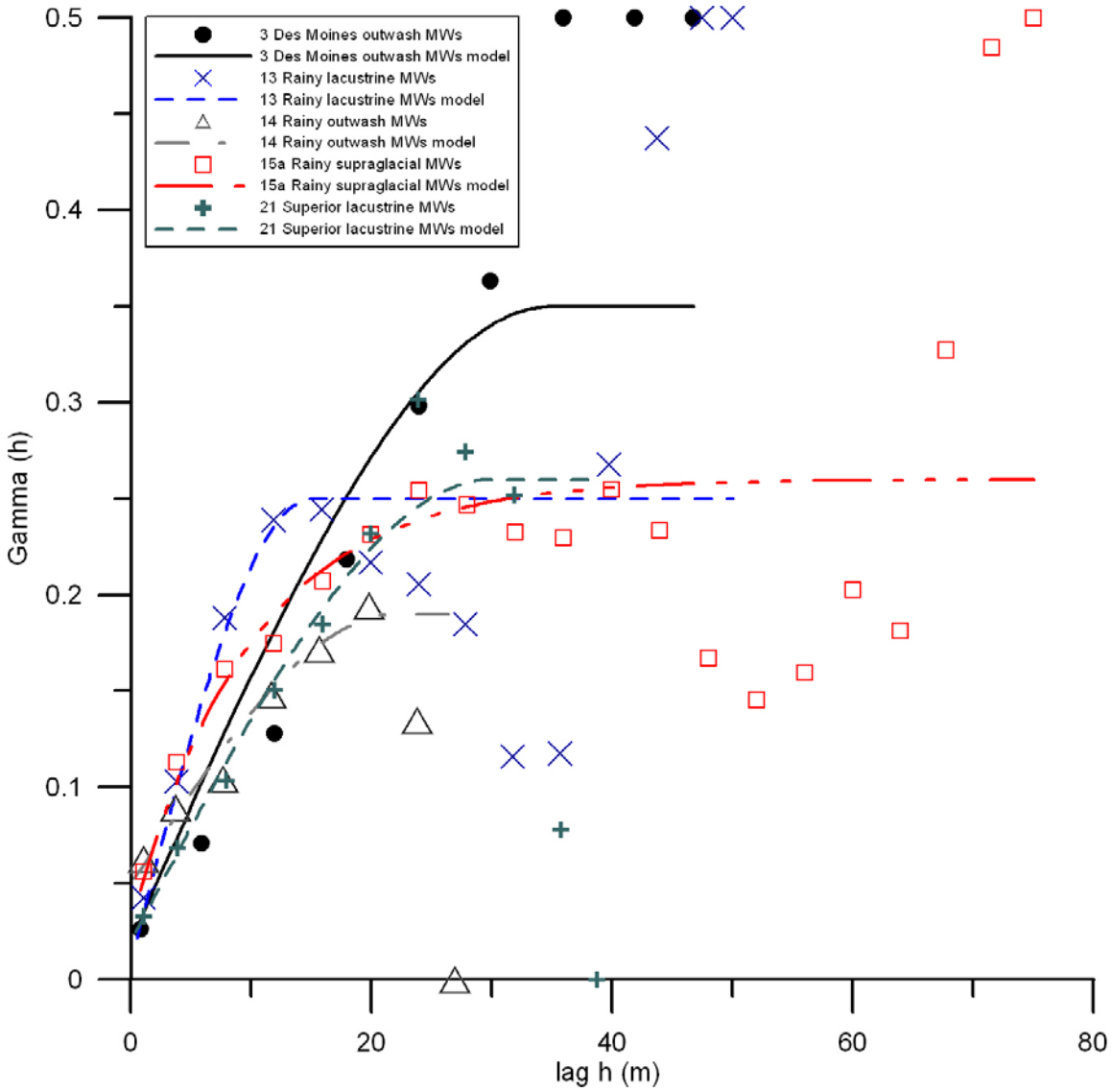

Figure 27. Vertical Variogram Comparison among Data from Monitoring Wells (3 = Des Moines Outwash, 13 = Rainy Lacustrine, 14 = Rainy Outwash, 15 = Rainy Supraglacial, 21 = Superior Lacustrine)

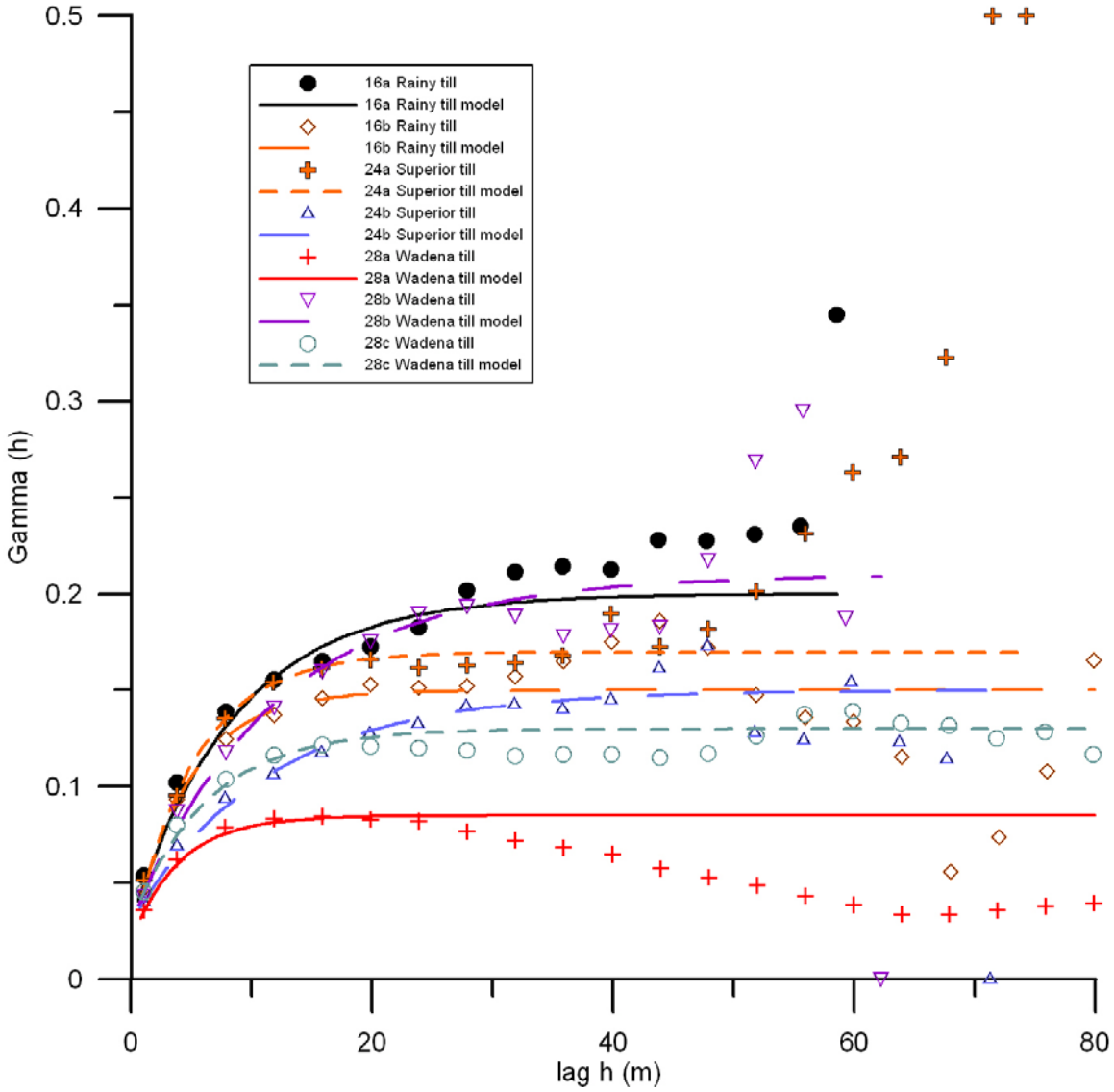

Figure 28. Vertical Variogram Results for Rainy, Superior, and Wadena Till Plain Geomorphological Zone, based on Private Well Log Data

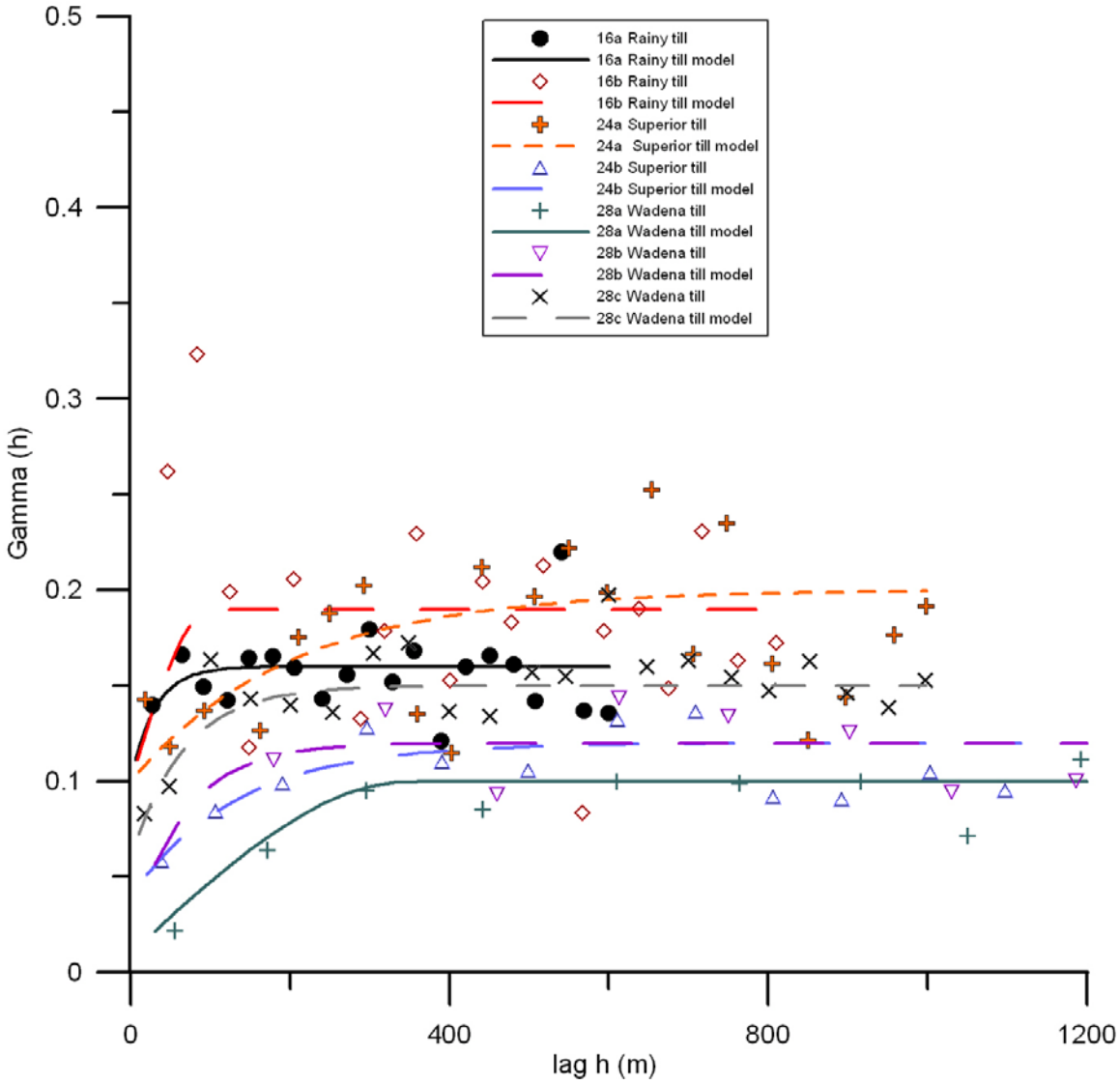

Figure 29. Lateral Variogram Results for Rainy, Superior, and Wadena Till Plain Geomorphological Zone, based on Private Well Log Data

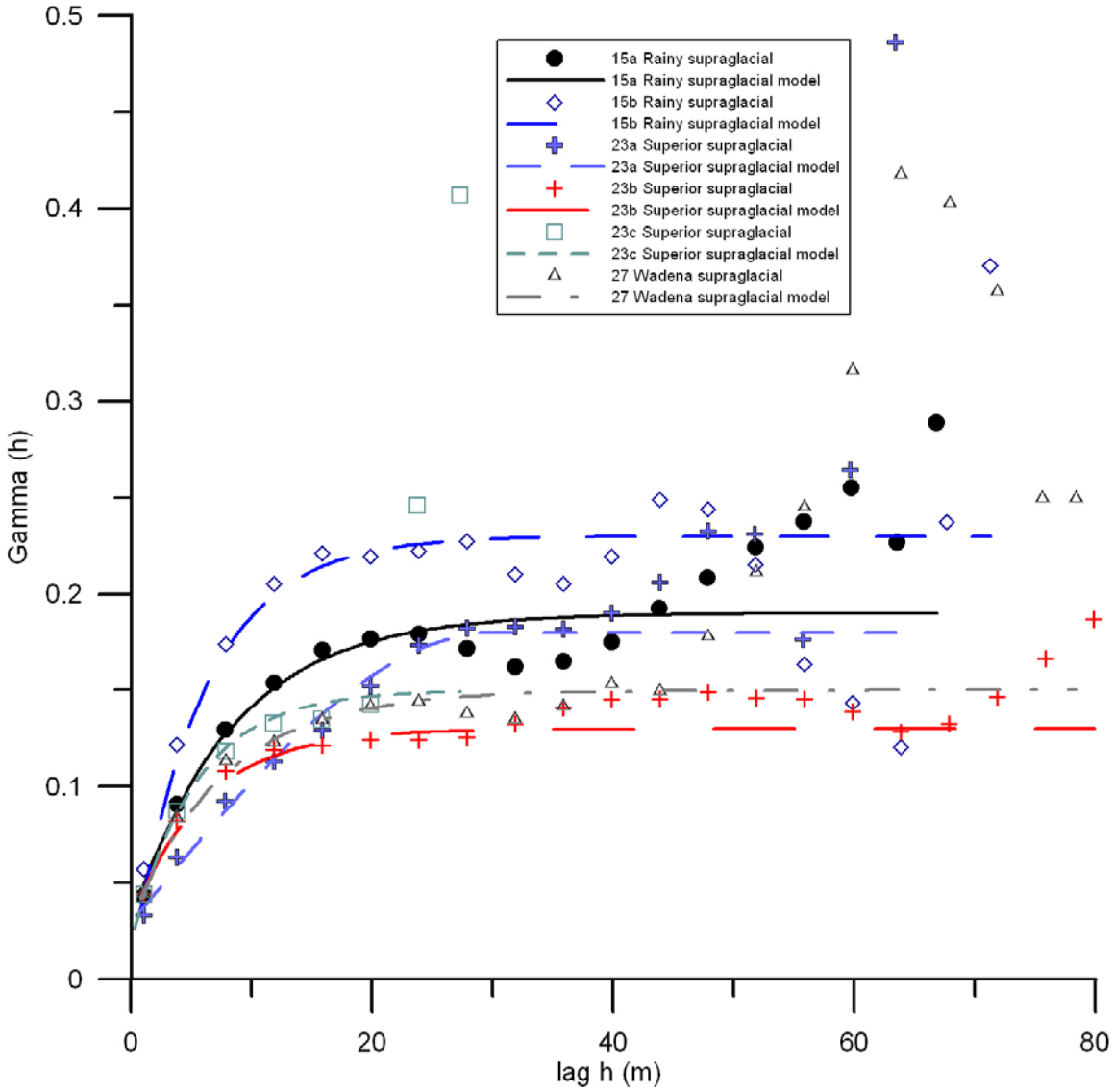

Figure 30. Vertical Variogram Comparison among Data from Supraglacial Geomorphological Zones (15 = Rainy, 23 = Superior, 27 = Wadena) based on Private Well Log Data Only

Although a second range was determined for the lateral variogram of the complete data set, the individual data sets did not show a second range. The strong data support of the complete data set, with countless data pairings across geomorphological boundaries, is believed to be the source for determining its second range.

Three-dimensional subsurface data may exhibit greater correlation along a particular strike and dip. SAGE (Isaaks & Co. 2001) software is designed to calculate 37 directional variograms that simultaneously address various azimuthal and dip directions. Several of the richer data sets were explored using SAGE to determine whether the data showed larger indicator variogram range in a particular direction and/or dip. CWI data and the onsite monitoring well data both showed a lack of structure in directional variograms constructed with a range of search parameters for dip angles, bandwidths, and lags. This is attributed to a lack of data support for directional variograms and/or a lack of anisotropy in the deposits.

Periodicity is exhibited in several of the vertical variograms (e.g. data sets 12, 15a, 15b, 26). Ritzi (2000) determined that as c_v approached unity, periodicity disappeared. The c_v values of the listed cases range from 0.83 to 1.13. Vertical variograms without periodicity (e.g. all data, 16a, 22, 23a, 24a, 24b, 28a, 28b) have c_v values that range from 0.57 to 1.23. This broader range with less periodicity counters Ritzi's findings. An explanation is that Ritzi's synthetic binary datasets tested constant $\overline{L}$ with varying standard deviation and therefore varying c_v, whereas the data sets explored here are not controlled.

The CWI data and monitoring well data sets have similar numbers of binary intervals per borehole. The similarity is due to higher quality data (i.e. more detailed logging) at monitoring wells offset by their relatively shallower drilling depths. EnDriP data were logged with significantly greater detail due to both the rotosonic technology and the scientific purpose of the data collection.

Similar binary mean thicknesses are found in the subdivided zones of Rainy till plains (16a, 16b), the Superior till plains (24a, 24b), and the Wadena till plains (28a, 28b, 28c) (Figure 20). Somewhat different values are found in the subdivided zone of the Rainy lacustrine (13a, 13b), Rainy supraglacial (15a, 15b), and Superior supraglacial (23a, 23b, 23c) settings.

As with the binary T-PROGS analysis, the five material categories have both similarities and differences when comparisons are made among subsets of like geomorphological zone, sets representing a deposit type but ignoring the lobe of origin, and sets developed using different technologies in the same unit (Figure 20).

While Weissmann and Fogg (1999) specifically addressed individual sequences of unconformity-bounded alluvial fan deposits, the current study addresses the entire package of sediments – including any unconformities – in geomorphic terrain zones. Because of the erosional and depositional processes that are so prevalent, especially in a region of multiple ice advances, the focus has been to demonstrate what the data indicate throughout the drift sequence in particular geomorphologic zones or subzones. The numerous unconformities in the subsurface do not bound any volumes of material in the investigation, but rather are factors that affect the statistical results for the entire

subsurface package. T-PROGS was developed for use in alluvial fan settings, where its capability for determining juxtapositional tendencies was important. In glaciated settings, the importance of this aspect of the software is limited because of the underlying processes of glacial deposition and erosion.

Figure 31 highlights the relationship between binary mean thickness and vertical variogram range. For each vertical variogram range, there are two mean thicknesses: one for the low-K material and one for the high-K material. The high-K data, whether low-quality CWI or high-quality monitoring well or rotosonic data, all plot within a band (with one exception, 15a EnDriP, which was an analysis supported by only seven boreholes).

The low-K materials, however, plot in two groups. The low-quality CWI data all have higher mean thicknesses than the high-K data, while the high-quality monitoring well and rotosonic data generally have lower mean thicknesses than the high-K data (two exceptions are 13b MWs and 21 MWs, which are both supported only by small numbers of boreholes and are both in lacustrine settings).

The low-K, high-quality data are assumed to have relatively low mean thicknesses due to careful logging of thin clays that may go undetected or unlogged during private well log drilling.

The high-K data have a best-fit line with a slope similar to that of the low-K, low-quality data, suggesting a consistency in the overall relationship of range to mean thickness.

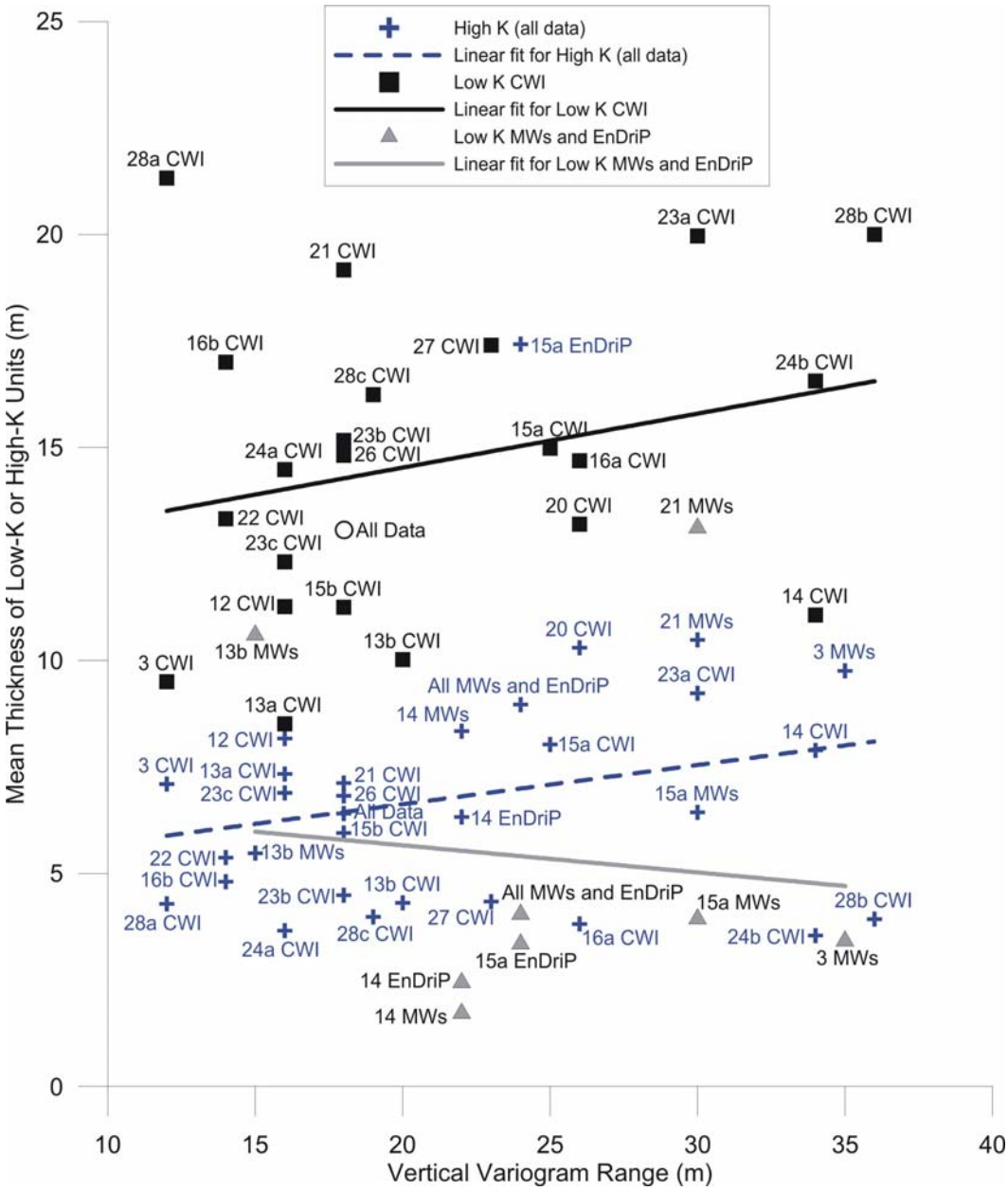

Figure 31. Vertical Range vs. Mean Thickness for All Data Sets

The relationship between vertical and lateral correlation was explored by comparing the values of this ratio for data sets with fair- or good-quality lateral variograms. These data are presented in Table 8. The ratios vary across a large range, but have a mean value of 9.4. The 95% confidence interval is 4.1 assuming a normal distribution, indicating a range of 5.3 to 14.7. An analysis using EPA software ProUCL indicated that the data have a gamma distribution and an upper confidence level of 13.3. Overall, the data suggest that, in the absence of stronger information, the ratio of lateral to vertical structure is on the order of approximately 10. This information can serve in a T-PROGS analysis as a suitable approximation for required lateral Markov chain information.

Table 8. Ratios of Lateral:Vertical Range for Cases of Fair to Good Quality Lateral Variograms

Data Set	Data Type(s)	Geomorph Setting	Number of Boreholes	Vertical Variogram Range (m)	Lateral Variogram Range (m)	Lateral Variogram Quality	Lateral Range / Vertical Range
All data	CWI, MW, rotosonic	all, including minor	11,388	18.0	60	good	3.3
All MWs and EnDriP	MWs and EnDriP	several	219	24.0	120	fair	5.0
3	CWI, MWs, EnDriP	Des Moines outwash	1,420	12.0	200	fair	16.7
3a	CWI, MWs, EnDriP	Des Moines outwash		35.0	200	fair	5.7
13a	CWI	Rainy lacustrine	1,350	16.0	50	fair	3.1
15aCWI	CWI	Rainy supraglacial	388	25.0	50	fair	2.0
15b	CWI	Rainy supraglacial	320	18.0	200	fair	11.1
15a MWs	MWs	Rainy supraglacial	51	30.0	250	fair	8.3
16a	CWI	Rainy till	393	26.0	90	fair	3.5
21	CWI	Superior lacustrine	74	18.0	125	fair	6.9
22	CWI	Superior outwash	470	14.0	20	fair	1.4
23a	CWI	Superior supraglacial	76	30.0	75	fair	2.5
23b	CWI	Superior supraglacial	450	18.0	200	fair	11.1
24a	CWI	Superior till	542	16.0	600	fair	37.5
24b	CWI	Superior till	270	34.0	400	good	11.8
26	CWI	Wadena outwash	292	18.0	150	fair	8.3
27	CWI	Wadena supraglacial	77	23.0	100	good	4.3
28a	CWI	Wadena till	185	12.0	350	good	29.2
28b	CWI	Wadena till	107	36.0	200	fair	5.6
28c	CWI	Wadena till	803	19.0	200	fair	10.5
						Average:	9.4
						Confidence Interval (95%):	4.1

An inspection of the vertical ranges and binary mean thicknesses of the data sets (Figure 20) indicates a mixture of ranges being between the mean thicknesses or being outside the range of mean thicknesses. Proce et al. (2004) found a similar relationship in a buried bedrock valley aquifer.

Stationarity in the various geomorphologically separated data sets can be explored by a variety of statistics. Proportions, mean thicknesses, vertical range, and lateral range all show some degree of variability (Figure 20, Figure 31). However, even within subdivided units of a particular geomorphological zone, differences can be found. In terms of proportions, similar proportions of binary data are observed in the subsets for Rainy supraglacial (15a, 15b), Rainy till plain (16a, 16b), Superior till plain (24a, 24b), and Wadena till plain (28a, 28b, 28c). Different proportions are found in the Rainy lacustrine zones (13a, 13b). The southern Superior supraglacial zone (23b) is different from zones 23a and 23c.

Comparisons of results from different geographically distinct subsets of the same landform sediment assemblage yield mixed findings. Similar vertical ranges and sills are found in Rainy lacustrine zones (13a, 13b). The Rainy supraglacial zones (15a, 15b) have similar range but different sills. Vertical ranges and sills are somewhat different in Rainy till plain zones (16a, 16b) and Superior till plain zones (24a, 24b). Larger differences are apparent in the Superior supraglacial (23a vs. 23b and 23c) and Wadena till plain (28b vs. 28a and 28c) zones.

Among lateral ranges from variograms that are described as “good” or “fair” quality, similar ranges are observed in Superior till plain (24a, 24b) and Wadena till plain

(28a, 28b, 28c). Differences are noted in Rainy supraglacial (15a, 15b) and the two main Superior supraglacial zones (23a, 23b).

In summary, the subdivided till plains show the strongest stationarity in comparisons among their geographically divided zones. The subdivided supraglacial and lacustrine environments show a lack of statistical stationarity.

Incomplete data may bias results (Ritzi and Allen-King 2007, Ramanathan et al. 2008). The nature of drilling data is that the glacial drift units are not fully penetrated, except in the case of a hole that extends to bedrock. The consequence is that the deepest encountered glacial drift material is logged with a thickness less than actual. In the case of water well installation, it is typically a sand (beneath a till) that is targeted by the drilling, and the sand is not necessarily fully penetrated.

Concentrated clusters of data can have an unwanted effect on the statistical or geostatistical assessment of a study area, and declustering methods have been developed to remove this bias. In this study, clustering occurs, however, the clusters are helpful for determining lateral variogram structure. They do not directly assist with lateral transition probability analysis, because there is no actual lateral search.

Clusters of high-quality data illustrate an important aspect of the complexity of glacial facies structure. At Camp Ripley's Landfarm vicinity (Figure 32), located in Rainy Supraglacial terrain, drilling data are relatively dense. Yet, even when simplified into binary categories, they indicate thin layer thicknesses and limited lateral correlation. While this study is geared toward an understanding of bulk statistical properties in

various landforms, it is clear that site-specific data are needed for site-specific assessment (e.g. for localized groundwater contamination investigations).

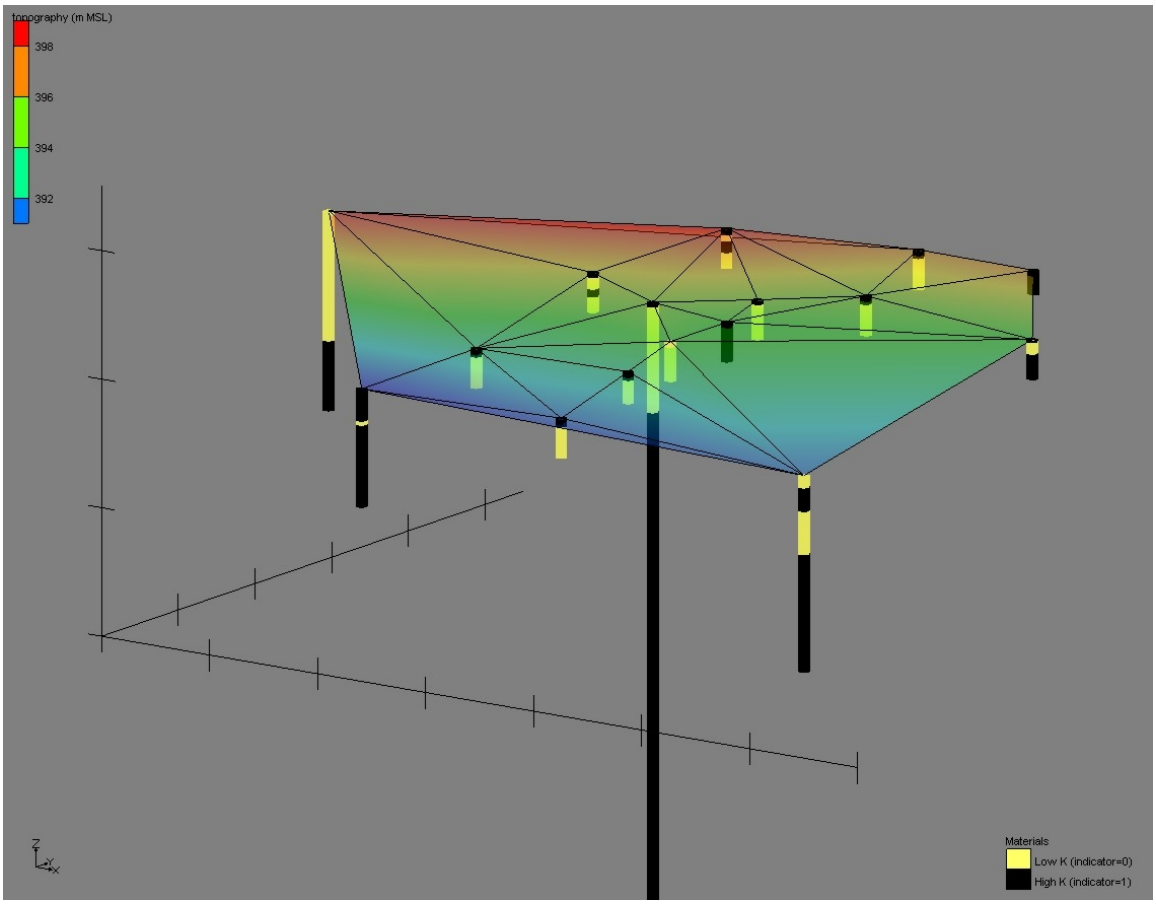

Figure 32. Oblique View of Binary Data in Camp Ripley Landfarm Vicinity (V.E.=10x. Lateral tick spacing 100 m; Vertical tick spacing 10 m)

The degree of logged stratigraphy in each tested zone varied (Table 3), but averaged about 50%. This suggests that a significant portion of the upper drift went into the geostatistical calculations. So, while the "cookie cutter" approach to grouping the

drilling data into sets based on surficial geomorphology is not expected to be perfect, it does address, on average, the upper half of the drift.

Conclusions

Variogram analysis in the case of each data set showed that the glacial drift has clear, measurable correlation in the vertical direction, as each vertical variogram showed very well-supported structure.

The rationale for subdividing the overall data set into data sets of specific ice lobe and depositional setting was to search for consistency in correlation structure of like settings, so that results of this study could have applications in areas of sparser data. The benefit would be in the design of sampling strategies for water resources evaluations at a larger scale and for groundwater contaminant fate and transport studies at a finer scale. Comparison of the various vertical variograms in this study demonstrated that, generally, data sets differed in their vertical range and/or sill even if they represented subdivisions of the same overall lobe and sediment type. Notable exceptions were in Rainy lacustrine areas 13a/13b/13MWs), and in some cases of like sediment types in different lobe settings (e.g. Rainy and Superior lacustrine, and Superior and Wadena outwash). This lack of stationarity is attributed to the fundamental complexity of the glacial drift in the study area, resulting from different depositional processes in different locales. It is expected that the complexities of glacial deposition would yield different statistical results at finer and finer scales and at different locations due to site-specific factors.

Overall, the degree of variability among different analyzed data sets suggests overlapping geostatistical parameter values (Figure 20), with generally as much variability within subdivided zones of a given landform assemblage as between different landform assemblages. Geographically subdivided areas suggest that stationarity is not present in the broad data sets, and may be limited at more local scales. It should be noted that at smaller scales, this complexity becomes more apparent (e.g. Figure 32). Site-specific factors in glacial depositional processes are therefore expected to cause deviation from the statistical properties of the collective CWI data located in the same landform assemblage. Vertical variogram comparisons would be expected to demonstrate monitoring well and rotosonic data having similar or shorter ranges than the corresponding CWI data in the same geomorphological zone. The rationale is that careful logging during the drilling and sampling process would capture thin units and result in shorter calculated range. In some cases, this proved to be true (Rainy lacustrine 13b MWs and 13b CWI, Rainy outwash 14 EnDriP and 14 CWI, Rainy supraglacial 15a EnDriP and 15a CWI, Rainy supraglacial 15a MWs and 15a CWI). However, in other cases, the CWI data had a larger range than the more detailed data (Des Moines outwash 3 MW and 3 CWI, Rainy supraglacial 15a MWs and 15a CWI, Superior lacustrine 21 MWs and 21 CWI). These unexpected cases are attributed to localized geologic factors.

Lateral variogram comparisons among different data sets were generally not feasible, because too many data sets had poor-quality lateral variograms or no apparent structure.

The lateral variogram search parameters allowed a reasonable approach to assessing the lateral structure. However, glacial depositional processes are complicated and involve complex geometries. For example, a till deposit may blanket an irregular underlying material, and its upper surface may vary also, due to factors at the time of deposition or to post-depositional processes. A lacustrine deposit may fill in the depressions in an undulating bottom of a basin, and its horizontal upper surface may be modified by later erosion. So, while the lateral variogram search parameters provide a means of estimating lateral structure, they do not fully access units with irregular geometry. Still, enough lateral variograms were generated of fair to good quality to determine a relationship between the lateral and vertical range of individual data sets, suggesting a ratio of about 10. This ratio provides a means of estimating the ratio between mean lens thicknesses and mean lens lengths in T-PROGS analyses.

Geographically subdivided till plains show strong statistical stationarity (except in vertical sill), but subdivided supraglacial or lacustrine settings do not. This suggests that the processes responsible for broad till plains associated with a particular ice lobe are fairly uniform in terms of the hydrostratigraphic framework they create. Supraglacial environments, by nature, are more complex and localized than the subglacial depositional setting generally responsible for the till plains.

The three main till plains have nearly uniform proportions of low-K and high-K materials. The vertical ranges of their subareas cover an overlapping range of values. Yet the Rainy till has a much smaller lateral range compared to the Wadena and especially the Superior till plains. Their mean thicknesses of high-K materials are all on

the order of 4 m. In terms of mean thicknesses of low-K materials, the Rainy and Superior till plains subzones are in the range of 14 to 17 m, but the Wadena is 16 to 21 m. The implication is that the Wadena deposited more massive fine-grained units than the other two lobes, which have more interbedded sandy materials. This is consistent with Goldstein (1989) and Mooers (1988).

Several comments may be made regarding the usefulness of each of the tested geostatistical methods. Variography is better for identifying complex structure, such as multiple ranges, if present, in data. This information can be related to depositional processes that created the hydrostratigraphic framework. In the current study, a second range was observed in the complete data set, but not in smaller data sets, even those with relatively abundant data. This may be attributed to enough data pairs that were comprised of material in the variogram calculation in adjacent geomorphological zones. These pairs, and the second range, represent aspects of the bulk glacial drift that is not observed in the subsets of data. Lateral variography, however, depends on data of suitably close spacing. Given proper data density, variography can potentially indicate not only the lateral correlation structure, but also possible anisotropic directional structure areally or in full 3D.

The T-PROGS analysis does not give information ranges. T-PROGS is not used to model lateral correlation directly but must rely on indirect information or assumptions (e.g. Weissmann et al. 1999).

Numerous, low-quality drilling data associated with water well logs (the CWI data) give information on major lithofacies, at least ideally. This sort of data may be

useful for large-scale water resources studies. Monitoring wells, with continuous split-spoon sampling, and rotosonic drilling and sampling technology provide far more detail on smaller facies. This higher resolution data is more appropriate for local studies of groundwater movement and contaminant transport.

Uncertainty in subsurface interpolation is due to a combination of factors, including the areal distribution of data locations, the depth of the drilling data (degree of penetration of subsurface units of interest), the completeness and accuracy of drilling logs (which is dependent on the drilling and sampling method), interpretation of the data, and the fundamental complexity of the subsurface material geometry. The 3-D mapping or interpolation that is performed on a data set is affected by these sources of uncertainty. Kriging can provide a measure of the uncertainty distribution, indicating zones of relatively high or low uncertainty in the estimate. Simulation using transition probabilities allows a stochastic interpretation of the subsurface as a means of addressing uncertainty.

GEOSTATISTICAL APPROACHES TO GROUNDWATER MODELING IN GLACIAL DRIFT

Approach

Groundwater modeling in glaciogenic terrain is problematic because of the distribution of material types resulting from glacial depositional and erosional processes. These materials have widely varying hydraulic conductivity values and complicated geometries. Thin units of limited lateral extent may exert an important influence on groundwater flow, which, dependent on scale, may be relevant to water resources analysis or contaminant transport studies.

In this study, the results of geostatistical modeling for the multi-county study area are applied to a numerical model focused on Camp Ripley. Recharge distribution is based on prior studies, while hydraulic conductivity is varied according to indicator kriging or transition probability geostatistics results. A set of water levels at monitoring wells serves as calibration targets and as a means of comparing the efficacy of the methods to modeling the subsurface.

Study Area

Location

The study area for the groundwater modeling analysis is comprised of Camp Ripley and associated areas west and south of the property (Figure 33). Together, this 460 km^2 region has been determined to have a suitable western no-flow boundary, as discussed below.

Surface Water

The modeling area is bounded on the east by the Mississippi River and on the north by the Crow Wing River (Figure 33). The Crow Wing has two dams: the Sylvan dam along the northeastern site boundary and the Pillager dam approximately 12 km upstream of the Sylvan dam. The Little Elk River is along the southwest edge of the study area and is a tributary to the Mississippi. Within and outside the site boundaries are numerous lakes and large wetlands in low areas near the rivers and elsewhere. Drainages from the Camp Ripley are minimal; only a few small creeks leave the site and are tributaries to the Mississippi, Crow Wing, or Little Elk Rivers.

The water levels of several lakes close to the Camp Ripley site boundary are monitored frequently by the Minnesota Department of Natural Resources (MDNR 2006). Long-term data from six of these lakes suggest that water levels generally fluctuate by much less than 1 m (Figure 34).

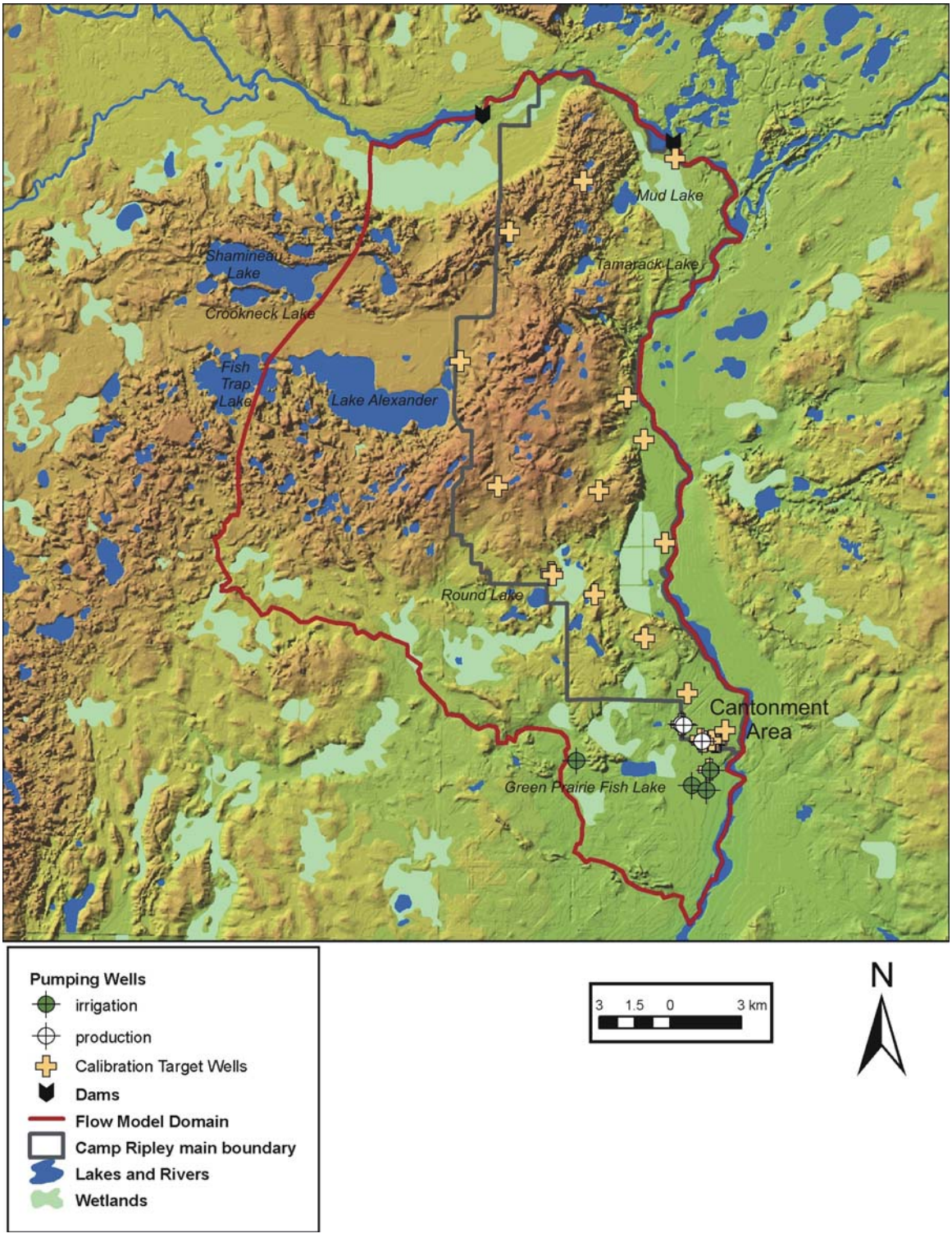

Figure 33. Hydrologic Features in the Flow Modeling Domain

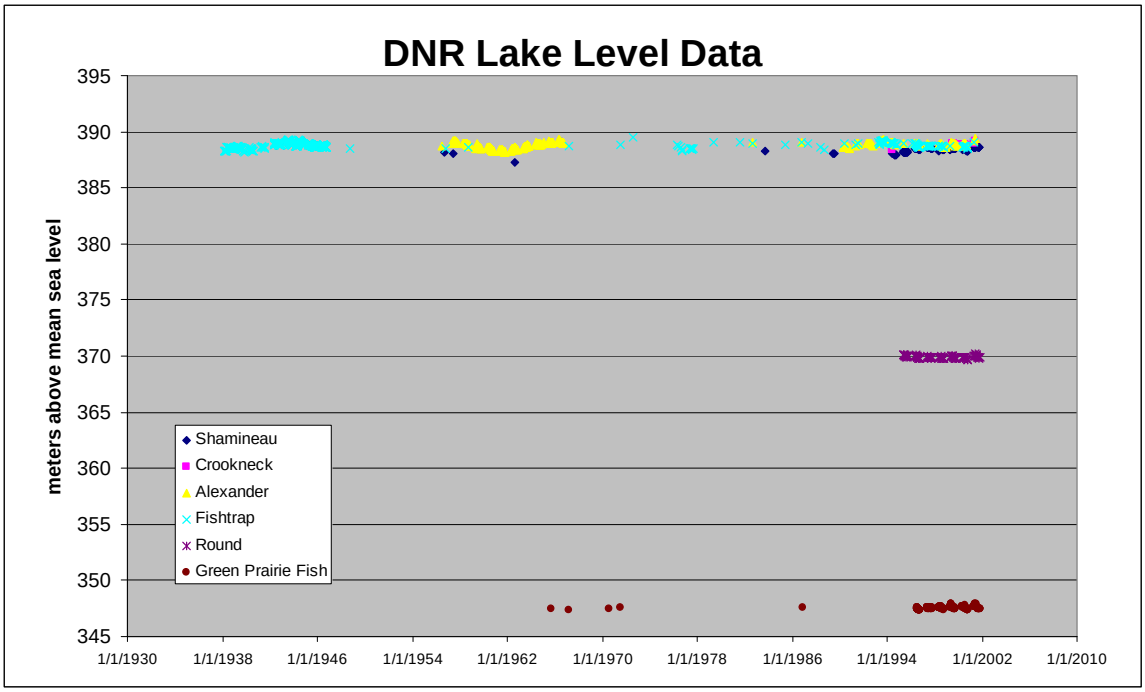

Figure 34. Water Levels at Six Lakes near Camp Ripley (data from MDNR 2006)

Aquifer Recharge

Recharge to an aquifer can be a difficult parameter to measure and is often estimated regionally by relying on numerical model calibration.

St. George (1994) used a detailed groundwater model to study an area that includes the Itasca moraine to the northwest of Camp Ripley. Because the climate of that study area is similar to the climate of Camp Ripley and because that area has similar glacial geologic materials, St. George's estimates of recharge are relevant to the Camp Ripley model. St. George delineated recharge zones on the basis of geomorphological map units. Mooers (1996) (see University of Minnesota-Duluth Department of

Geological Sciences 1997) provides mapping of the geomorphological units in the Camp Ripley region (Figure 35). These units were grouped into six categories (Table 9), which were then compared to relevant units in St. George's study (Table 10). For two of the categories, an adequate match in St. George's units was not available, so estimates were made for the recharge values.

Lindgren (2002) modeled groundwater in a broad study area northwest of the Camp Ripley vicinity. He compiled available estimates of recharge to the surficial aquifer based on hydrograph analyses and to confined aquifers as leakage through till calculated by Darcy's Law or through groundwater modeling analysis. His calibrated model results were 18 to 25 cm/yr (5e-4 to 7e-4 m/d) of recharge to the surficial aquifer and typically 2.3 cm/yr as leakage through surficial till.

At least in the case of the sandy outwash plain, the estimate in Table 10 compares closely to the value in a similar setting in Minnesota found by using a hydrographic method (Helgesen and Lindholm 1977).

Table 9. Mapping Units of Mooers (1996) in the Camp Ripley Study Area

Grouping in GMS	Code	Geomorphic Association	Glacial Phase	Topographic Expression	Sedimentary Association
A	RSt3S	Rainy lobe	St. Croix	Hummocky	Supraglacial drift complex
B	RSt3O	Rainy lobe	St. Croix	Hummocky	Outwash
C	RSt1O	Rainy lobe	St. Croix	Level	Outwash
C	RSt1Och	Rainy lobe	St. Croix	Level	Outwash
B	RSt3I	Rainy lobe	St. Croix	Hummocky	Ice contact
D	RSt1L	Rainy lobe	St. Croix	Level	Lacustrine
A	SSt3S	Superior lobe	St. Croix	Hummocky	Supraglacial drift complex
E	SSt1Lsw	Superior lobe	St. Croix	Level	Lacustrine
F	OHo1P	Organic deposits	Holocene	Level	Peat
C	DBe1O	Des Moines lobe	Bemis	Level	Outwash
G	WHe2T	Wadena lobe	Hewitt	Rolling to undulating	Till plain
C	RSt3Och	Rainy lobe	St. Croix	Hummocky	Outwash
G	SSt2T	Superior lobe	St. Croix	Rolling to undulating	Till plain
C	F_1A	Fluvial		Level	Alluvium

Table 10. Calibrated Recharge Values of St. George (1994) for Units Relevant to Camp Ripley and Estimated Recharge Values

Grouping in GMS	St. George's (1994) Landforms	Sediment Classification	Calibrated Recharge (cm/yr)	Calibrated Recharge (m/d)
B	Collapsed outwash	Loamy sand	7.6	2.08E-04
G	Till plain (Wadena)	Sandy loam	0.15	4.11E-06
C	Outwash fan	Sand	15.2	4.16E-04
A	Outwash plain	Sand	21.3	5.84E-04
	Other materials:			Estimated Recharge (m/d)
D, E	Fine lacustrine			1.00E-04
F	Peat			1.00E-04

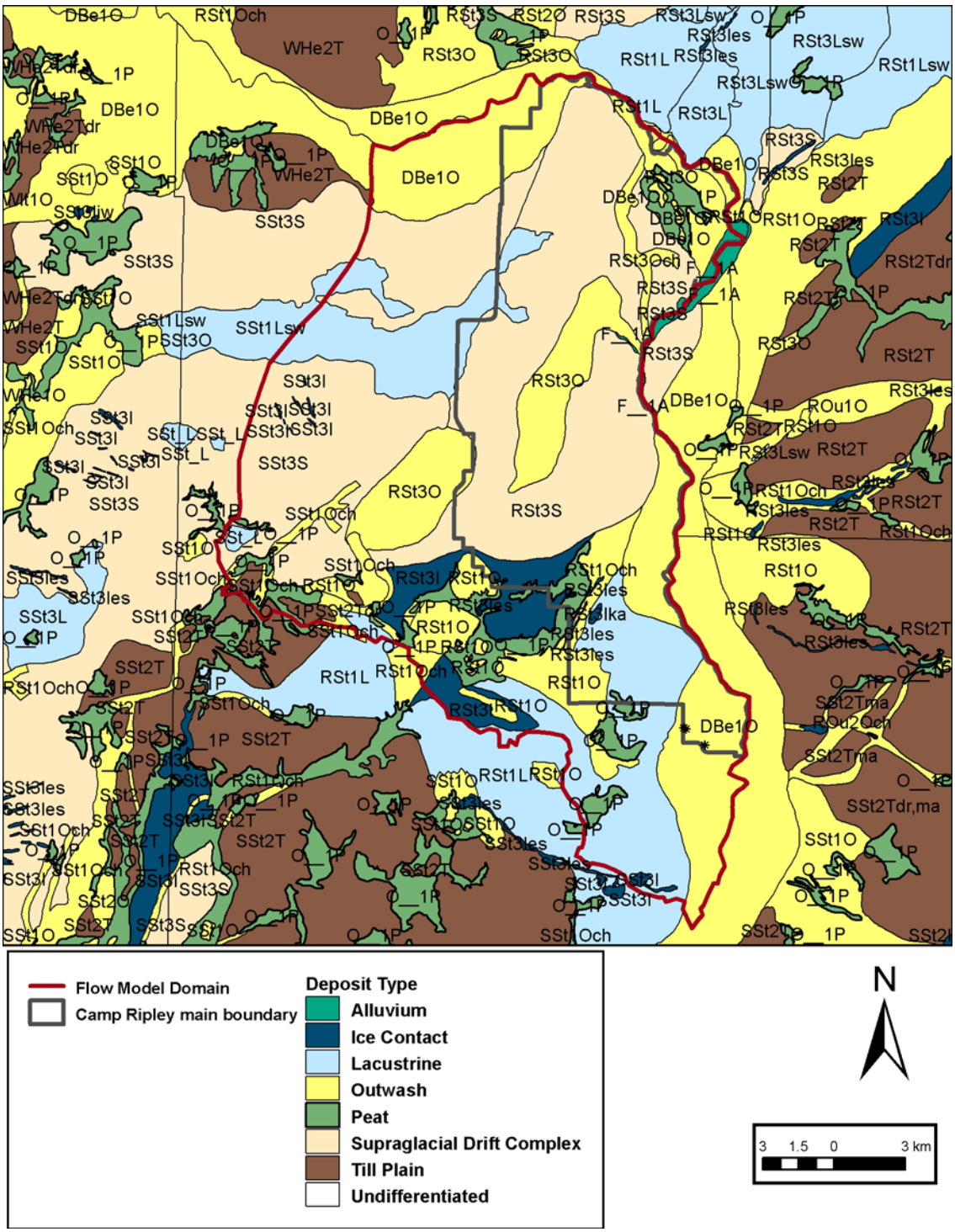

Figure 35. Geomorphological Zones used as Recharge Zones

Hydraulic Conductivity

Hydraulic conductivity (K) can be estimated in a variety of ways. One method is to use grain size analyses, in which geologic samples are separated according to the amounts retained on standard screen openings of various sizes. Then information from plots of the grain size distribution is used with empirical formulas to estimate K. UMD staff performed grain size analyses for a variety of geologic samples obtained during the EnDriP project (UMD Department of Geological Sciences 2002) (Table 11). These samples provide information for essentially all major materials present in the Camp Ripley subsurface. The results are similar to expected values in standard texts (e.g., Freeze and Cherry 1979) and compare well to similar units determined by St. George (1994) through model calibration in a similar study area. Lindgren (2002) reviewed many sources of information regarding hydraulic conductivity in materials in the vicinity of a nearby flow modeling area with Wadena lobe sediments at the surface. Through model calibration, he arrived at horizontal hydraulic conductivity with a range of 1.5 to 107 m/d for surficial and confined aquifer materials and 0.3 to 61 m/d for till confining units. Vertical hydraulic conductivity was generally 1/10 that of the horizontal value for the aquifers and 8e-4 to 8e-2 m/d for most confining units. Person et al. (2007), in another model of an area northwest of the current study, arrived at calibrated values of 3 m/d for moraines, 6 m/d for stagnation moraine, 10 m/d for ground moraine, and 61 m/d for outwash.

Table 11. Geometric Mean Hydraulic Conductivities from UMD Grain Size Analyses

	Geometric Mean K (m/d)				
Unit	Hazen	Krumbein and Monk	Puckett	Harleman	Geometric Mean (All Methods) (m/d)
Dense clay loam till	1.06E-03	7.34E-01	8.63E-03	1.13E-01	2.96E-02
Lacustrine clay	1.13E-03	1.60E-01	1.35E-01	1.20E-01	4.13E-02
Red sandy till	8.14E-03	3.97E+01	8.25E-01	8.69E-01	6.94E-01
Lacustrine silt	1.69E-02	8.19E-01	1.13E+00	1.80E+00	4.09E-01
Red/brown sandy loam till	2.40E-02	2.78E+01	1.12E+00	2.38E+00	1.16E+00
Silty fine sand	3.26E-02	6.17E+00	1.11E+00	3.15E+00	9.16E-01
Saprolith	6.06E-02	1.44E+01	2.60E+00	6.47E+00	1.96E+00
Fine sand	3.60E-01	9.32E+00	2.40E+00	2.80E+01	3.87E+00
Medium sand	3.72E+00	4.77E+01	2.55E+00	3.08E+02	1.93E+01
Coarse sand/gravel	5.15E+01	2.50E+02	2.76E+00	3.02E+03	1.02E+02

Source: unpublished UMD data.

Pumping Stresses

Pumping stresses in the modeling domain include the active wells H, L, and N, which are located in the Cantonment Area at the south end of Camp Ripley and several irrigation wells (Figure 33). The effect of scattered private wells is assumed to be negligible, and they were not included in the model.

The MDNR requires water appropriation permits for groundwater or surface water withdrawals of more than 10,000 gal/d or 1 million gal/yr. Through the permitting process, long-term pumping rate information is available for the on-site production wells and the wells that they have replaced (1988–2002 from MDNR appropriation permits and

2001–2004 from unpublished Camp Ripley data). These values are summarized in Table 12. Irrigation wells (unique numbers 214597, 214434, 214433, and 121834), which are located south and west of the Cantonment Area, are also included in the model, with pumping rates based on average withdrawal rates over 1988–2002. This information is also included in Table 4. On the basis of the MDNR appropriation database, no other large groundwater users are in the modeling domain.

Table 12. Pumping in the Study Area

Unique Number or Name	Type	Ground Elevation (m)	Well Depth (m)	Historical Average Pumping Rate (10^6 gal/yr)	Peak-Year Pumping Rate (10^6 gal/yr)	Historical Average Pumping Rate (m^3/d)	Peak-Year Pumping Rate (m^3/d)
H	Production	348.54	18.6	27.6	42.9	285.9	444.4
L	Production	348.54	29.9	20.9	34.9	216.5	361.6
N	Production	348.54	31.1	24.3	30	251.7	310.8
121834	Irrigation	350.5	19.5	16.7	16.7	173	173
214597	Irrigation	344.4	21.6	37.7	77.4	390.6	801.9
214433	Irrigation	344.4	18	57.8	44.1	598.8	456.9
214434	Irrigation	344.4	16.5	37.8	27.2	391.6	281.8

Groundwater Levels

UMD staff collected hand measurements of water levels at numerous wells, and they collected continuous (at 30-min intervals) automated measurements of groundwater levels at four wells. The data show that long-term fluctuations at the wells are generally within a range of only 0.3 m. This suggests that water level measurements across the site

and region are useful in calibrating a regional-scale steady-state model. Average continuous data values were therefore combined with average monitoring well hand measurements and static water level information to create a set of target water levels for calibration of the model (Table 13). The wells listed in Table 13 are those that represent the regional flow system, as indicated by inspections of data on well screen location and water levels. Wells determined to be finished in perched zones were not included as calibration points.

Table 13. Calibration Targets for Relevant Monitoring Wells

Well ID	Easting (m)	Northing (m)	Target Head (m)
534167	395713.1	5103620.3	345.40
534166	395674.8	5103571.0	345.43
534080	395606.4	5103592.0	344.97
534078	395621.3	5103629.0	345.31
530010	395516.4	5103646.8	345.95
530009	395483.3	5103650.6	346.01
523491	396036.0	5104078.4	341.38
495630	386414.9	5114383.3	383.13
470668	394207.9	5104332.4	342.47
470506	390511.6	5109814.5	367.89
466292	394448.2	5105660.8	344.36
466289	388661.0	5110757.8	364.69
466286	388659.7	5110652.2	367.13
451233	390700.7	5114207.2	367.28
451232	392631.7	5107977.1	351.74
451231	393496.0	5112003.4	345.95
451230	393933.1	5128276.4	356.62
451229	386919.5	5125175.3	373.08
224577	395075.5	5103609.4	343.81
214597	395363.3	5102427.1	340.77
150536	395131.6	5103608.2	345.34
150535	394988.1	5103728.7	343.20
671611	390044.3	5127315.1	369.42
671608	392609.4	5116367.9	351.74
578602	384820.6	5119692.9	381.61
536841	391907.9	5118146.1	359.97
466287	388726.6	5110647.0	367.28

Methodology

Numerical Flow Model

Conceptual Flow Model

Before a numerical groundwater flow model is constructed, it is important to describe a conceptual model of the site's groundwater flow system. For Camp Ripley and nearby areas to the west and southwest, precipitation (as rainfall or snowmelt) infiltrates and becomes aquifer recharge. It is assumed that only a small amount of water runs off, on the basis of the fact that only a few very minor creeks are in the entire study area. This internal drainage is also demonstrated by closed topographic depressions that are dry in the bottom (e.g., along Easy Street in northern Camp Ripley), and it is consistent with predominantly sandy soil and subsoil.

Lakes are assumed to be either flow-through lakes, representing the groundwater flow system, or perched features. Although perched groundwater may be present locally as the result of a low-permeability lacustrine clay or fine-grained till, the main groundwater flow system is assumed to be part of the regional flow system, discharging directly to the main nearby rivers (Mississippi, Crow Wing, Little Elk), to wetlands, or to pumping wells.

Flow in the subsurface is complicated by countless irregular contacts between different types of glacial depositional units with widely different permeability. The uncertainty in subsurface correlation is apparent even at the scale of the Landfarm Spread

Site, an area of relatively dense data in the southwest part of Camp Ripley. Here, boreholes 50 to 100 m apart show little apparent correlation in their stratigraphic contacts because the subsurface changes occur at a scale finer than the borehole spacing.

Model Selection

The U.S. Geological Survey's MODFLOW 2000 code (Harbaugh et al. 2000) was selected to model groundwater flow. MODFLOW is the world's standard for modeling groundwater flow through porous media, in part because of its documentation, verification, and adaptability. MODFLOW can handle a variety of hydrologic and geologic inputs. It is a finite-difference model, relying on a three-dimensional (3D) grid for the solution space. MODFLOW 2000 includes parameter estimation capabilities (Hill et al. 2000), which provide a means of optimal estimation of model inputs based on nonlinear regression techniques.

The Groundwater Modeling System (GMS) (EMRL 2005) is a preprocessor and postprocessor for MODFLOW and other codes, and it includes related tools for subsurface analysis. GMS allows the modeler to work from map information to design a grid that matches the study area's hydraulic boundaries. Many forms of model input may be imported in spreadsheet form, facilitating accurate model setup. GMS also has the option of using geostatistics and transition probability geostatistics (TPROGS) to populate the subsurface permeability framework of its MODFLOW models.

Grid Design and Boundary Conditions

The extent of a modeling domain is determined by evaluating a study area's hydrologic and geologic factors for their potential as natural boundaries to groundwater flow. Examples are specified head boundaries, such as those along rivers in direct connection with the groundwater flow system, or no-flow boundaries, such as known or assumed divides in the groundwater flow system.

Much of Camp Ripley is bounded by the Mississippi and Crow Wing Rivers (Figure 33). By inspecting water level data for wells across the region to the west of Camp Ripley, the location of a mainly north-to-south trending flow divide was estimated. This divide extends from the Crow Wing River on the north to the Little Elk River to the south and is assumed to coincide with streamlines trending north and south form the Lake Alexander vicinity. The no-flow boundary is between two large lakes, Lake Alexander and Fishtrap Lake. Fishtrap Lake is connected to Lake Alexander. The channel, however, rarely has much flow because the water elevations of the two lakes are nearly equal (Minnesota Pollution Control Agency 1999). Because of the regional groundwater flowfield and the low surface water gradient between these lakes, the no-flow boundary condition is supported for the western edge of the modeling domain (Figure 36).

The model grid was constructed with uniform 200-m cells (Figure 37). The bottom of the modeling domain is the saprolith (weathered bedrock) surface (Figure 40). The upper boundary of the model is the ground surface. Digital Elevation Model (DEM) data at 60-m spacing were obtained for the region. This data set provides strong control of the upper surface of the glacial drift sequence (Figure 41). Although the locations of

the DEM grid nodes do not exactly match the locations of model cell centers, the DEM data were interpolated to the cells by GMS, and they provide a highly accurate upper surface elevation for the geologic package. An inspection of cell elevations along the major rivers showed that the river stage was accurately incorporated into the model by relying on the DEM data at 60-m spacing. These cells along the Mississippi, Crow Wing, and Little Elk Rivers were each fixed as specified heads. A side view and an oblique view of the grid are shown in Figure 38 and Figure 39, respectively.

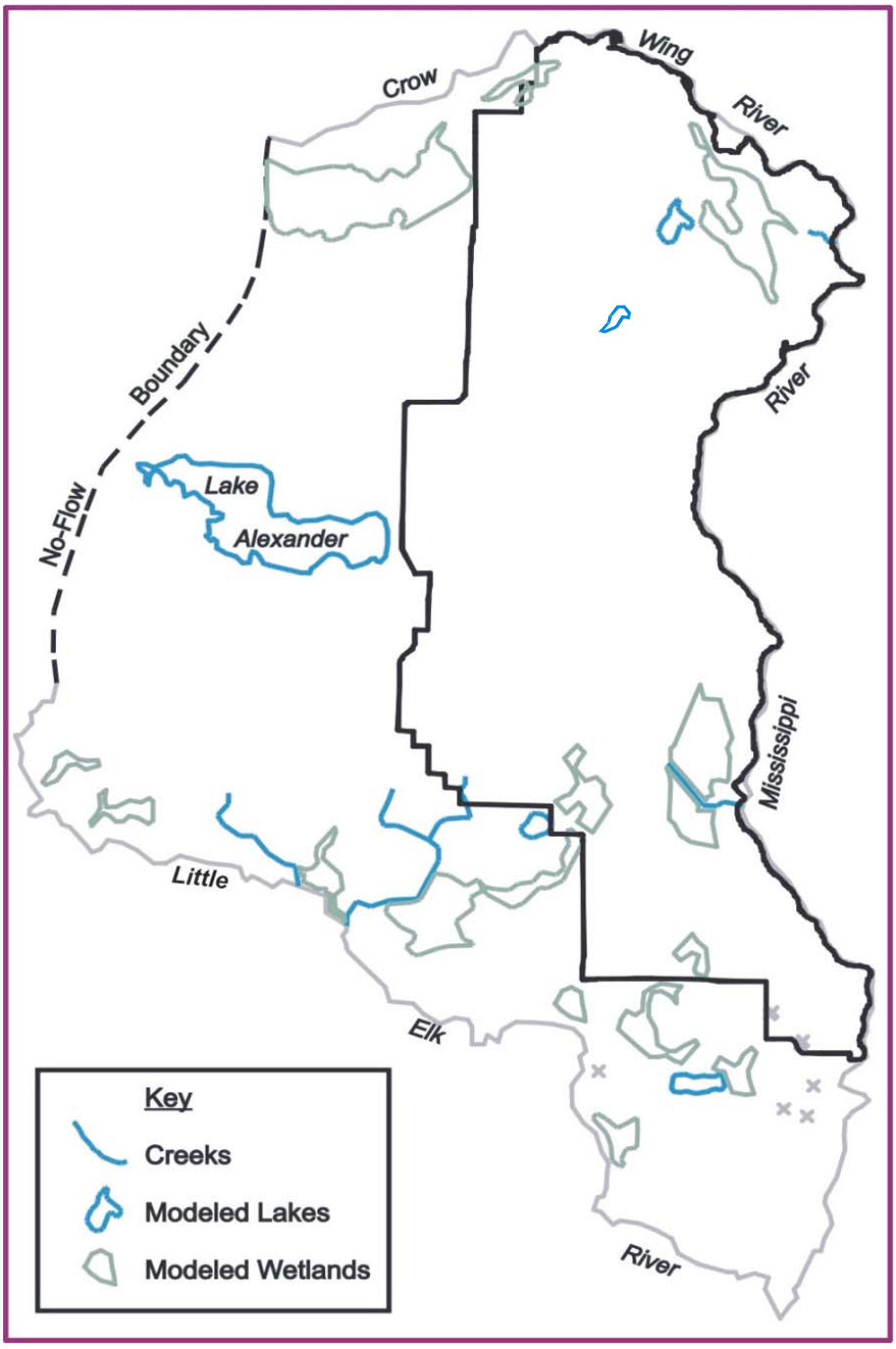

Figure 36. External and Internal Boundary Conditions

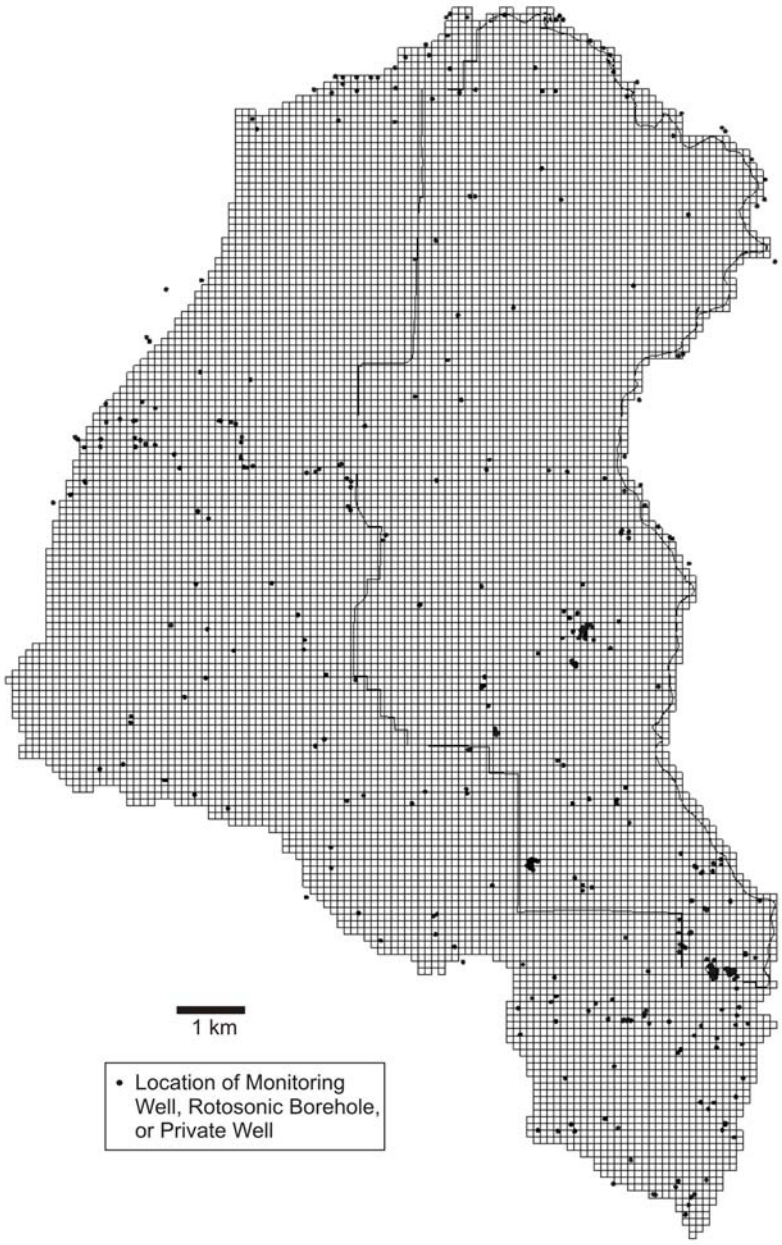

Figure 37. Model Grid and Borehole Locations

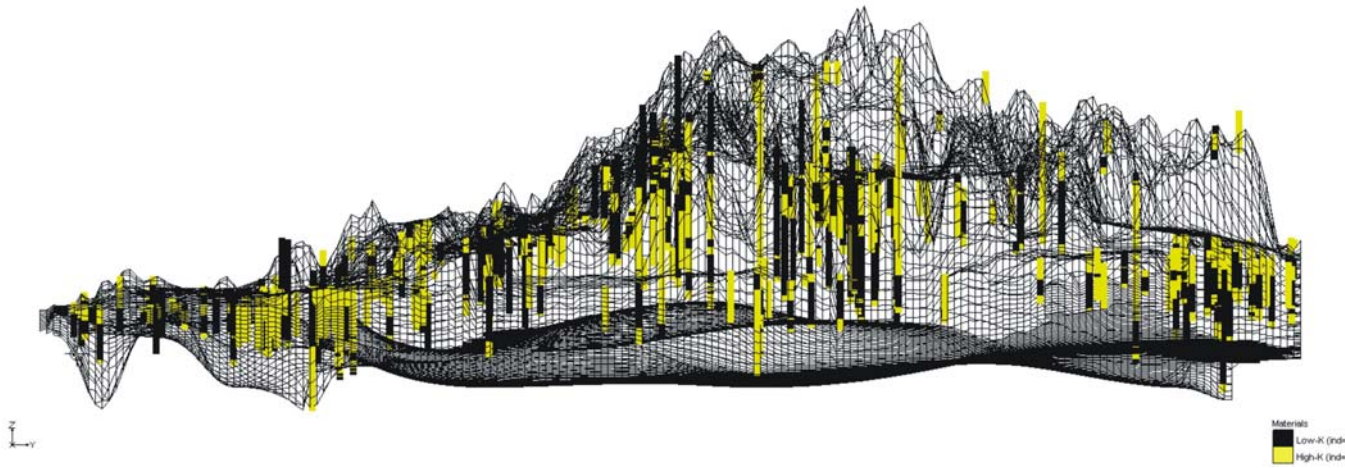

Figure 38. View of Model Grid and Drilling Data from the East

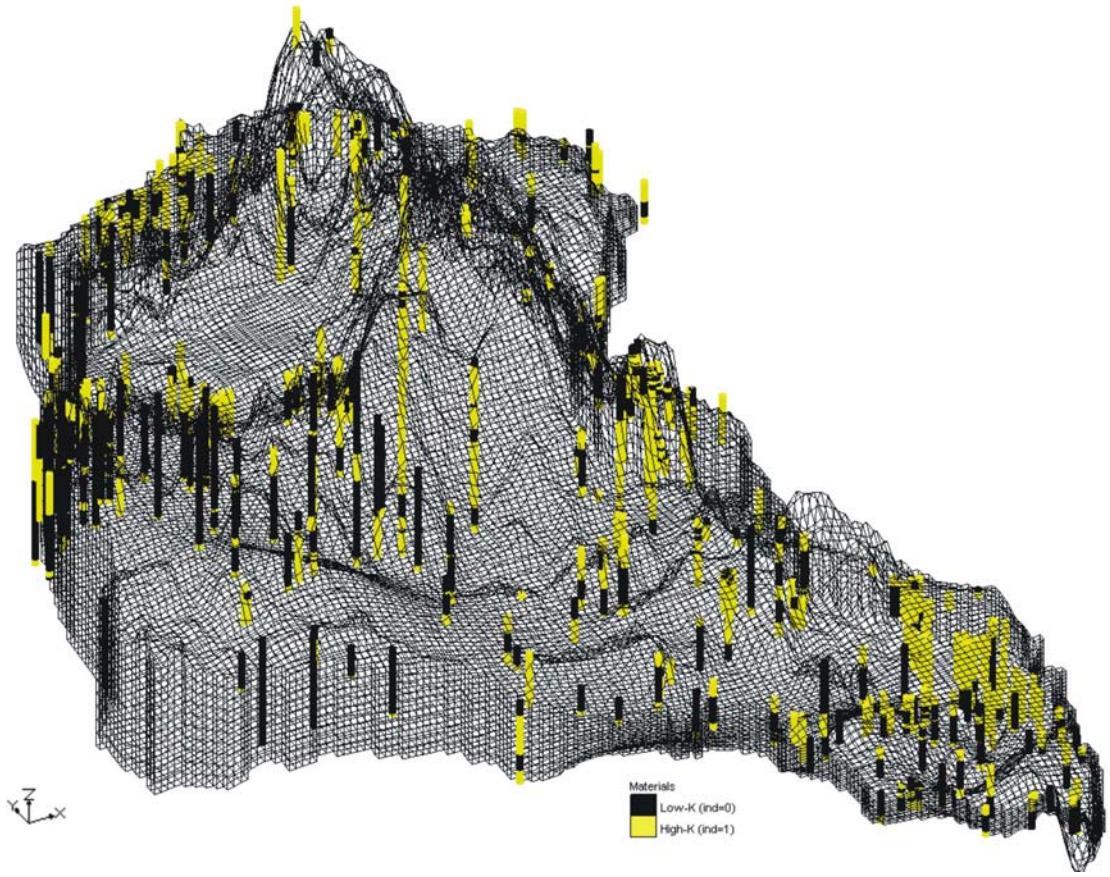

Figure 39. Oblique View of Model Grid and Drilling Data from the Southwest

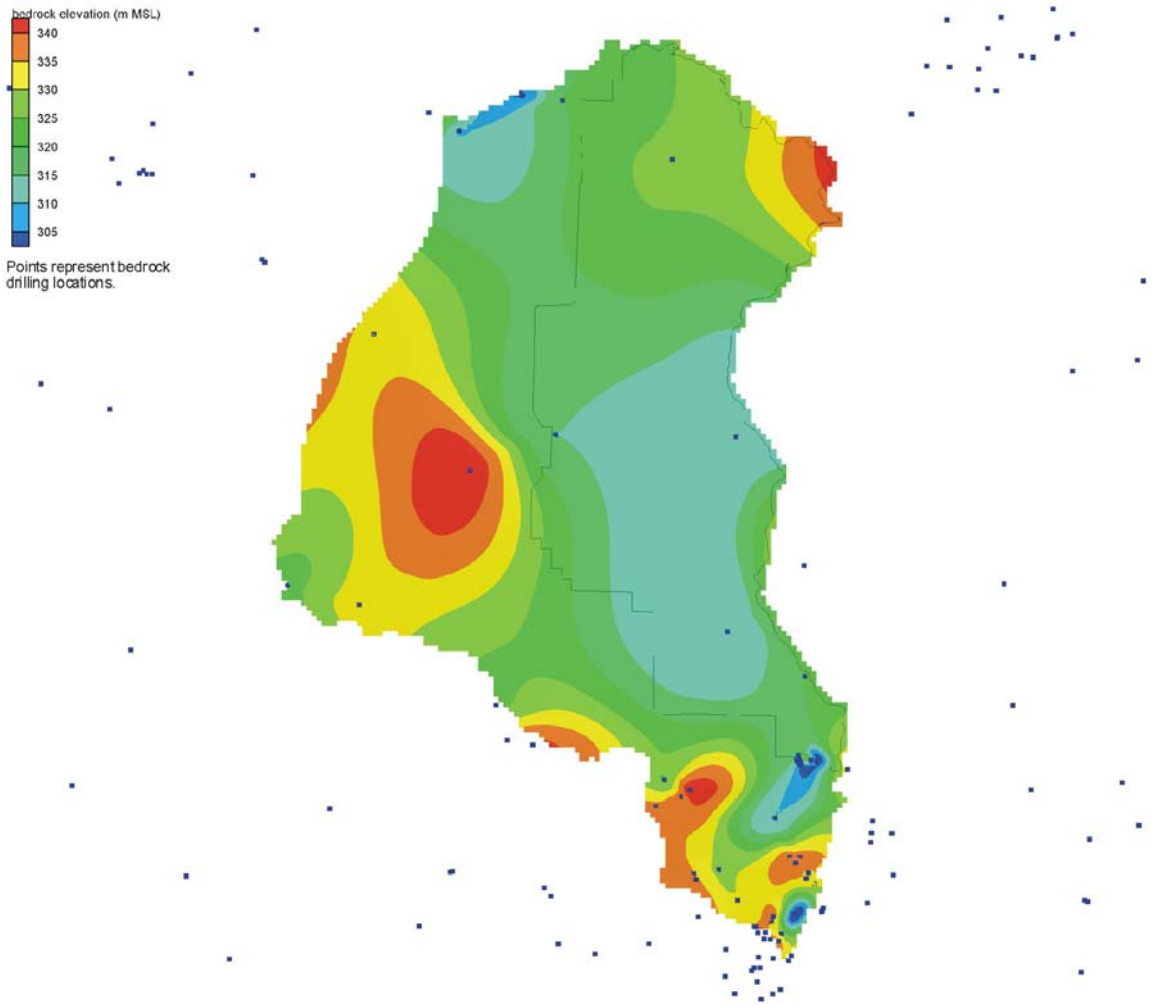

Figure 40. Bedrock Surface Elevation in Model Domain

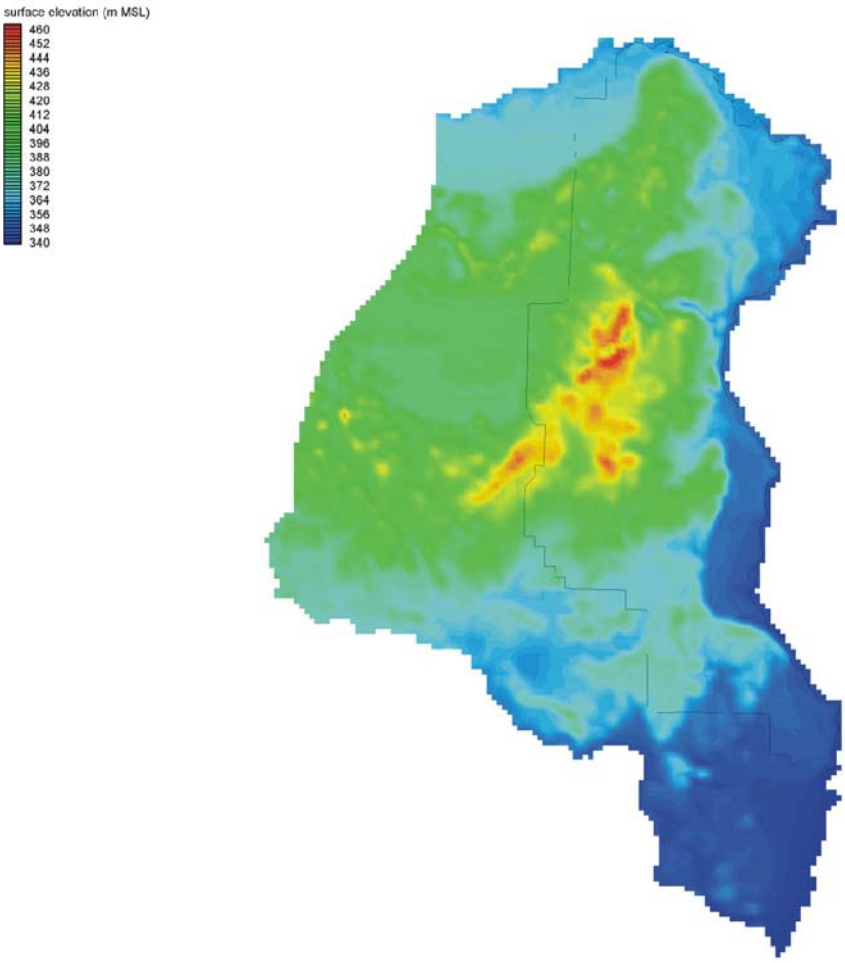

Figure 41. Topographic Surface Modeled with 60-m DEM Data

Ten layers were modeled by dividing the glacial drift thickness evenly throughout the modeling domain. As a result, some locations, such as those along major rivers, have 10 thin, saturated model cells, whereas other locations, such as those on the St. Croix moraine, have 10 thick cells, and one or more cells below the ground surface may be unsaturated.

Input Parameters

Interior creeks, lakes, and wetlands are important hydrologic features in a groundwater flow model (Figure 33 and Figure 36). These were determined to represent an expression of the water table in many instances. In MODFLOW, these types of features can be accommodated in several ways.

The creeks were modeled by using the Drain Package of MODFLOW. A tool in GMS allows the tracing of linear features such as creeks, and cells along the traces may be automatically assigned as drain cells. Drain cells require two input parameters: elevation and conductance. Elevations were assigned to cells on the basis of the creek stage. Conductance per unit length was assigned on the basis of estimated values of creek sediment thickness, width, and vertical permeability.

Wetlands were also modeled by using the Drain Package, through the use of another mapping tool in GMS. Wetlands were delineated as polygons, which were each assigned an elevation (wetland elevation) and a conductance per unit area (on the basis of estimated values of wetland sediment thickness and vertical permeability).

Large lakes (Alexander, Round, Green Prairie Fish, Mud, and Tamarack) were assumed to be in direct contact with the regional flow system and were modeled as specified heads. In this manner, the lakes' levels remain steady, allowing the lakes to be a continuous source or sink for groundwater. In the case of a flow-through lake, the lake would be a source at one end and a sink at the other. A value for conductance per unit area was assigned to the lake sediments on the basis of estimated values of sediment

thickness and vertical permeability. Many other lakes at the site were not modeled because they are assumed to be perched on the basis of their typical water level.

For recharge, the calibrated estimates of St. George (1994), along with two rough estimates based on material character, were used as inputs in the flow models (Table 10 and Figure 35).

Pumping stresses in the study area were modeled by calculating or estimating average groundwater withdrawals, as described above. These pumping rates were incorporated in the 3D model by assigning the withdrawal across each individual well's screened interval. In a case where a well screen's top and bottom elevations straddle two or more model layers, GMS (EMRL 2005) automatically divides the pumping rate across the model layers on the basis of the proportion of well screen present in each.

The final input parameter type, hydraulic conductivity, is distributed through the use of 3D geostatistics, as described below.

Geostatistical Modeling of the Subsurface

The geological structure of the subsurface of Camp Ripley and its vicinity poses a challenge in flow model construction because of the products of the glacial depositional events. The distances between boreholes are such that the correlation of units throughout the site is quite uncertain, because average lens lengths are less than the average borehole spacing. An understanding of the distribution of materials is important to the model because the hydraulic conductivities of the units vary so widely.

For this reason, modeling of the geologic framework was performed geostatistically. Evaluations are made using three approaches: binary indicator

variography with indicator kriging, binary transition probability geostatistics, and 5-category transition probability geostatistics. In addition, a simple model was analyzed, consisting of a single K value for all glacial drift. This base case provides a point of comparison to the geostatistical results.

Indicator Kriging Approach

Relying on the indicator variography, ordinary kriging is performed, using the indicator dataset along with the variogram parameters and appropriate search parameter values. Indicator kriging results provide a cell-by-cell array of indicators values, ranging from 0 to 1, throughout a three-dimensional grid representing the study area. In a sense, the indicator kriging results represent the probability of a cell being of "low" K or of "high" K.

For a flow model, the indicators need to be converted into K values to populate the flow model's K array. In this study, K is assumed to vary between the high and low values measured in the field, and to assign K values that are smoothly proportioned across this range. K values for the array of indicator kriging results can be determined with the following equation:

$$\mathbf{K(ind) = K_{min} * 10}^{(\log(Kmax) - \log(Kmin)) * \text{indicator}}$$

Equation 14

where K(ind) = K of a model cell as a function of indicator kriging result

K_{min} = minimum field measurement of K

K_{max} = maximum field measurement of K

Indicator = indicator kriging result for model cell (ranging between 0 and 1)

Equation 14 is used to populate the numerical flow model's K arrays based on the indicator geostatistical results from analysis of binary indicator data for subsurface materials.

Transition Probability Approach

The transition probability geostatistics (TPROGS) (Carle 1999) approach determines the volumetric proportions, mean thicknesses, mean lens lengths, and juxtapositional tendencies of a site's hydrogeologic units. It may then be used in conditional simulation - stochastic model runs of multiple, equally probable spatial distributions of the hydrogeologic units - while the hard data are honored. The results of a simulation are multiple realizations of the cell-by-cell material types. Field-based K measurements could then be tied to the material types to create each layer's material distributions. TPROGS analyses may be performed within GMS, and results may be imported by GMS into a stochastic MODFLOW flow model or a stochastic inverse model for parameter (K) estimation.

To implement TPROGS in GMS, a site's hydrogeology should be simplified into a maximum of five units. For Camp Ripley, the 10 glacial hydrogeological materials identified by EnDriP were converted to five units on the basis of the similarities in both depositional setting and hydraulic conductivity values (Table 14). Monitoring well, EnDriP, and CWI data in the model domain were fit to these categories.

Table 14. TPROGS Categories Based on EnDriP Interpretations

EnDriP Material Name	TPROGS Unit Grouping	Binary Indicator	5-Category Indicator
Dense clay loam till	Tills	0	5
Red/brown sandy loam till	Tills		
Red sandy till	Tills		
Lacustrine clay	Lacustrine clay		4
Silt loam	Lacustrine silt	1	3
Lacustrine silt	Lacustrine silt		
Silty fine sand	Lacustrine silt		
Fine sand	Lacustrine sand		2
Medium sand	Lacustrine sand		
Coarse sand/gravel	Outwash		1

The transition probability geostatistical approach relies on the same GMS borehole data as the indicator approach. GMS includes the T-PROGS software to facilitate the analysis with a clear understanding of inputs and graphical outputs. A software limitation is a maximum of five categories, which is a reasonable number, given the nature of the study area. An initial step, therefore, is to group the materials into proper categories. In a case of too many material types, they may be grouped according to both relative K values and depositional setting. For this study area, materials were grouped in two ways. First, they were grouped into two categories: low-K (tills, lacustrine clay), and high-K (outwash, lacustrine sand, lacustrine silt). A second analysis was performed on all five categories (Table 14).

The ratio of mean lateral lens length to mean vertical lens thickness was assigned on the basis of the ratio of lateral:vertical variogram ranges as determined in the prior

section. Though a range of ratios were present in the various data sets, an average of about 10 was indicated.

Calibration and Parameter Estimation

Comparison of the output obtained through flow model calibration based on each method is performed to evaluate the effectiveness of the geostatistical characterizations for matching a set of target heads. For the indicator kriging case, various plausible minimum and maximum K values for the study area's materials were tested. Indicator kriging results across the 3D model range between 0 and 1. By manually adjusting the values for the K distribution end members, the cell-by-cell distribution of K is interpolated, and calibration statistics are generated.

For the cases of the single equivalent porous media for the glacial drift, the binary T-PROGS analysis, and the 5-category T-PROGS analysis, PES, the calibration tool contained in MODFLOW 2000 (Hill et al. 2000), was used to estimate parameters of the model's hydraulic conductivity while calibrating the model to the target heads. Initial values used to begin the parameter estimation process are shown in Table 19. These values were bounded by appropriate minimum and maximum values, allowing PES to have a range of values to explore. For the two T-PROGS analyses, stochastic inverse parameter estimation was performed. In this manner, the subsurface in each case was modeled as 20 separate, equally probably realizations, and PES was performed for each one while attempting to match the target head data.

In each calibration process, the match between simulated head values and measured heads at target wells provides an indication of the model's calibration. Three

equations for addressing the bulk accuracy of the model are the mean error (ME), mean absolute error (MAE), and root mean squared error (RMSE) equations (Anderson and Woessner 1992). The ME is calculated simply as the mean difference between simulated and measured heads. The MAE is the mean absolute value of the difference between simulated and measured heads. The RMSE, which is generally the best measure of error, is the square root of the average squared difference between simulated and measured heads.

Results

Four cases were examined for their accuracy in modeling the hydrogeologic framework and, in turn, the calculated heads in the study area. These included a single-K or equivalent porous medium approach, binary indicator kriging, binary transition probability geostatistics, and 5-category transition probability geostatistics. All model runs relied on calibration statistics derived through comparisons with the same set of target heads. All sought to determine horizontal hydraulic conductivity values, with vertical hydraulic conductivity consistently assumed to be one-tenth of the horizontal value.

A summary of all determinations for K values, along with the associated errors, is presented in Table 15. The details are described below.

Table 15. Summary of Hydraulic Conductivity Results and Associated Error Measurements

Case	Hydraulic Conductivity (m/d)	Calibration Method	ME (m)	MAE (m)	RSME (m)
Single K (equivalent porous medium)	6.4	Inverse modeling with PES	-0.17	2.51	3.68
Binary Indicator Kriging	K_{low} = 0.05 K_{high}= 10	Process of altering K_{low} and/or K_{high} to determine combination with lowest RMSE	0.22	2.56	3.43
Binary T-TROGS	K_{low} = 0.37 K_{high} = 17	Stochastic inverse modeling with PES, geometric mean of valid solutions	0.66	3.00	3.85
5-category T-PROGS	Outwash = 69 Lacustrine Sand = 23 Lacustrine Silt = 2.9 Lacustrine Clay = 0.54 Tills = 0.23	Stochastic inverse modeling with PES, geometric mean of valid solutions	0.07	2.91	3.88

Initial modeling was directed at determining a single hydraulic conductivity (K) value for the entire glacial drift package. The equivalent porous medium determined using inverse modeling with PES (Hill et al. 2000) was 6.4 m/d. This relates well to the range of values of drift materials in Table 11 and by St. George (1994), Lindgren (2002), and Person et al. (2007).

The indicator kriging approach relied on a variogram analysis for the study area. This analysis was performed by including all borehole data from within or directly adjacent to the modeled area (Figure 42). This includes 220 onsite boreholes associated with monitoring wells, EnDriP wells and soil borings, and production wells, as well as

218 private wells from the CWI database. The variography for this binary data showed a vertical variogram of excellent quality with a range of 32 m (Figure 43). The lateral variogram was fair in quality and suggested a range of 125 m (Figure 44). These results and the associated sills are similar to those determined in the earlier analysis for the set of Camp Ripley monitoring wells and EnDriP boreholes, though half of the data in the flow modeling study area are private well logs.

Kriging relied on this variogram information to interpolate between data points and determine an estimate, ranging from 0 to 1, for the indicator value in each cell in the variable 3D grid of the flow model (e.g. Figure 45). To calibrate the flow model, various combinations of the K_{low} and K_{high} end members were tested using Equation 14 for their suitability in creating a flow model that best matches the target head values. As a measure of calibration, ME, MAE, and RMSE values were determined for each pair of K extremes in a series of forward model runs. The RMSE values are displayed in Table 16. The minimum RMSE value coincides with a K_{low} value of 0.05 m/d and a K_{high} value of 10 m/d, as illustrated in Figure 46. The K_{low} end member matches up closely with laboratory estimates for clay loam till and lacustrine clay, while the K_{high} value matches closely with medium sand (Table 11). Flow model results with these K values as the minimum and maximum are shown in Figure 47. Localized highs in the southern end of the study area are the result of high recharge rates based on the DNR surficial mapping assigned to low-permeability cells based on drilling data.

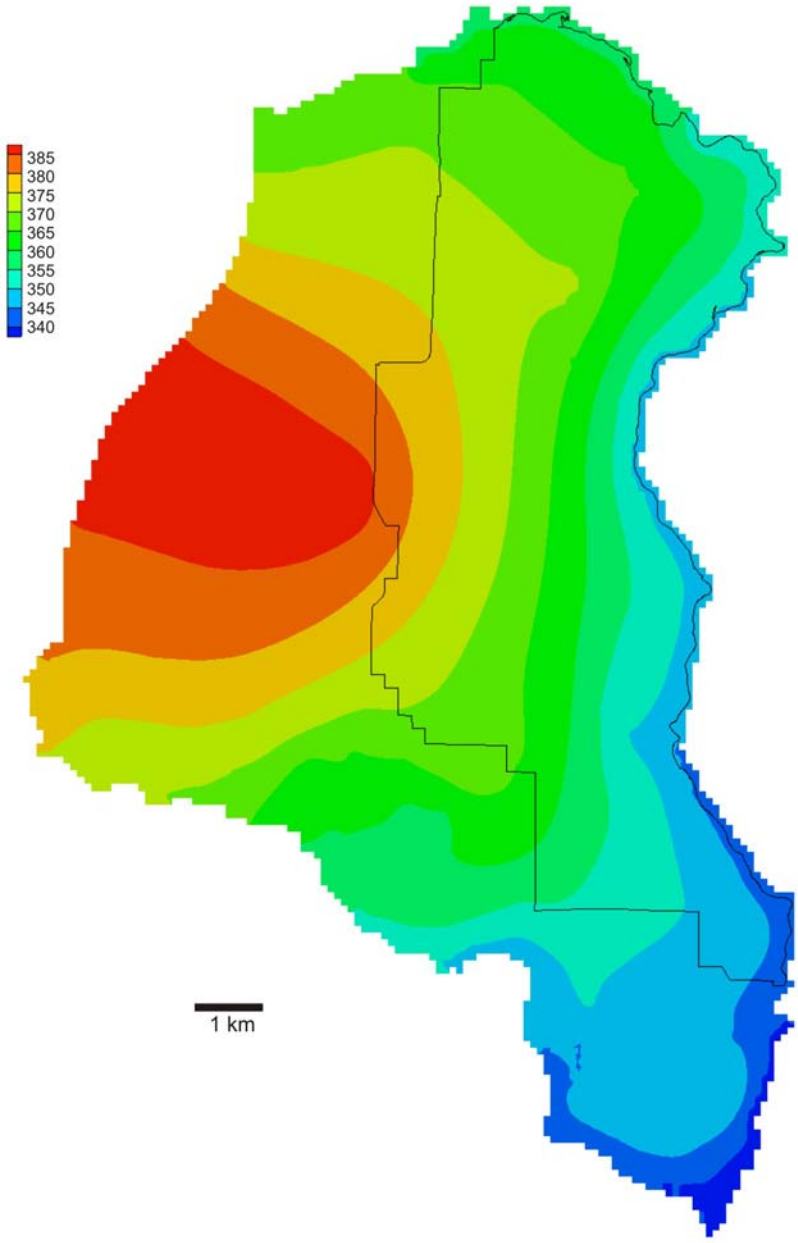

Figure 42. Heads Resulting from Single-K Approach

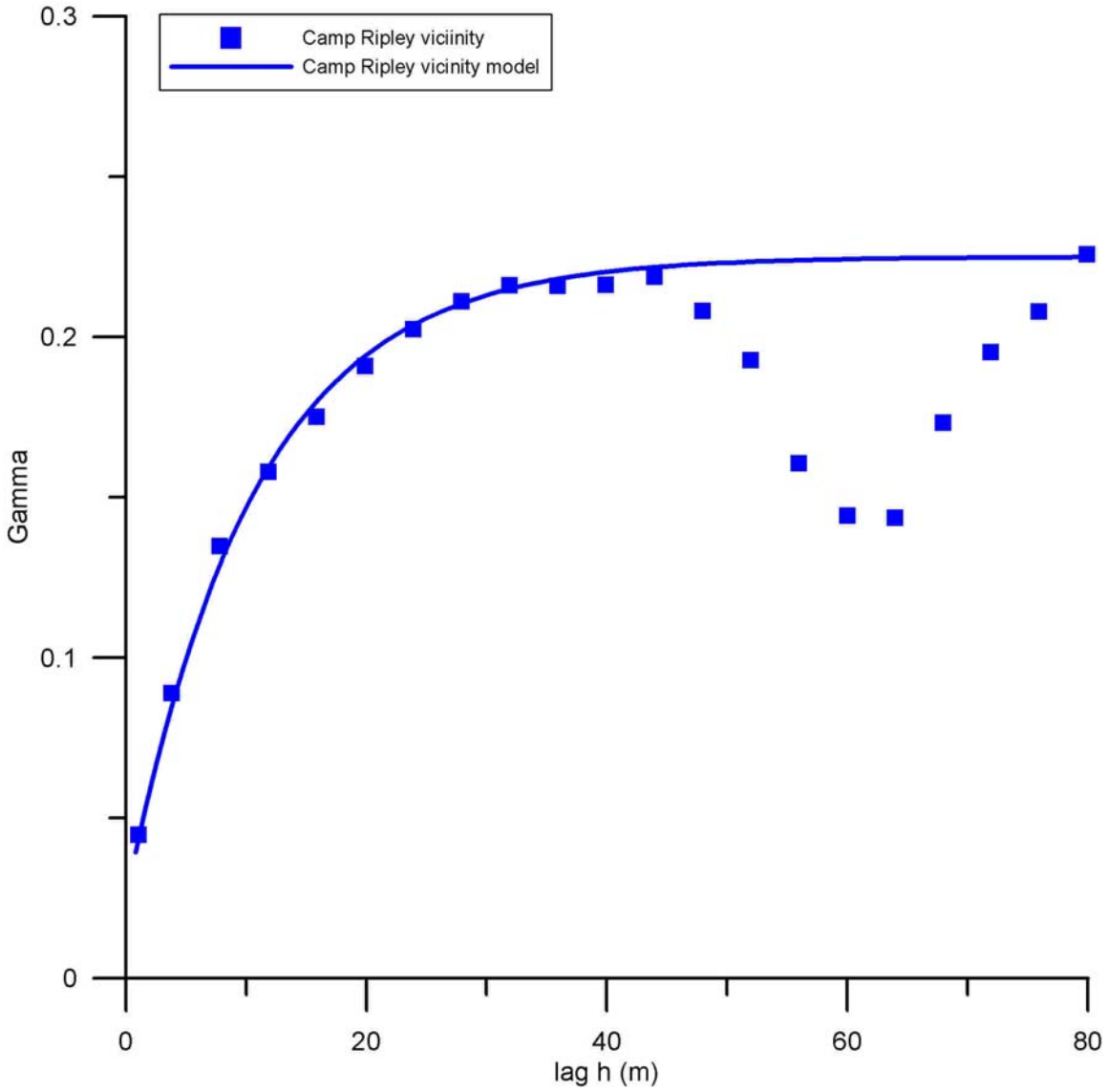

Figure 43. Vertical Indicator Variogram for Camp Ripley Vicinity

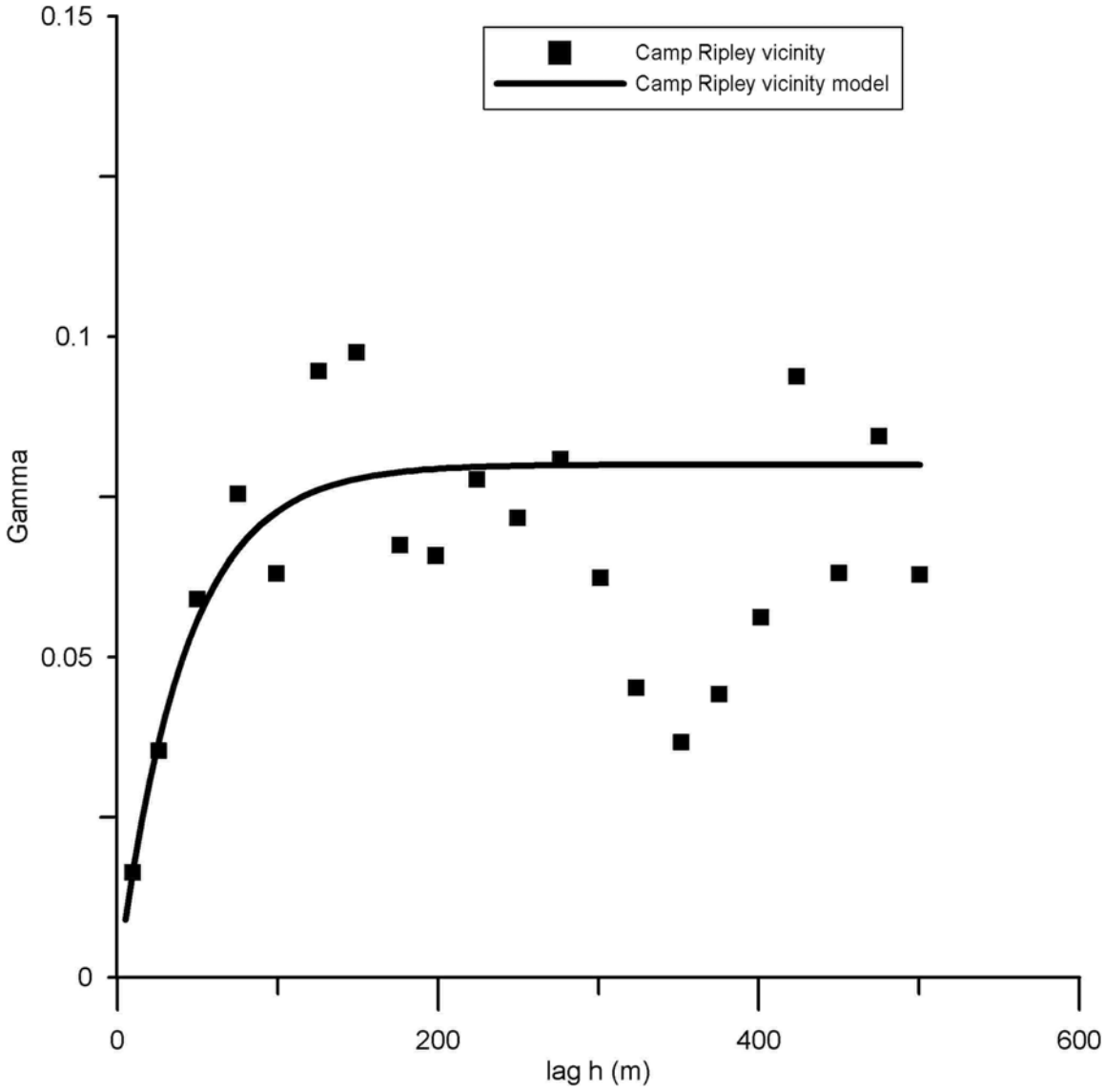

Figure 44. Lateral Indicator Variogram for Camp Ripley Vicinity

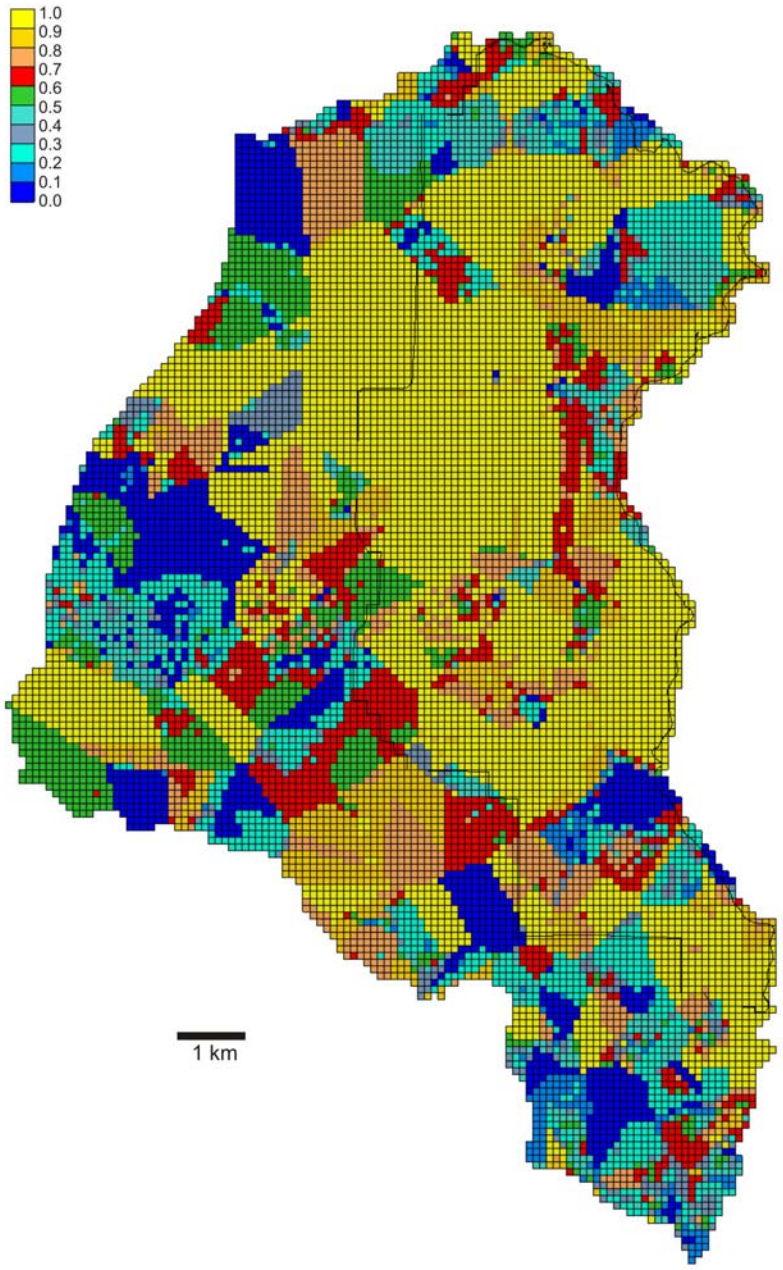

Figure 45. Example of Indicator Kriging Results for Model Layer 5

Table 16. Root Mean Squared Errors (m) from Indicator Kriging Output and Various K_{high} and K_{low} Values

K high (m/d)	**1000**		5.15	5.01				4.89			4.84	4.77
	100	4.57	4.50	4.48				4.55			4.61	4.64
	50					4.29		4.35		3.84		
	25					3.95						
	10	6.03	4.22	3.51	3.44	3.43	3.44	3.45	3.50	3.56	3.54	3.81
	7.5					3.69		3.63				
	5					4.62		4.35				
	1	46.25	33.32	24.12				16.58			11.09	
	0.1	350.06	255.64	176.63				116.94				
		1E-04	**0.001**	**0.01**	**0.025**	**0.05**	**0.075**	**0.1**	**0.25**	**0.5**	**1**	**10**
		K low (m/d)										

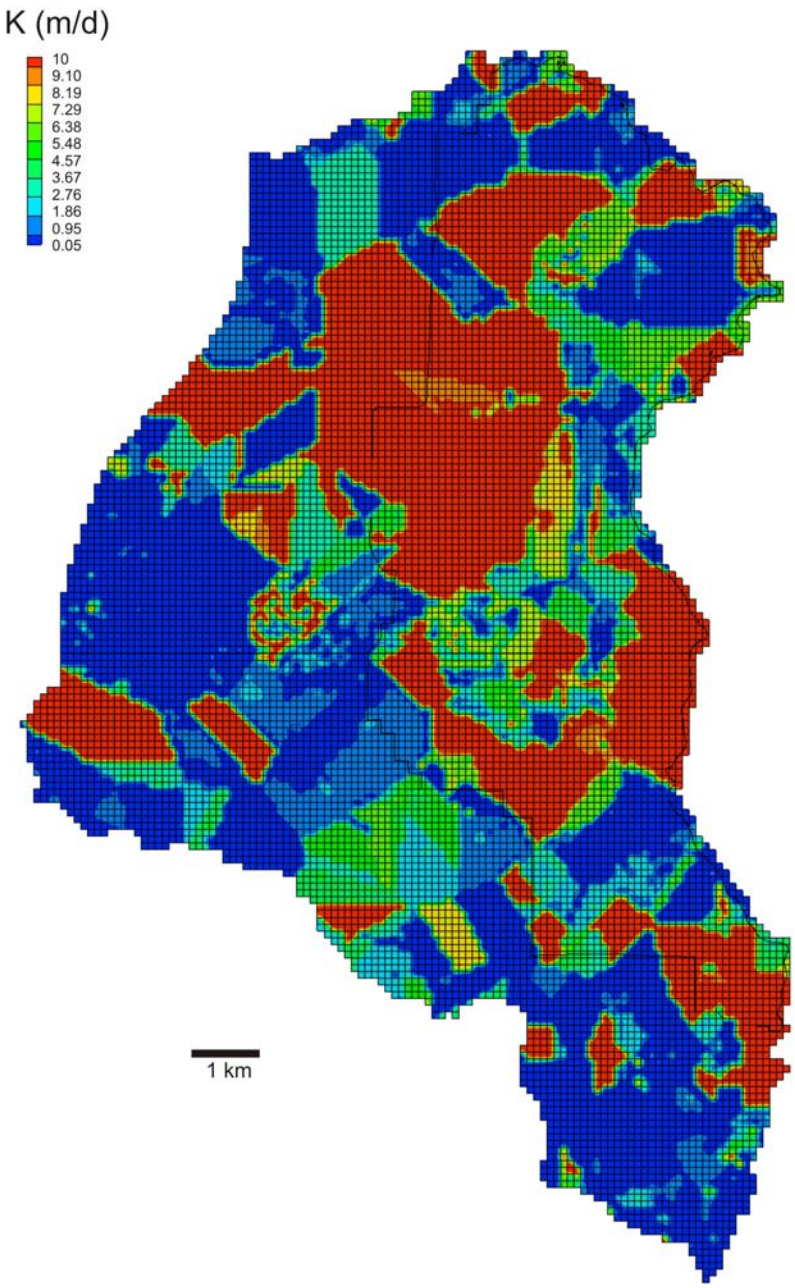

Figure 46. Hydraulic Conductivity Values Assigned to Layer 5

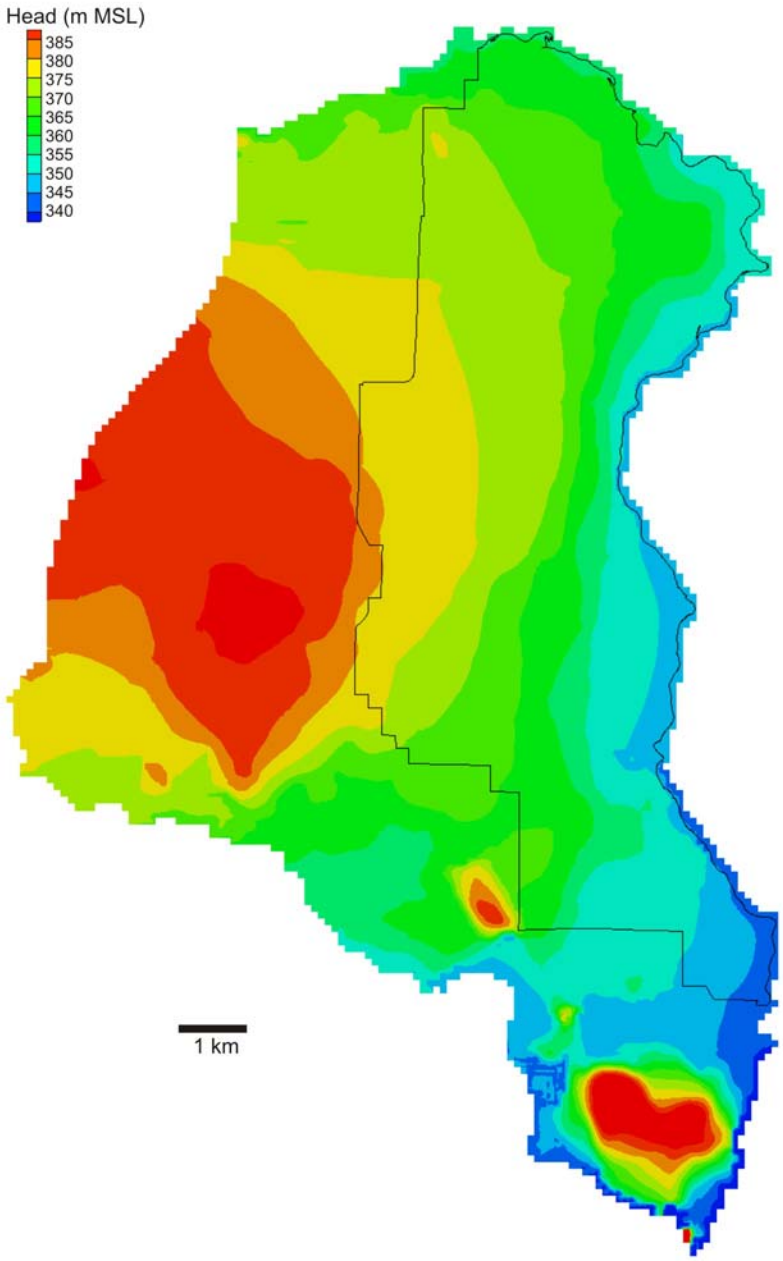

Figure 47. Heads Resulting from Optimal Klow and Khigh Values

For the binary analysis, results are shown in Figure 48, and proportions and mean lens thicknesses are presented in Table 17. The mean thicknesses differ from those determined earlier for the multi-county study area. Though the low-K material's mean thickness is similar (8.9 m vs. 11.0 m), the high-K thickness is double that of the multi-county analysis (12.9 m vs. 6.4 m). This may be attributed to a greater proportion of thick alluvial sands in the Camp Ripley data (especially near the Mississippi River and in the Cantonment Area) compared to the multi-county area.

TSIM was used to create 20 realizations of the binary hydrostratigraphic framework. For the lateral direction, mean lens lengths were assumed to be roughly ten times the vertical lens thickness, as investigated in the earlier study. Each realization is a statistically valid and equally probable model that honors the hard data. However, the hard data are far apart relative to both the assumed lateral correlations of the units and the grid spacing. The results of different realizations, therefore, are all quite similar, with random results according to material proportions except at hard data locations. An example result for model layer 1 is shown in Figure 49.

In GMS, Modflow was run in stochastic inverse parameter estimation mode for each realization to determine the K_{low} and K_{high} values. These 20 PES analyses required 5 hours on a 2.26-GHz Intel Pentium 4 computer or 1.2 hours on a 3.0-GHz Intel Core 2 Quad computer. Starting K values and allowed ranges are included in Table 17. Of these runs, 17 converged on a set of solutions (Table 18). The heads resulting from the geometric mean values for K_{low} and K_{high} are shown in Figure 50.

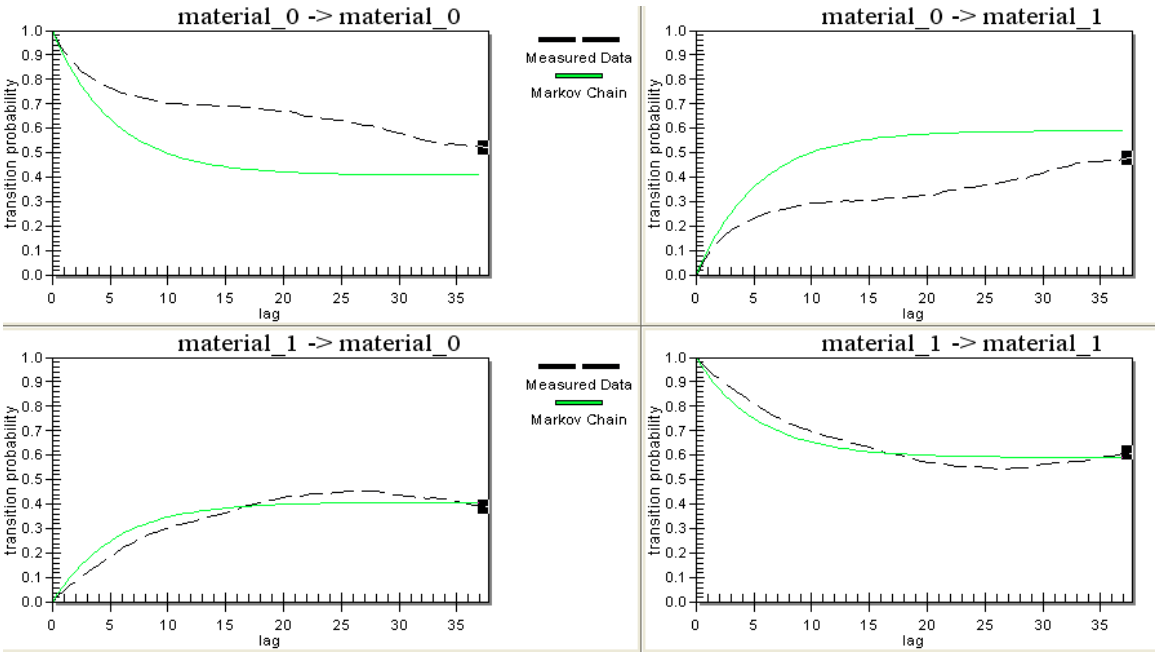

Figure 48. Binary T-PROGS Results

Table 17. Binary T-PROGS Summary

Material	Indicator	Proportion	Mean Lens Thickness (m)	Initial Modeled K (m/d)	Minimum Allowed K (m/d)	Maximum Allowed K (m/d)
Low K	0	0.41	8.9	0.1	0.0001	100
High K	1	0.59	12.9	10	0.1	1,000

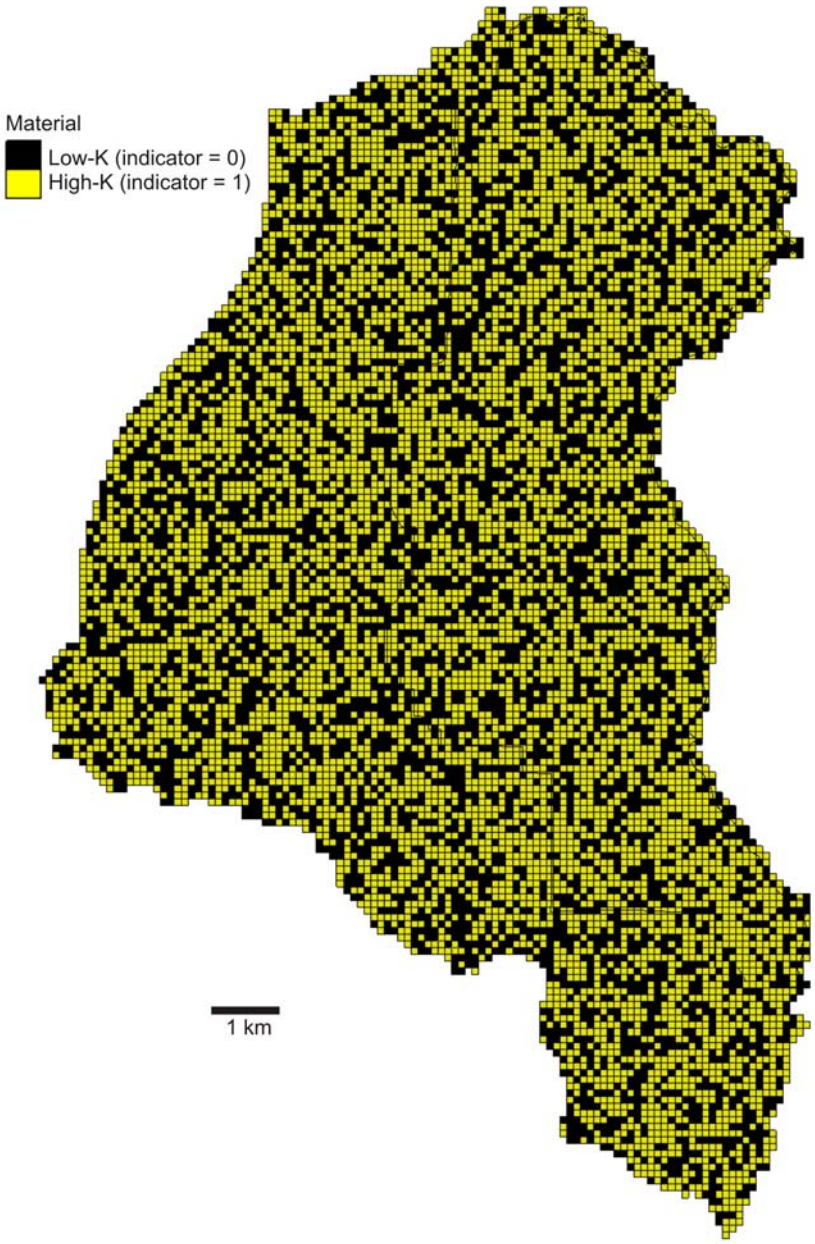

Figure 49. Example of Binary T-PROGS Results for Layer 1

Table 18. Estimated Hydraulic Conductivity Values from 17 Realizations of the Binary T-PROGS Model

	K_{low} (m/d)	K_{high} (m/d)
K values (m/d):	2.55	17.18
	2.40	14.50
	0.10	10.00
	0.12	16.67
	0.32	18.65
	0.13	17.19
	0.16	21.59
	0.44	19.41
	2.06	15.56
	0.18	19.46
	0.14	16.82
	1.44	15.23
	0.31	19.45
	0.35	17.97
	0.20	19.70
	1.35	15.49
	0.10	17.29
geometric mean (m/d):	0.37	16.96
mean (m/d):	0.73	17.19

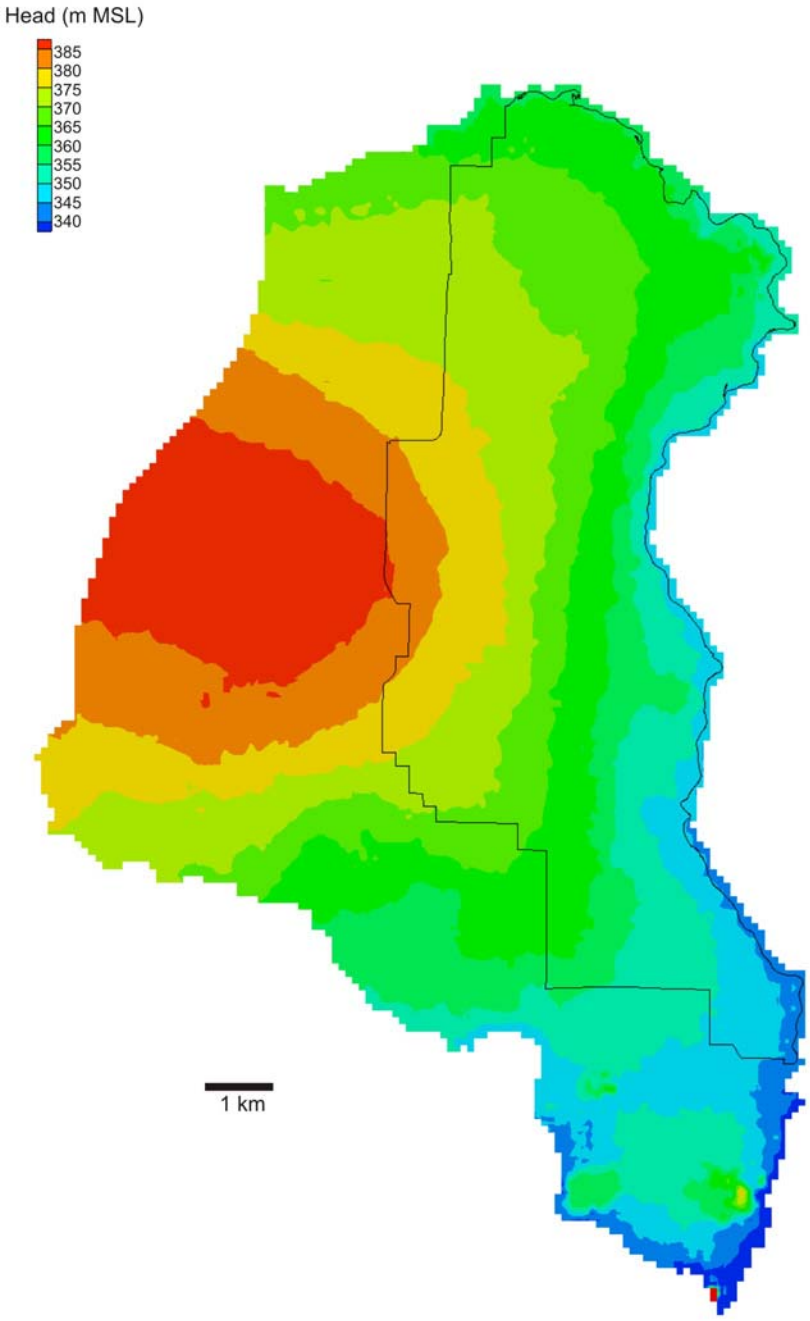

Figure 50. Heads Resulting from Binary T-PROGS Approach

For the 5-category analysis, results are illustrated in Figure 51, and proportions and mean thicknesses are presented in Table 19. Here, too, the mean thicknesses differ somewhat from those of the multi-county study area.

TSIM was used to create 20 realizations of the hydrostratigraphic framework based on the five material types. An example for one model layer is shown in Figure 52. For the lateral direction, mean lens lengths were again assumed to be roughly ten times the vertical lens thickness. In GMS, Modflow was run in stochastic inverse mode for each realization to determine the K values for each of the five material types. These PES analyses required 13 hours on a 2.26-GHz Intel Pentium 4 computer or 2.5 hours on a 3.0-GHz Intel Core 2 Quad computer. Starting K values and allowed ranges are included in Table 20. Of these runs, 17 converged on a set of solutions, though three had unreasonably high values for one of the parameters. The remaining 14 solutions are presented in Table 20. The heads derived from the geometric mean K values for the five material types are shown in Figure 53.

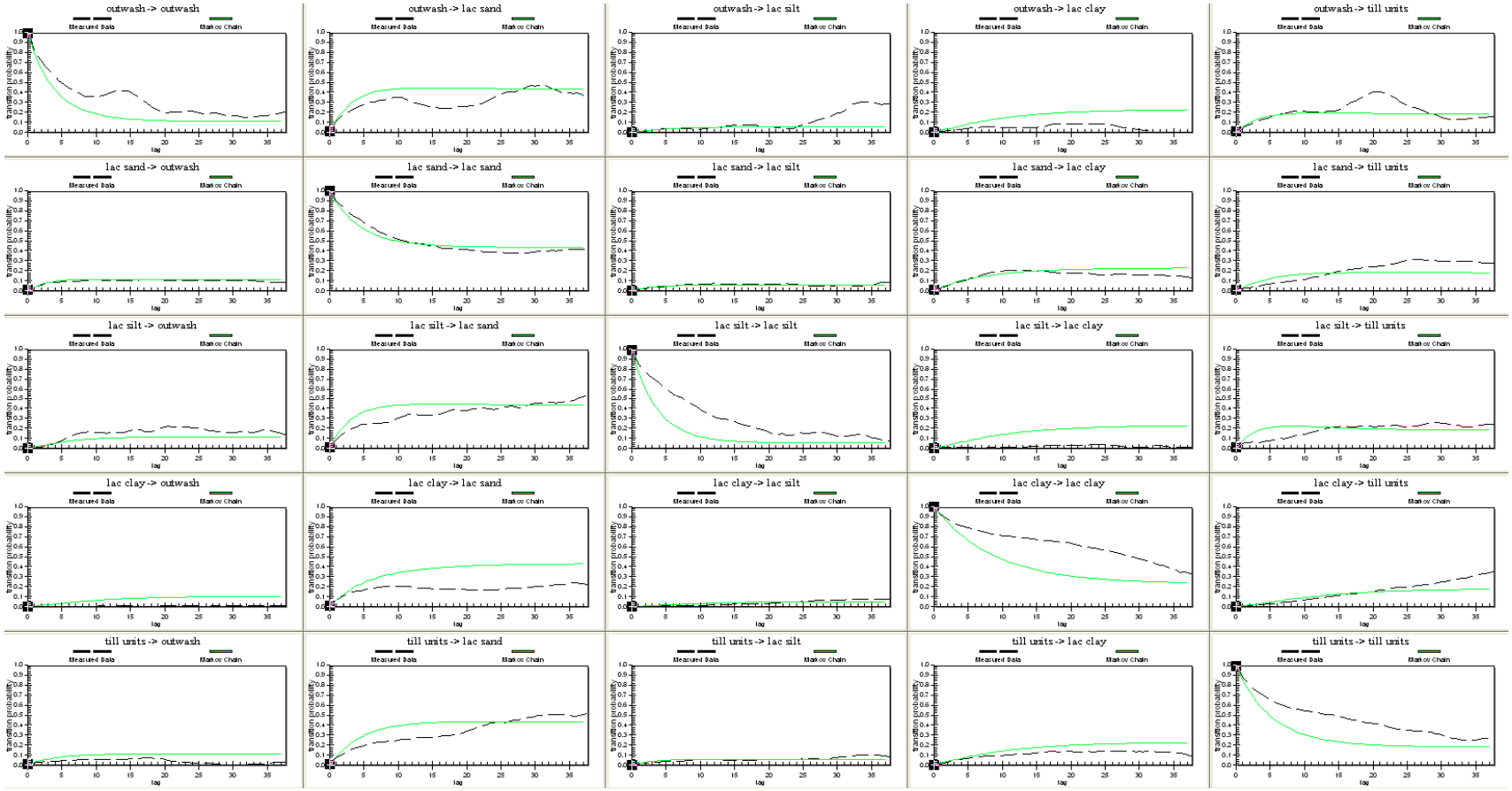

Figure 51. Five-Category T-PROGS Results

Table 19. Five-Category T-PROGS Summary

EnDriP Material Name	TPROGS Unit Grouping	5-Category Indicator	Proportion	Mean Lens Thickness (m)	Initial Modeled K (m/d)	Minimum Allowed K (m/d)	Maximum Allowed K (m/d)
Dense clay loam till	Tills	5	0.11	4.5	0.1	0.0001	10
Red/brown sandy loam till	Tills						
Red sandy till	Tills						
Lacustrine clay	Lacustrine clay	4	0.43	7.7	0.1	0.00001	10
Silt loam	Lacustrine silt	3	0.05	3.8	1	0.01	10
Lacustrine silt	Lacustrine silt						
Silty fine sand	Lacustrine silt						
Fine sand	Lacustrine sand	2	0.24	11.6	20	0.1	1,000
Medium sand	Lacustrine sand						
Coarse sand/gravel	Outwash	1	0.17	6.2	50	1	1,000

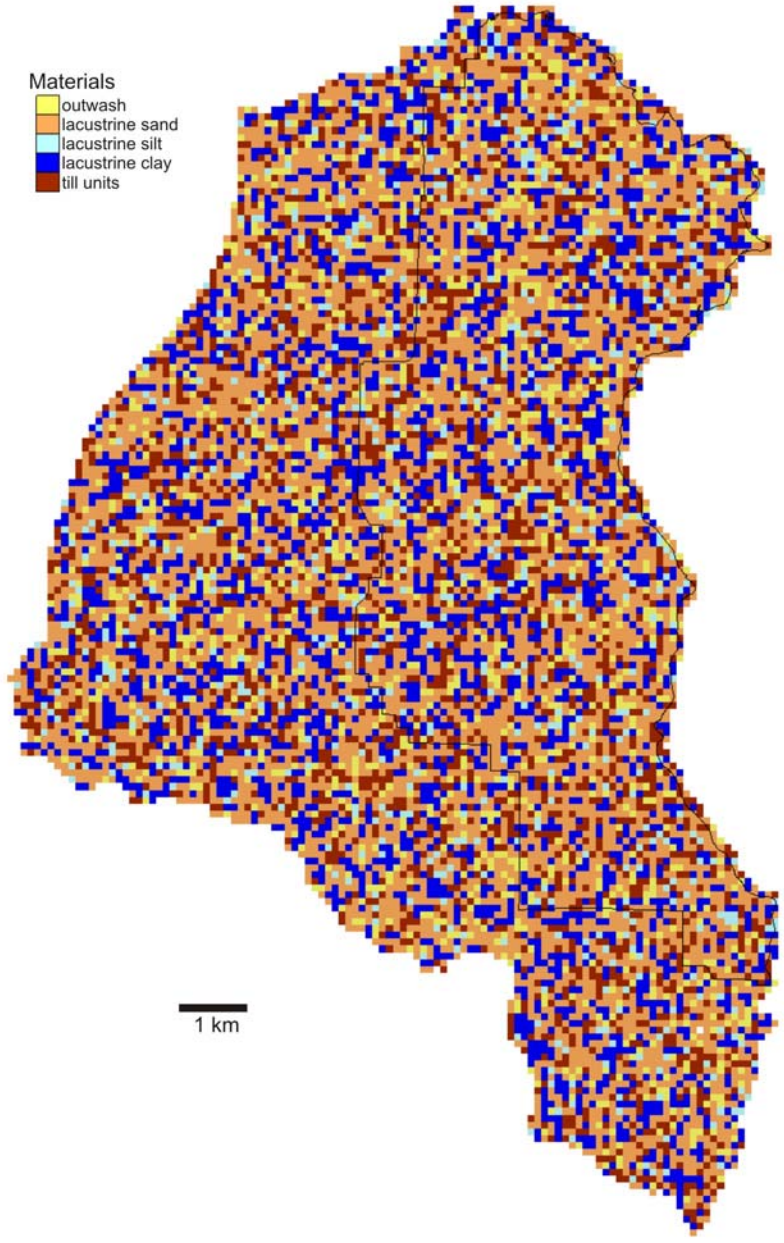

Figure 52. Example of 5-Category T-PROGS Simulation

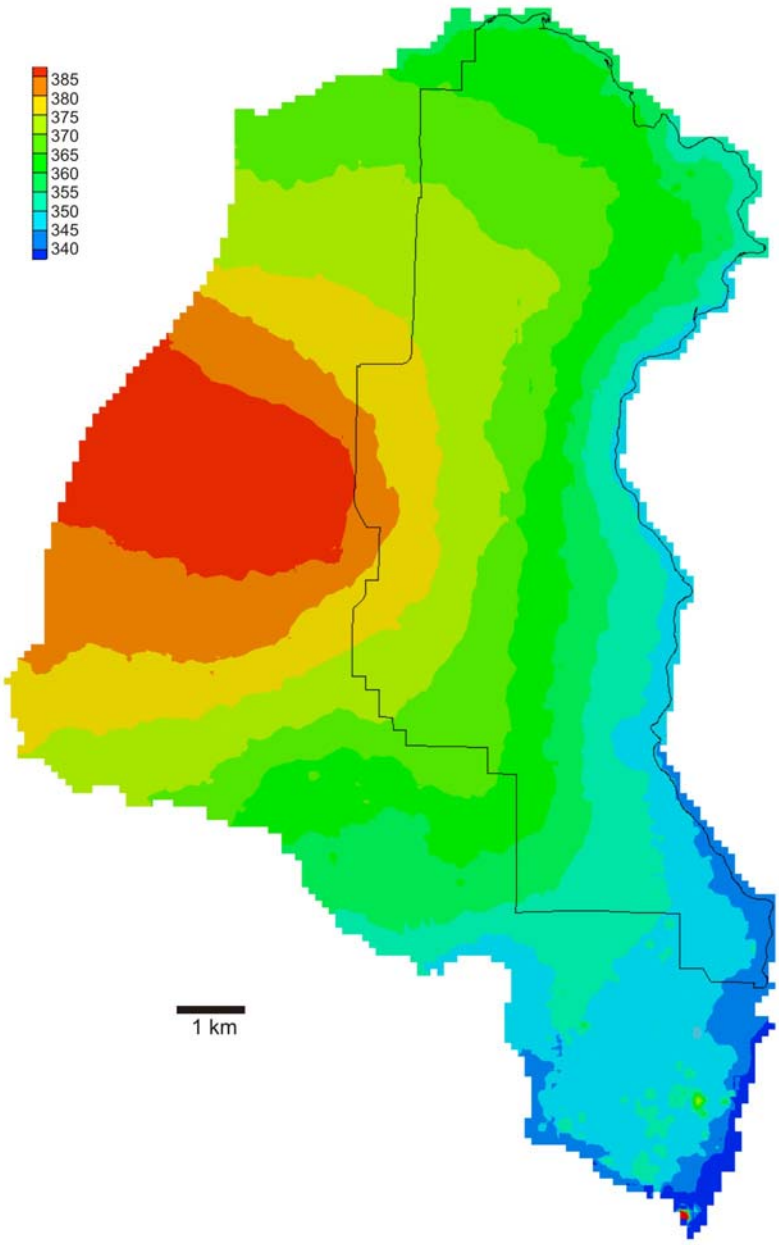

Figure 53. Heads Resulting from 5-Category T-PROGS Approach

Table 20. Estimated Hydraulic Conductivity Values from 14 Realizations of the 5-Category T-PROGS Model

Materials:	1	2	3	4	5
K values (m/d):	193.60	32.71	0.00065	0.00010	0.04354
	31.54	20.89	20.05	5.08	0.45
	12.74	22.52	55.43	1.95	0.30
	9.97	25.65	48.09	0.73	0.49
	150.40	20.05	5.65	6.63	0.18
	204.30	24.88	12.29	0.04571	0.11
	168.50	21.44	24.02	0.13	0.13
	67.74	20.41	6.80	5.64	2.48
	49.16	21.74	32.43	10.06	0.24
	37.76	21.49	148.40	0.50	0.35
	264.00	29.63	0.00078	2.11	0.13
	92.72	23.22	0.21	0.35	0.10
geometric means (m/d):	69.34	23.45	2.88	0.54	0.23
means (m/d):	106.87	23.72	29.45	2.77	0.42

Discussion and Conclusions

The three geostatistical approaches to modeling the hydrostratigraphic framework and the baseline single-K solution yielded a variety of K values and associated RMSE values. The four solutions were fairly consistent with each other. The single-K solution of 6.4 m/d is in between the K_{low} and K_{high} values determined in the binary indicator kriging case (0.05 and 10 m/d, respectively) and the binary T-PROGS case (geometric means of 0.37 and 17 m/d, respectively). The 5-category T-PROGS approach yielded higher geometric mean K values for the permeable materials: 69 m/d for outwash and 23 m/d for lacustrine sand. For the less-permeable materials, it yielded K values that were somewhat higher than those of the indicator kriging or binary T-PROGS runs: 0.54 for lacustrine clay and 0.23 for till units. The lacustrine silt, accounting for only a small

proportion of the data, had the most inconsistent K determinations (Table 20) and likely a negligible effect on the 5-catorogy T-PROGS results. The final T-PROGS values differ by varying degrees from their initial values in both cases (Table 17 and Table 19).

In the end, the four approaches yielded fairly similar head distributions (Figure 42, Figure 47, Figure 50, and Figure 53) and RMSE values (Table 15). The indicator kriging approach yielded the smallest RMSE, and the single-K approach was second lowest. However, all four methods produced RMSE values within the narrow range of 3.43 to 3.88 m.

The kriging and transition probability approaches differ in terms of their complexity, relevance and application to particular sites, and underlying assumptions. The transition probability approach requires that all of a site's lithologic data can be grouped appropriately into two to five material categories based on relative permeability. With indicator kriging, the gradational K values between hard data locations must be acceptable. The indicator kriging approach has the benefit of direct measurements, if possible, of the lateral correlation, while transition probability requires an assumed ratio of mean lens thicknesses to mean lens lengths. Calibration of the indicator kriging method required a tedious series of manual modifications to the Modflow model's K array using a wide range of Klow and Khigh values. Calibration of the T-PROGS runs, in contrast, requires an hours-long series of inverse model runs which are performed automatically.

Three-dimensional, geostatistically modeled hydrogeology continues to develop and has made some inroads at conferences focused on 3D geological modeling (e.g. Berg

and Thorleifson 2001, Thorleifson and Berg 2002a, Berg et al. 2004, Russell et al. 2006, Thorliefson et al. 2007). An end goal of such hydrogeological modeling is not simply the hydrostratigraphic model, but accurately and appropriately populating K arrays in numerical models, a challenge identified by Sharpe et al. (2001) and Anderson (1989). Modflow 2000 (Harbaugh et al. 2000, Hill et al. 2000), with current graphical user interfaces such as GMS and powerful desktop computers, is capable of incorporating a high level of detail in its hydrogeological input. The geostatistical structure of a study area's hydrostratigraphy, whether determined with indicators or transition probabilities, and whether analyzed deterministically or stochastically, can be incorporated into a flow model with a high level of representativeness subject to the density of available data.

On the basis of the geostatistical modeling and numerical modeling, the results of this study suggest that, for a regional groundwater model in complex glaciated terrain, detailed modeling of the geostatistical framework as input to the flow model does not provide significant improvement over an equivalent porous medium approach. It is possible that in other study areas, distinct geostatistical signatures may be determined for various spatial portions of the model, and these would require separate modeling and blending for use as flow model input.

REFERENCES

Abert, C.C., C.P. Weibel, and R.C. Berg, 2000, Three-Dimensional Geologic Mapping of the Villa Grove Quadrangle, Douglas County, Illinois: U.S. Geological Survey Open-File Report 00-325. http://pubs.usgs.gov/of/of00-325/abert.html

Anderson, M.P., 1989, Hydrogeologic facies models to delineate large-scale spatial trends in glacial and glaciofluvial sediments: Geological Society of America Bulletin, vol. 101, p. 501-511.

Anderson, M.P., and W.W. Woessner, 1992, Applied Groundwater Modeling: Simulation of Flow and Advective Transport, Academic Press, Inc., San Diego, CA.

Beckers, J. and E.O. Frind, 2001, Simulating Groundwater Flow and Runoff for the Oro Moraine Aquifer System. Part II. Automated Calibration and Mass Balance Calculations: Journal of Hydrology, vol. 243, p. 73-90.

Berg, R.C., and L.H. Thorleifson (conveners) 2001. Geologic Models for Groundwater Flow Modeling: Workshop Extended Abstracts. Illinois State Geological Survey, Open File Series 2001-1, 62 p.

Berg, R.C., H. Russell, and L.H. Thorleifson (conveners) 2004. Three-Dimensional Geological Mapping for Groundwater Applications: Workshop Extended Abstracts. Illinois State Geological Survey, Open File Series 2004-8, 100 p.

Boyce, J.I, and N. Eyles, 2000, Architectural element analysis applied to glacial deposits: internal geometry of a late Pleistocene till sheet, Ontario, Canada: Geological Society of America Bulletin, vol. 112, no. 1, p. 98-118.

Burow, K.R., B.C. Jurgens, L.J. Kauffman, S.P. Phillips, B.A. Dalgish, and J.L. Shelton, 2008, Simulations of Ground-Water Flow and Particle Pathline Analysis in the Zone of Contribution of a Public-Supply Well in Modesto, Eastern San Joaquin Valley, California: U.S. Geological Survey Scientific Investigations Report 2008–5035, 41 p.

Carle, S. F. and G. E. Fogg, 1996, Transition probability-based indicator geostatistics: Mathematical Geology, vol. 28, no. 4, p. 453-476.

Carle, S. F. and G. E. Fogg, 1997, Modeling spatial variability with one and multidimensional continuous-lag Markov chains: Mathematical Geology, vol. 29, 7, p. 891-918.

Carle, S.F., 1997, Implementation schemes for avoiding artifact discontinuities in simulated annealing: Mathematical Geology, v. 29, p. 231-244.

Carle, S.F., 1999, T-PROGS: Transition Probability Geostatistical Software, Version 2.1, University of California, Davis, CA.

Carle, S.F., E.M. LaBolle, G.S. Weissmann, D. Van Brocklin, and G.E. Fogg, 1998, Geostatistical simulation of hydrofacies architecture: a transition probability/Markov approach: in Fraser, G.S. and J.M. Davis, eds., 1998, Hydrogeologic models of sedimentary aquifers: Tulsa, -Oklahoma, SEPM (Society for Sedimentary Geology), p. 147-170.

Carney, L.M., and H.D. Mooers, 1998, “Landform Assemblages and Glacial History of a Portion of the Itasca Moraine, North-Central Minnesota,” in C.J. Patterson and H.E. Wright, Jr., eds., Contributions to the Quaternary of Minnesota, Minnesota Geological Survey Report of Investigations 49, St. Paul, MN.

Carney, L.M., and H.D. Mooers, 1998, Landform assemblages and glacial history of a portion of the Itasca moraine, north-central Minnesota: in Patterson, C.J. and Wright, H.E., Jr., eds., Contributions to the Quaternary of Minnesota: Minnesota Geological Survey Report of Investigations 49, St. Paul, Minnesota, p.85-96.

Clayton, L., J. Teller, and J. Attig, 1985, Surging of the southwestern part of the Laurentide ice sheet: Boreas, vol. 14, p. 285.

Dai, Z., R. W. Ritzi, and D. F. Dominic, 2005, Improving permeability semivariograms with transition probability models of hierarchical sedimentary architecture derived from outcrop analog studies: Water Resources Research, vol. 41, W07032, doi:10.1029/2004WR003515.

Dai, Z., R.W. Ritzi, D.F. Dominic, and Y.N. Rubin, 2003, Relating spatial correlation of permeability to sedimentary architecture in outcrop-analog studies: Geological Society of America Annual Meeting, Seattle, Abstracts with Program,

Damico, J., R.W. Ritzi, and D.F. Dominic, 2002, Characterizing aquifer heterogeneity in the Aberjona River valley, Massachusetts: Geological Society of America Annual Meeting, Denver, Abstracts with Program,

Damico, J.R., R.W. Ritzi, and D.F. Dominic, 2001, Geostatistical analysis of the distribution of lithofacies in the Aberjona Valley aquifer near Woburn, Massachusetts: Geological Society of America Annual Meeting, Boston, Abstracts with Program,

Davis, J.C., 2002, Statistics and data analysis in geology (third edition): New York, John Wiley & Sons, 638 p.

Desbarats, A.J., M.J. Hinton, C.E. Logan, and D.R. Sharpe, 2001, Geostatistical mapping of leakance in a regional aquitard, Oak Ridges Moraine area, Ontario, Canada: Hydrogeology Journal, vol. 9, p. 79-96.

Deutsch, C.V. and A.G. Journel, 1992, GSLIB Geostatistical Software Library and User's Guide: New York, Oxford University Press, 340 p.

Dominic, D.F., R. W. Ritzi, and Z. Dai, 2003, Modeling multi-scale heterogeneity in buried-valley aquifers using indicator geostatistics: Geological Society of America Annual Meeting, Seattle, Abstracts with Program,

Dominic, D.F., R.W. Ritzi, E.C. Reboulet, and A.C. Zimmer, 1998, Geostatistical analysis of facies distributions: elements of a quantitative facies model, in Fraser, G.S. and J.M. Davis, eds., 1998, Hydrogeologic models of sedimentary aquifers: Tulsa, Oklahoma, SEPM (Society for Sedimentary Geology), p. 137-146.

Environmental Modeling and Research Laboratory (EMRL), 2005, Groundwater Modeling System version 5.1, Brigham Young University.

Eyles, N., 1983, Glacial geology: an introduction for engineers and earth scientists: New York, Pergamon Press, 409 p.

Eyles, N., and Miall, A.D., 1984, Glacial facies, in Walker, R.G., ed., Facies models (second edition): Toronto, Canada, Geological Association of Canada, p. 15 38.

Fleming, A.H., 1998a, Using glacial terrain models to define hydrogeological settings in heterogenous depositional systems, in Fraser, G.S. and J.M. Davis, eds., 1998, Hydrogeologic models of sedimentary aquifers: Tulsa, Oklahoma, SEPM (Society for Sedimentary Geology), p. 25-46.

Fleming, A.H., 1998b, Using glacial terrain models to characterize aquifer system structure, heterogeneity and boundaries in an interlobate basin, northeastern Indiana, in Fraser, G.S. and J.M. Davis, eds., 1998, Hydrogeologic models of sedimentary aquifers: Tulsa, Oklahoma, SEPM (Society for Sedimentary Geology), p. 47-68.

Fogg, G. E., C. D. Noyes and S. F. Carle, 1998, Geologically based model of heterogeneous hydraulic conductivity in an alluvial setting: Hydrogeology Journal, vol. 6, 1, p. 131-143.

Fogg, G.E., 1986, Groundwater flow and sand body interconnectedness in a thick, multiple-aquifer system: Water Resources Research, vol. 22, no. 5, p. 679-694.

Fraser, F.S., and Bleuer, N.K., 1987, Use of facies models as predictive tools to locate and characterize aquifers in glacial terrains, in Proceedings of the NWWA Focus Conference

on Midwestern Ground Water Issues: Dublin, Ohio, National Water Well Association, p. 123 143.

Fraser, G.S. and J.M. Davis, eds., 1998, Hydrogeologic models of sedimentary aquifers: Tulsa, Oklahoma, SEPM (Society for Sedimentary Geology), 188 pp.

Freeze, R.A., and J.A. Cherry, 1979, Groundwater, Prentice-Hall, Inc., Englewood Cliffs, NJ.

Gödeke, S., H. Geistlinger, A. Fischer, H.-H. Richnow, and M. Schirmer, 2008, Simulation of a reactive tracer experiment using stochastic hydraulic conductivity fields: Environmental Geology, vol. 55, p. 1255–1261. DOI 10.1007/s00254-007-1073-3

Goetz Troost, K. and B.B. Curry, 1992, Genesis and Continuity of Quaternary Sand and Gravel in Glacigenic Sediment at a Proposed Low-Level Radioactive Waste Disposal Site in East-Central Illinois: Environmental Geology and Water Sciences, v. 18, no. 3, p. 159-170.

Goldstein, B.S., 1989, Lithology, sedimentology, and genesis of the Wadena drumlin field, Minnesota, U.S.A.: Sedimentary Geology vol. 62, p. 241-277.

Goldstein, B.S., 1998, "Quaternary Stratigraphy and History of the Wadena Drumlin Region, Central Minnesota," in C.J. Patterson and H.E. Wright, Jr., eds., Contributions to the Quaternary of Minnesota, Minnesota Geological Survey Report of Investigations 49, St. Paul, MN.

Harbaugh, A.W., Banta, E.R., Hill, M.C., and McDonald, M.G., 2000, MODFLOW-2000, the U.S. Geological Survey modular ground-water model -- User guide to modularization concepts and the Ground-Water Flow Process: U.S. Geological Survey, Reston, VA, Open-File Report 00-92, 121 p.

Harbaugh, A.W., et al., 2000, MODFLOW 2000, The U.S. Geological Survey Modular Ground Water Model - User Guide to Modularization Concepts and the Ground Water Flow Process, Open File Report 00 92, U.S. Geological Survey, Reston, VA.

Harris, K.L., and Knaeble, A.R., 2003, Surficial geology, pl. 3 of Harris, K.L., project manager, Geologic atlas of Pope County, Minnesota: Minnesota Geological Survey County Atlas C-15, pt. A, 5 pls., scale 1:100,000.

Harris, K.L., Knaeble, A.R., and Berg, J.A., 1999, Surficial geology, pl. 2 of Quaternary stratigraphy—Otter Tail area, west central Minnesota: Minnesota Geological Survey Regional Hydrogeologic Assessment RHA-5, pt. A, 2 pls.

Harris, K.L., West, S.A., Tipping, R.G., 1998, Geologic setting of the Buffalo aquifer: a buried tunnel valley of the Red River Lobe, in Patterson, C.J. and Wright, H.E. (ed.) Contributions to Quaternary Studies in Minnesota, Minnesota Geological Survey Report of Investigations 49, p. 103-113.

Helgesen, J.O., 1977, Ground-water appraisal of the Pineland Sands area, central Minnesota: U.S. Geological Survey Water-Resources Investigations Report 77-102, 49 p.

Helgesen, J.O., and G.F. Lindholm, 1977, Geology and Water-Supply Potential of the Anoka Sand-Plain Aquifer, Technical Paper No. 6, Minnesota Department of Natural Resources, Division of Waters, St. Paul, MN.

Herzog, B.L., D.R. Larson, C.C. Abert, S.D. Wilson, and G.S. Roadcap, 2003, Hydrostratigraphic modeling of a complex., glacial-drift aquifer system for importation into MODFLOW: Ground Water, vol.41, no. 1, p. 57-65.

Hill, M.C., Banta, E.R., Harbaugh, A.W., and Anderman, E.R., 2000, MODFLOW-2000, the U.S. Geological Survey modular ground-water model -- User guide to the Observation, Sensitivity, and Parameter-Estimation Processes and three post-processing programs: U.S. Geological Survey, Reston, VA, Open-File Report 00-184, 210 p.

Hill, M.C., et al., 2000, MODFLOW 2000, The U.S. Geological Survey Modular Ground Water Model - User Guide to the Observation, Sensitivity, and Parameter Estimation Processes

and Three Post Processing Programs, Open File Report 00 184, U.S. Geological Survey, Reston, VA.

Hobbs, H.C., 1998, Use of 1-2 millimeter sand-grain composition in Minnesota Quaternary studies, in Patterson, C.J., and Wright, H.E., Jr., eds., Contributions to Quaternary studies in Minnesota: Minnesota Geological Survey Report of Investigations 49, p. 193-208.

Hobbs, H.C., 2001a, Surficial geology of the Brainerd quadrangle, Cass and Crow Wing Counties, Minnesota: Minnesota Geological Survey Miscellaneous Map M-112, scale 1:24,000.

Hobbs, H.C., 2001b, Surficial geology of the Gull Lake quadrangle, Cass and Crow Wing Counties, Minnesota: Minnesota Geological Survey Miscellaneous Map M-113, scale 1:24,000.

Isaaks & Co., 2001, SAGE2001 General Purpose Software for Variography: Redwood City, California.

Isaaks, E.H., and R.M. Srivastava, 1989, Applied geostatistics: New York, Oxford University Press, 561 p.

Johnson, M.D., and Mooers, H.D., 1998, Ice-margin positions of the Superior Lobe during Late Wisconsinan deglaciation, in Patterson, C.J., and Wright, H.E., Jr., eds., Contributions to Quaternary studies in Minnesota: Minnesota Geological Survey Report of Investigations 49, p. 7-14.

Johnson, N.M., 1995, Characterization of alluvial hydrostratigraphy with indicator semivariograms: Water Resources Research, vol. 31, no. 12, p. 3217-3227.

Johnson, N.M., and Dreiss, S.M., 1989, Hydrostratigraphic interpretation using indicator geostatistics: Water Resources Research, vol. 25, no. 12, p. 2501-2510.

Journel, A.G., 1983, Nonparametric estimation of spatial distributions: Mathematical Geology, vol. 15, no. 3, p. 445-468.

Journel, A.G., and Alabert, F., 1989, Non-Gaussian data expansion in the earth sciences: Terra Review, p. 123-134.

Killey, M.A., and C.B. Trask, 1984, Geotechnical Site Investigation for an Advanced Photon Source at Argonne National Laboratory, Illinois: Illinois State Geological Survey, EG 147.

Knaeble, A.R., 1996, Glaciotectonic thrusting along the St. Croix Moraine, Stearns County, Minnesota, in Meyer, G.N., and Swanson, L., eds., Text supplement to the geologic atlas, Stearns County, Minnesota: Minnesota Geological Survey County Atlas C-10, pt. C, p. 16-39.

Knaeble, A.R., 1998, Superior-Lobe glacial thrusting of glacial sediment and bedrock along the St. Croix Moraine, Stearns County, Minnesota, in Patterson, C.J., and Wright, H.E., Jr., eds., Contributions to Quaternary studies in Minnesota: Minnesota Geological Survey Report of Investigations 49, p. 15-26.

Knaeble, A.R., 2001, Surficial geology of the Baxter quadrangle, Cass, Morrison, and Crow Wing Counties, Minnesota: Minnesota Geological Survey Miscellaneous Map M-111, scale 1:24,000.

Knaeble, A.R., and Meyer, G.N., 2004, Quaternary stratigraphy, pl. 4 of Setterholm, D.R., project manager, Geologic atlas of Crow Wing County, Minnesota: Minnesota Geological Survey County Atlas C-16, pt. A, 6 pls., scale 1:100,000.

Knaeble, A.R., coordinator, 2006, Landforms, stratigraphy, and lithologic characteristics of glacial deposits in central Minnesota: Minnesota Geological Survey Guidebook 22, 44 p.

Koltermann, C.E. and S.M. Gorelick, 1996, Heterogeneity in sedimentary deposits: a review of structure-imitating, process-imitating, and descriptive approaches: Water Resources Research, vol. 32, no. 9, p. 2617-2658.

Lampe, D.C., and G.A. Olyphant, 2003, Geostatistical characterization of apparent hydraulic conductivity distributions within three highly heterogeneous glacial terrains of Indiana: Geological Society of America Annual Meeting, Seattle, Abstracts with Program, vol. 35, no. 6, p. 67.

Lindgren, R. J., 2002, Ground-water resources of the uppermost confined aquifers, southern Wadena County and parts of Otter Tail, Todd and Cass counties, central Minnesota, 1997-2000: U.S. Geological Survey Water Resources Investigation 02-4023, 50 p.

Lindgren, R.J., 1990, Simulation of ground-water flow in the Prairie Du Chien-Jordan and overlying aquifers near the Mississippi River, Fridley, Minnesota: U.S. Geological Survey, Water-Resources Investigations Report 90-4165.

Maji, R., E. Sudicky, S. Panday, and G. Teutsch, 2003, Effect of permeability and porosity conditioning on the prediction of dense chlorinated solvent migration patterns in a highly characterized fluvial aquifer: Geological Society of America Annual Meeting, Seattle, Abstracts with Program,

Martin, P.J. and E.O. Frind, 1998, Modeling a Complex Multi-Aquifer System: The Waterloo Moraine: Ground Water, vol. 36, no. 4, p. 679-690.

MDH (Minnesota Department of Health), 2006, County Well Index, http://www.health.state.mn.us/divs/eh/cwi/, accessed April 3, 2006.

Meriano, M., and N. Eyles, 2003, Groundwater flow through Pleistocene glacial deposits in the rapidly urbanizing Rouge River-Highland Creek watershed, City of Scarborough, southern Ontario, Canada: Hydrogeology Journal, vol. 11, p. 288-303.

Meyer, G., Knaeble, A., Tipping, R.G., 1995, Quaternary stratigraphy, plate 4 in Meyer, G. Project Manager, Geologic Atlas of Stearns County, Minnesota: County Atlas Series C-10, Part A, scale 1:200,000.

Meyer, G.N., 1986, Subsurface and till stratigraphy of the Todd County area, central Minnesota: Minnesota Geological Survey Report of Investigations 34, 40 p.

Meyer, G.N., 1997, Pre-Late Wisconsinan till stratigraphy of north-central Minnesota: Minnesota Geological Survey Report of Investigations 48, 65 p.

Minnesota Department of Natural Resources (MDNR), 2009, GIS Data Deli, http://deli.dnr.state.mn.us. Accessed May 2.

Minnesota Department of Natural Resources (MDNR), 2006, Lake Finder, http://www.dnr.state.mn.us/lakefind/index.html. Accessed April 3.

Minnesota Pollution Control Agency, 1999, Lake Assessment Program 1997, Fishtrap Lake (ID #49-0137), Morrison County, Minnesota, St. Paul, MN, Aug.

Mooers, H.D., 1988, Quaternary history and ice dynamics of the St. Croix phase of Last Wisconsin glaciation, central Minnesota: Minneapolis, University of Minnesota, Ph.D. dissertation, 200 p.

Mooers, H.D., 1989, On the formation of the tunnel valleys of the Superior lobe, central Minnesota: Quaternary Research, v. 32, no. 1, p. 24-35.

Mooers, H.D., 1990a, A glacial-process model: the role of spatial and temporal variations in glacial thermal regime: Geological Society of America Bulletin, v. 102, no. 2, p. 243-251.

Mooers, H.D., 1990b, Ice marginal thrusting of drift and bedrock: Thermal regime, subglacial aquifers, and glacial surges: Canadian Journal of Earth Sciences, v. 27, p. 849-862.

Mooers, H.D., 1996, Geomorphology of the Brainerd 1:100,000 Quadrangle and the Development of the Land Type Association Layer of the Ecological Classification System, Minnesota Department of Natural Resources, Division of Forestry, St. Paul, MN.

Paola C., J. Mullin, C. Ellis, D.C. Mohrig, J.B. Swenson, G. Parker, T. Hickson, P.L. Heller, L. Pratson, J. Syvitski, B. Sheets, and N. Strong, 2001, Experimental Stratigraphy: GSA Today, Vol. 11, No. 7 pp. 4–9.

Park, Y.-J., E.A. Sudicky, R.G. McLaren, and J.F. Sykes, 2003, Three-dimensional analysis of hydraulic and tracer response tests within moderately fractured rock based on a transition probability geostatistical characterization: Geological Society of America Annual Meeting, Seattle, Abstracts with Program, p.613.

Patterson, C.J., 1994, Tunnel valley fans of the St. Croix moraine, east-central Minnesota, USA: in W.P. Warren and D.G. Croot, eds., formation and deformation of glacial deposits: A.A. Balkema, Rotterdam, p. 69-87.

Patterson, W.E., K.A. Hardwick, R.W. Ritzi, and D.F. Dominic, 2001, Characterization of hierarchical heterogeneity at multiple scales using indicator geostatistics in the Mahomet buried- valley aquifer system: Geological Society of America Annual Meeting, Boston, Abstracts with Program,

Person, M., P. Roy, H. Wright, W. Gutowski, E. Ito, T. Winter, D. Rosenberry, and D. Cohen, 2007, Hydrologic response of the Crow Wing Watershed, Minnesota, to mid-Holocene climate change: Geological Society of America Bulletin, vol. 119 no. 3-4, p. 363-376. DOI: 10.1130/B26003.1

Proce, C.J., R.W. Ritzi, D.F. Dominic, Z.X. Dai, 2004, Modeling multiscale heterogeneity and aquifer interconnectivity: Ground Water, vol. 42, no. 5, p. 658-670.

Quinn, J.J., 1992, Modeling of groundwater flow, leachate migration, and geostatistical aspects of a portion of the Anoka sandplain, Minnesota [M.S. thesis]: University of Minnesota, Minneapolis, 158 p.

Quinn, J.J., 1998, Tunnel Valleys and Other Glacial Features near Anoka, Minnesota, in Patterson, C.J. and Wright, H.E., Jr., eds., Contributions to the Quaternary of Minnesota: Minnesota Geological Survey Report of Investigations 49, St. Paul, Minnesota, p. 27-34.

Quinn, J.J., R.J. Barnes, and H.D. Mooers, 1992, A three-dimensional geostatistical analysis of glacial-drift aquifers and aquitards: Geological Society of America, Annual Meeting, Cincinnati, Abstracts with Programs, v. 24, no. 7, p. 252-253.

Ramanathan, R, R.W. Ritzi, C.C. Huang, 2008, Linking hierarchical stratal architecture to plume spreading in a Lagrangian-based transport model: Water Resources Research, vol. 44 no. 4, W04503, DOI: 10.1029/2007WR006282.

Ritzi, R. W., and R. M. Allen-King, 2007, Why did Sudicky [1986] find an exponential-like spatial correlation structure for hydraulic conductivity at the Borden research site?: Water Resources Research, 43, W01406, doi:10.1029/2006WR004935.

Ritzi, R.W., 2000, Behavior of indicator variograms and transition probabilities in relation to the variance in lengths of hydrofacies: Water Resources Research, vol. 36, no. 11, p. 3375-3381.

Ritzi, R.W., D.F. Dominic, A.J. Slesers, C.B. Greer, E.C. Reboulet, J.A. Telford, R.W. Masters, C.A. Klohe, J.L. Bogle, and B.P Means, 2000, Comparing statistical models of physical heterogeneity in buried-valley aquifer: Water Resources Research, vol. 36, no. 11, p. 3179-3192.

Ritzi, R.W., D.F. Dominic, N.R. Brown, K.W. Kausch, P.J. McAlenney, and M.J. Basial, 1995, Hydrofacies distribution and correlation in the Miami Valley aquifer system: Water Resources Research, vol. 31, no. 12, p. 3271-3281.

Ritzi, R.W., D.F. Jayne, A.J. Zahradnik, A.A. Field, and G.F. Fogg, 1994, Geostatistical Modeling of Heterogeneity in Glaciofluvial, Buried-Valley Aquifers: Ground Water, vol. 32, no. 4, p. 666-674.

Ross, M., M. Parent, and R. Lefebvre, 2005, 3D geologic framework models for regional hydrogeology and land-use management: a case study from a Quaternary basing of southwestern Quebec, Canada: Hydrogeology Journal, vol. 13, p. 690-707.

Russell, H., R.C. Berg, and L.H. Thorleifson, (conveners) 2006. Three-Dimensional Geologic Mapping for Groundwater Applications: Workshop Extended Abstracts. Geological Survey of Canada, Open File 5048, 109 p.

Schneider, A.F., 1961, Pleistocene Geology of the Randall Region, Central Minnesota, Bulletin 40, Minnesota Geological Survey, Minneapolis, MN.

Schoenberg, M. E., 1990, Effects of present and projected ground-water withdrawals on the Twin Cities aquifer system, Minnesota: U.S. Geological Survey, Water-Resources Investigations Report 90-4001.

Seaberg, J.K., 2000, Metropolitan Area Groundwater Model -- Project Summary Overview of the Twin Cities Metropolitan Groundwater Model: Minnesota Pollution Control Agency. http://www.pca.state.mn.us/water/groundwater/mm-overview.pdf

Sharpe, D.R., L.D. Dyke, M. J. Hinton, S.E. Pullan, H.A.J. Russell, T.A. Brennand, P.J. Barnett, and A. Pugin, 1996, Groundwater prospects in the Oak Ridges Moraine area, southern Ontario: application of regional geological models: in Current Research 1996-E, Geological Survey of Canada, p. 181-190.

Sharpe, D.R., M.J. Hinton, H.A.J. Russell, and A.J. Desbarats, 2002, The need for basin analysis in regional hydrogeological studies: Oak Ridges Moraine, southern Ontario: Geoscience Canada, vol. 29, no. 1, p. 3-20.

Sminchak, J.R., D.F. Dominic, and R.W. Ritzi, 1996, Indicator geostatistical analysis of sand interconnections within a till: Ground Water, vol. 34, no. 6, p. 1125-1131.

Soller, D.R., S.D. Price, J.P. Kempton, and R.C. Berg, 1999, Three-Dimensional Geologic Maps of Quaternary Sediments in East-Central Illinois: U.S. Geological Survey, Geologic Investigations Series Map I-2669. http://pubs.usgs.gov/imap/i-2669/

St. George, L.M., 1994, A Landform-Based Approach to the Estimation of Groundwater Recharge in Complex Glacial Topography, M.S. thesis, University of Minnesota, Duluth, MN.

Stanford, S.A. and G.M. Ashley, 1998, Using three-dimensional geologic models to map glacial aquifer systems: an example from New Jersey: in Fraser, G.S. and J.M. Davis, eds., 1998, Hydrogeologic models of sedimentary aquifers: Tulsa, Oklahoma, SEPM (Society for Sedimentary Geology), p. 69-84.

Sudicky, E.A., 1986, A natural gradient experiment on solute transport in a sand aquifer: spatial variability of hydraulic conductivity and its role in the dispersion process: Water Resources Research, vol. 22, no. 13, p. 2069-2082.

Sun, A.Y., R.W. Ritzi, and D.W. Sims, 2008, Characterization and modeling of spatial variability in a complex alluvial aquifer: implications on solute transport: Water Resources Research, vol. 44, W04401, doi:10.1029/2007WR006119.

Tarboton, K.C., W.W. Wallender, G.E. Fogg, and K. Belitz, 1995, Kriging of regional hydrologic properties in the western San Joaquin Valley, California: Hydrogeology Journal, vol. 3, no. 1, p. 5-23.

Thorleifson, L.H., and R.C. Berg (conveners) 2002a. Three-Dimensional Geological Mapping For Groundwater Applications: Workshop Extended Abstracts. Geological Survey of Canada, Open File 1449, 87 p.

Thorleifson, L.H. and R.C. Berg, 2002b, Introduction – the need for high-quality three-dimensional geologic information for groundwater and other environmental applications, in Thorleifson, L.H. and R.C. Berg, eds., Three-dimensional geological mapping for groundwater applications: workshop extended abstracts: Geological Survey of Canada, Open File 449, p. v-vii.

Thorleifson, L.H., R.C. Berg, and H.A.J. Russell (conveners), 2007, Three-dimensional geologic mapping for groundwater applications: Minnesota Geological Survey, Open-File Report 07-4, 90 p.

U.S. Geological Survey, 1999, Sustainable growth in America's heartland: 3-D geologic maps as the foundation: Circular 1190. http://pubs.usgs.gov/circ/c1190

University of Minnesota-Duluth (UMD) Department of Geological Sciences, 1997, Geomorphology of Minnesota, 1:100,000 scale geomorphology data http://deli.dnr.state.mn.us/metadata.html?id=L280000062101

University of Minnesota-Duluth (UMD) Department of Geological Sciences, 2002, Environmental Drilling Field Report, prepared for Camp Ripley, January 29.

USDA (U.S. Department of Agriculture), 1994, Soil Survey of Morrison County, Minnesota, Soil Conservation Service.

Venteris, E.K., 2007, Three-dimensional modeling of glacial sediments using public water-well data records: an integration of interpretive and geostatistical approaches: Geosphere, vol. 3, no. 6, p. 456-468, doi: 10.11/1130/GES00090.1.

Walker, R.G., 1984, General introduction: facies, facies sequences and facies models, in Walker, R.G., ed. Facies models (second edition): Toronto, Canada, Geological Association of Canada, p. 19.

Weissmann, G. S. and G. E. Fogg, 1999, Multi-scale alluvial fan heterogeneity modeled with transition probability geostatistics in a sequence stratigraphic framework: Journal of Hydrology vol. 226, p. 48-65.

Weissmann, G. S., S. F. Carle and G. E. Fogg, 1999, Three-dimensional hydrofacies modeling based o n soil surveys and transition probability geostatistics: Water Resources Research, vol. 35, no.6, p. 1761-1770.

Wilson, S.D., G.S. Roadcap, B.L. Herzog, D.R. Larson, and D. Winstanley, 1998, Hydrogeology and ground-water availability in southwest McLean and southeast Tazewell counties, part 2: Aquifer modeling and final report: Illinois State Water Survey and Illinois State Geological Survey Cooperative Ground-Water Report 19.

Wright, H.E., Jr., 1972, Quaternary history of Minnesota, in Sims, P.K., and Morey, G.B., eds., Geology of Minnesota—A centennial volume: Minnesota Geological Survey, p. 515-547.

Wright, H.E., Jr., 1973, Tunnel valleys, glacial surges and subglacial hydrology of the Superior lobe, Minnesota, in Black, R.F., Goldthwait, R.P., and Willman, H.B., eds., The Wisconsinan Stage: Geological Society of America Memoir 136, p. 251-276.

Wright, H.E., Jr., and Ruhe, R.V., 1965, Glaciation of Minnesota and Iowa, in Wright, H.E., Jr., and Frey, D.G., eds., The Quaternary of the United States: Princeton, Princeton University Press, p. 29-41.

Wright, H.E., Jr., Matsch, C.L., and Cushing, E., 1973, Superior and Des Moines lobes, in Black, R.F., Goldthwait, R.P., and Willman, H.B., eds., The Wisconsinan Stage: Geological Society of America Memoir 136, p. 153-185.

Yarus, J.M., and R.L. Chambers, 2006, Practical geostatistics – an armchair overview for petroleum reservoir engineers: Journal of Petroleum Technology, November, p. 78-87.

Appendix A: Locations of Geomorphologically Grouped Data Sets

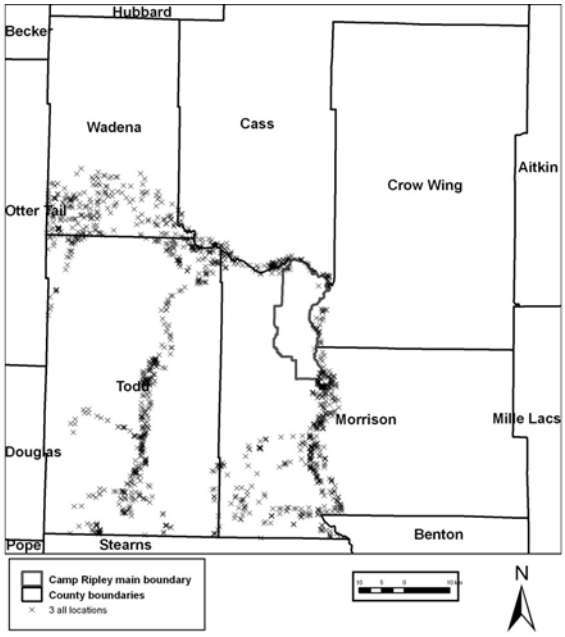

Des Moines outwash geomorphological setting, based on various data sources

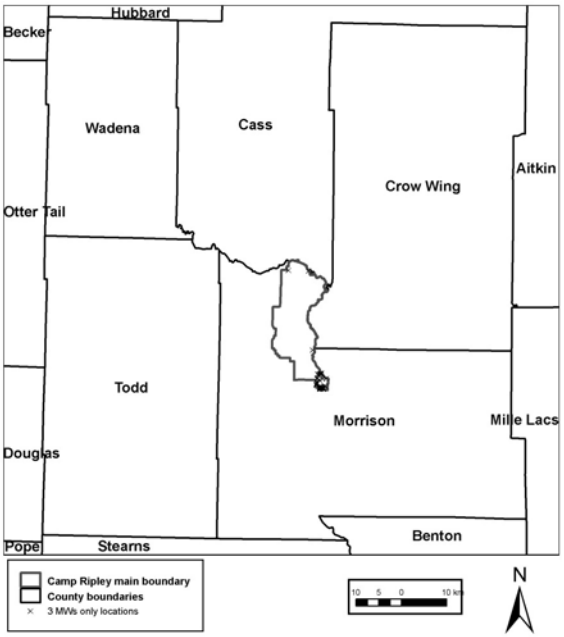

Des Moines outwash geomorphological setting, based on monitoring well data

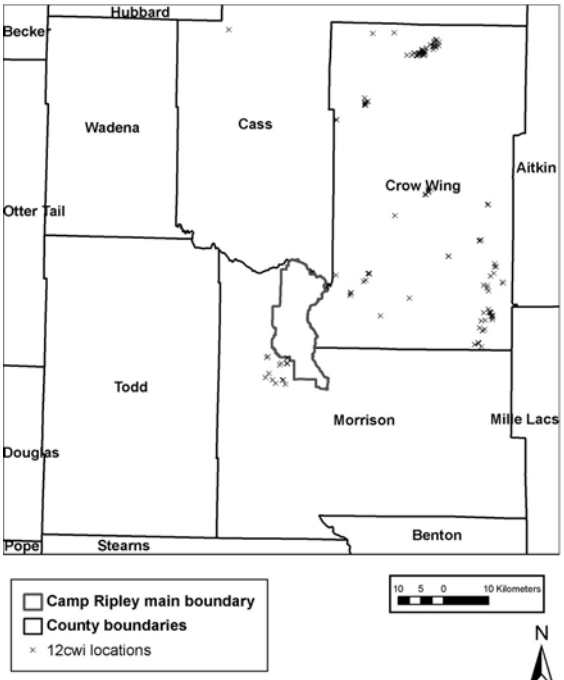

Rainy ice contact geomorphological setting, private well logs only

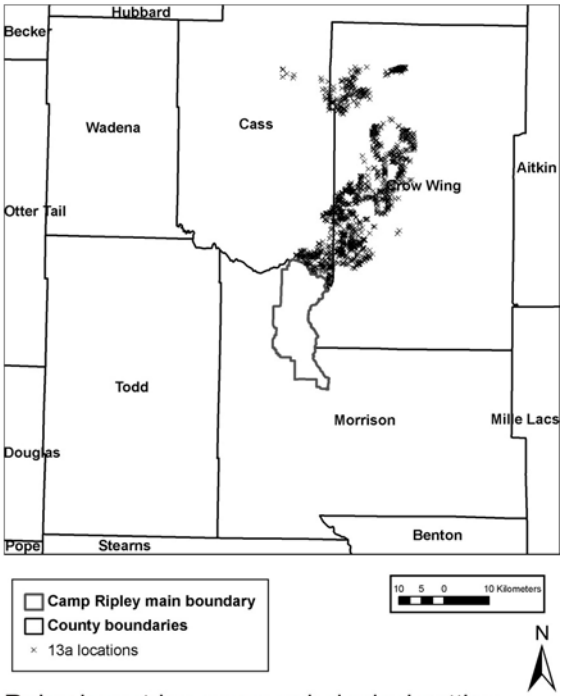

Rainy lacustrine geomorphological setting, northern region, private well logs only

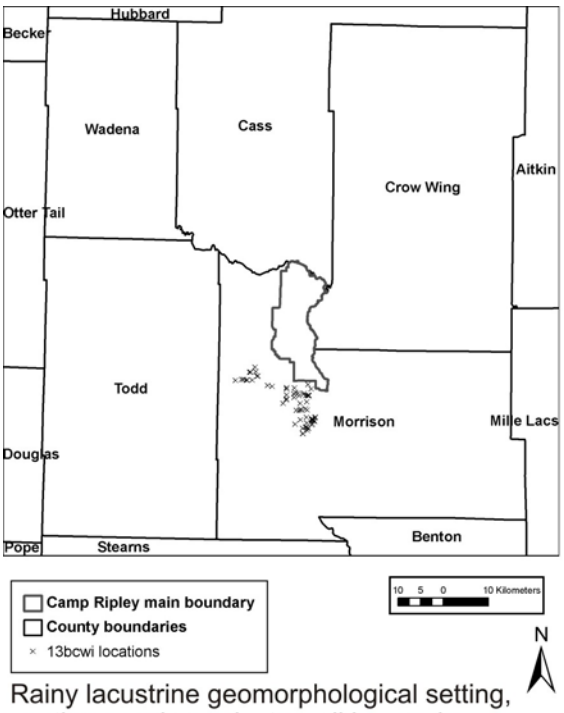

Rainy lacustrine geomorphological setting, southern region, private well logs only

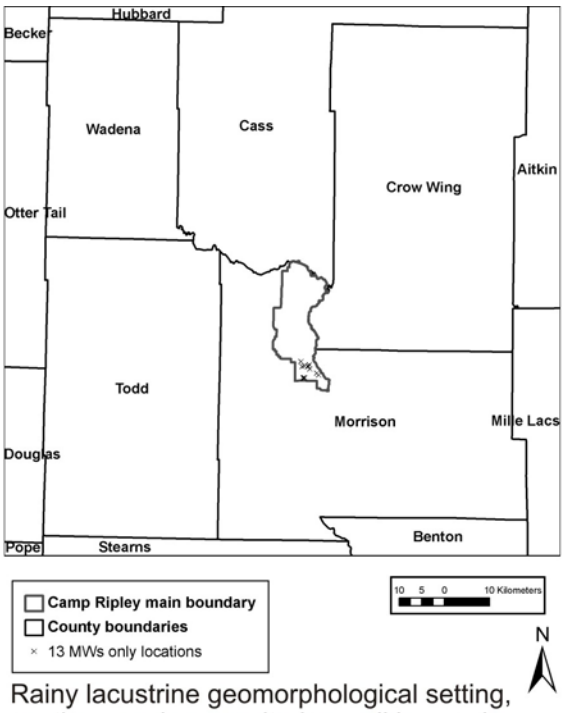

Rainy lacustrine geomorphological setting, southern region, monitoring well logs only

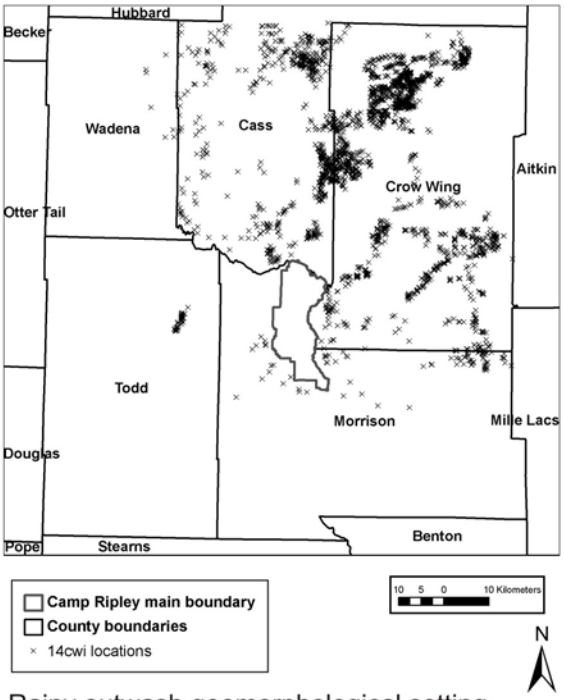

Rainy outwash geomorphological setting, private well logs only

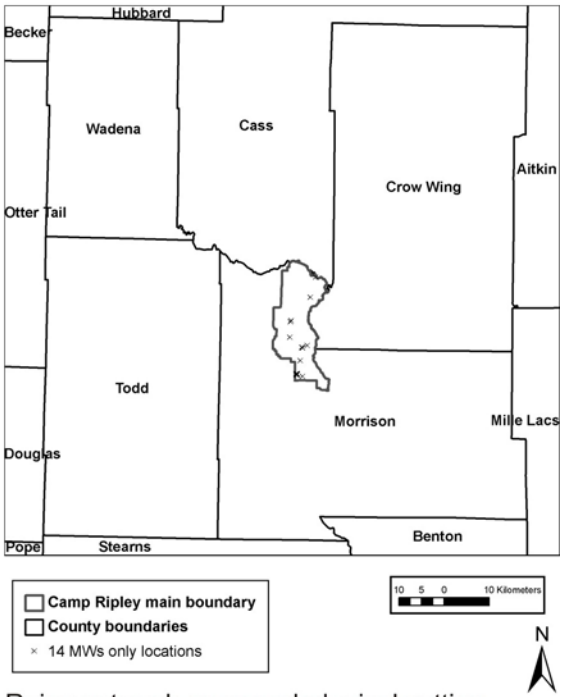

Rainy outwash geomorphological setting, monitoring well logs only

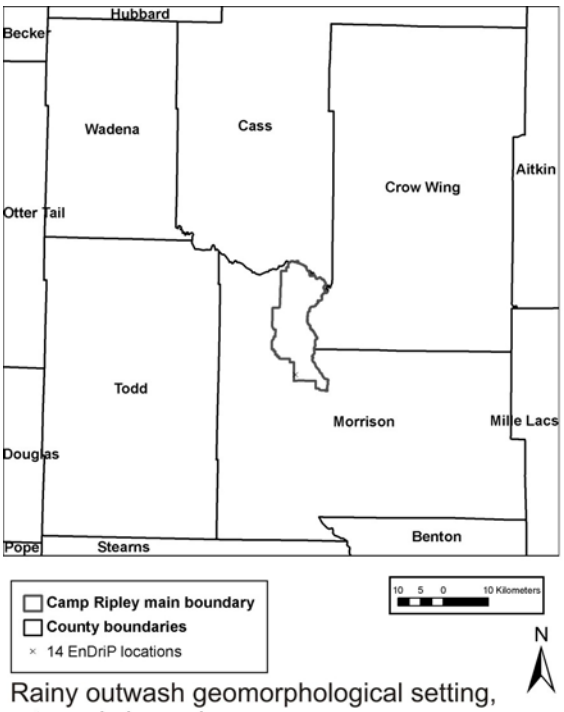

Rainy outwash geomorphological setting, rotosonic log only

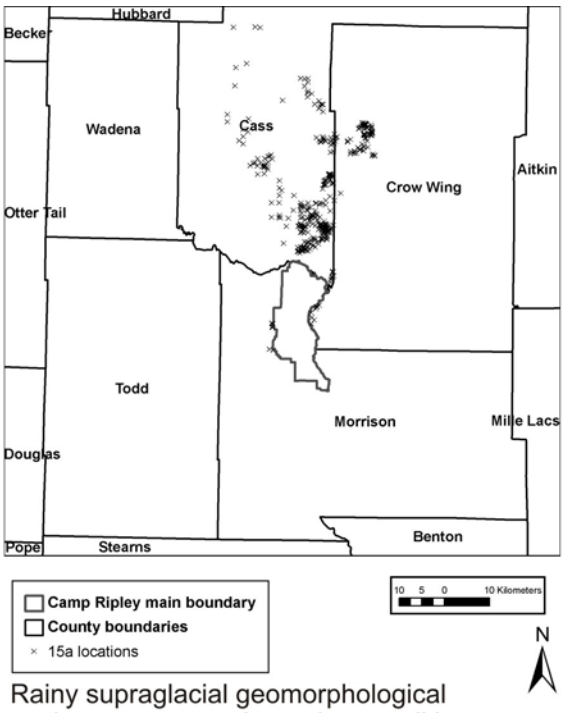

Rainy supraglacial geomorphological setting, western region, private well logs only

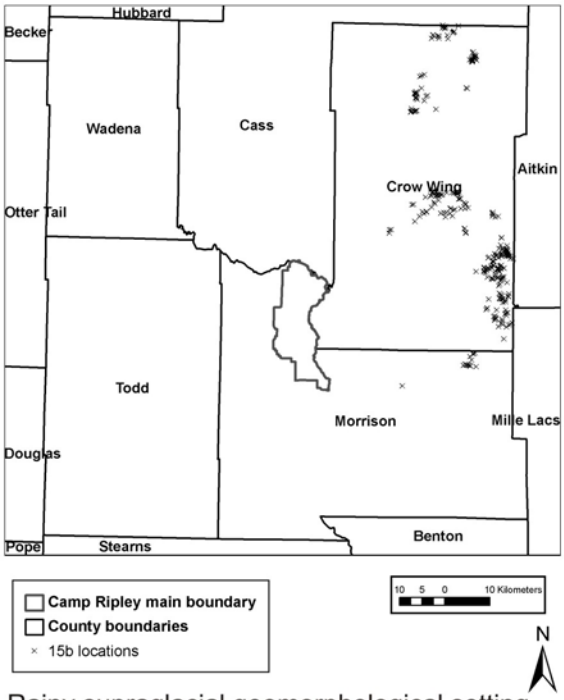

Rainy supraglacial geomorphological setting, eastern region, private well logs only

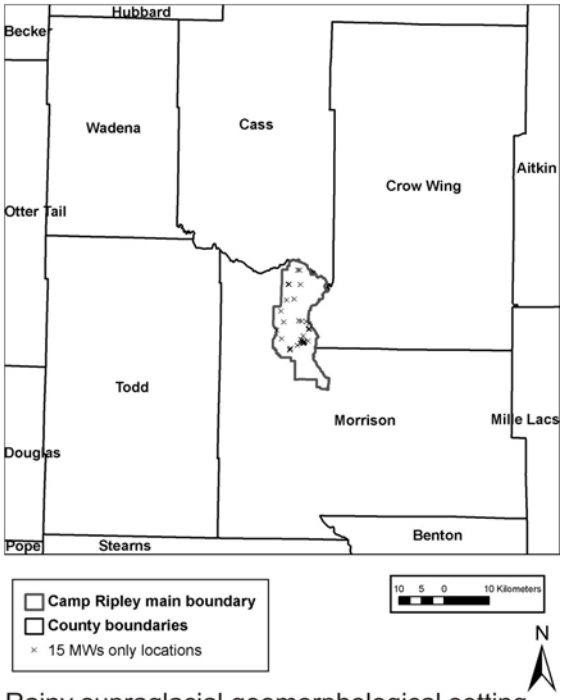

Rainy supraglacial geomorphological setting, western region, monitoring well logs only

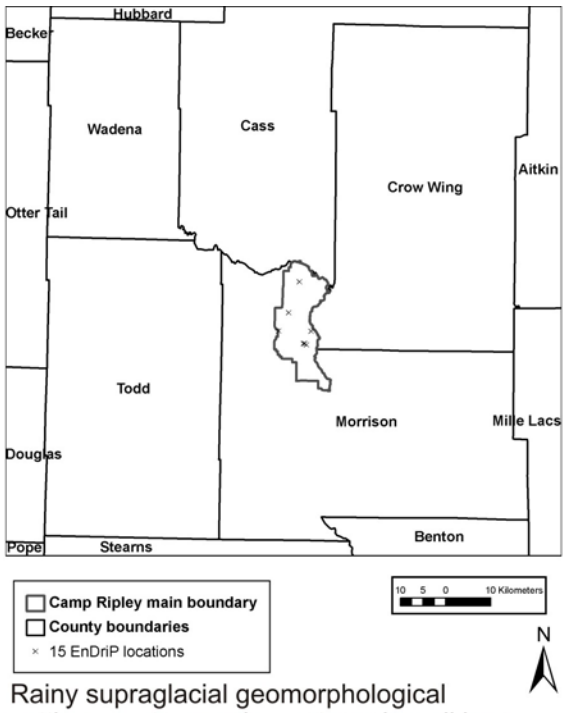

Rainy supraglacial geomorphological setting, western region, rotosonic well logs only

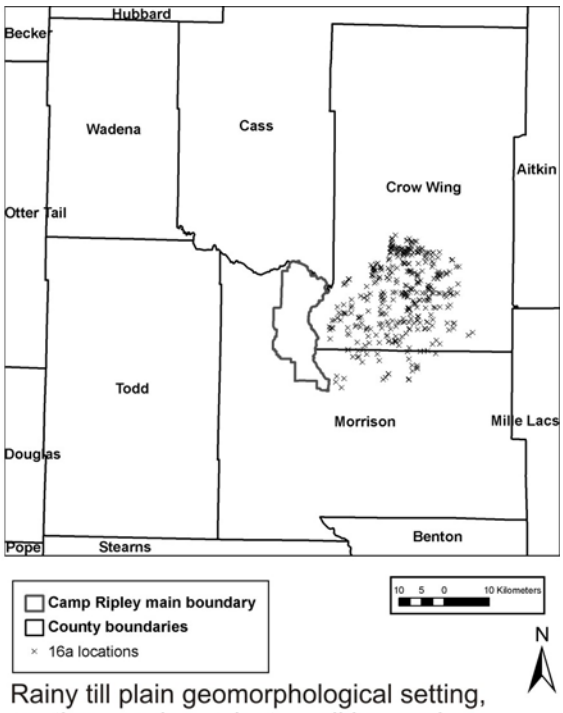

Rainy till plain geomorphological setting, southern region, private well logs only

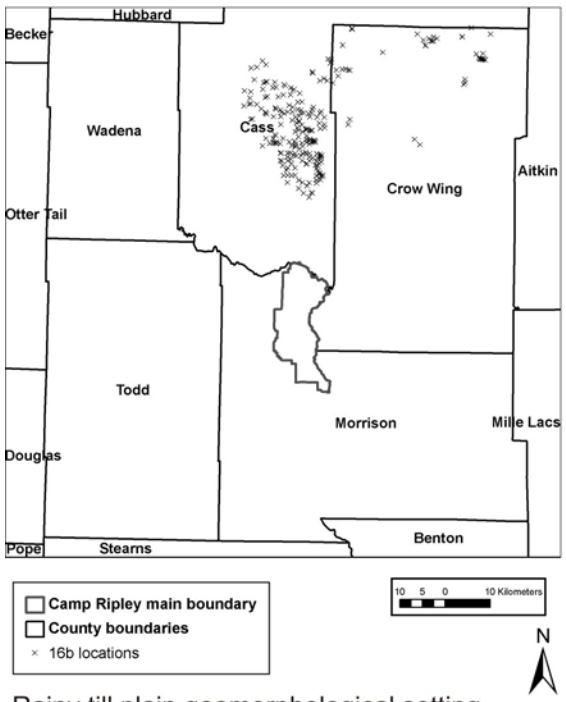

Rainy till plain geomorphological setting, northern region, private well logs only.

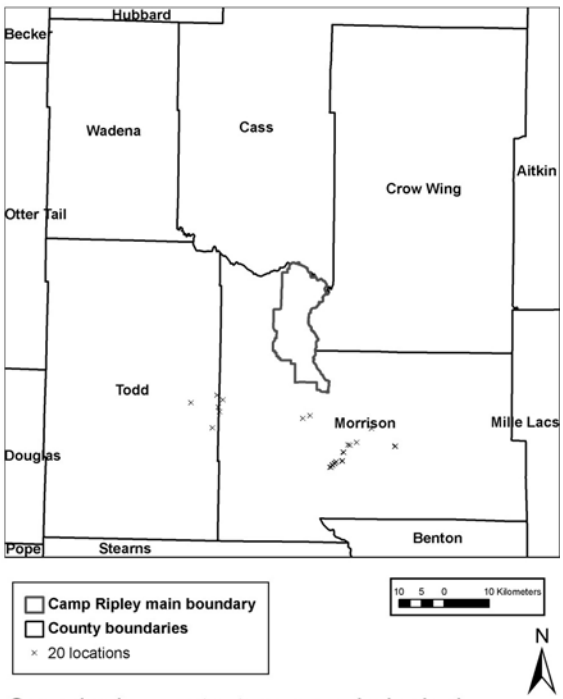

Superior ice contact geomorphological setting, private well logs only

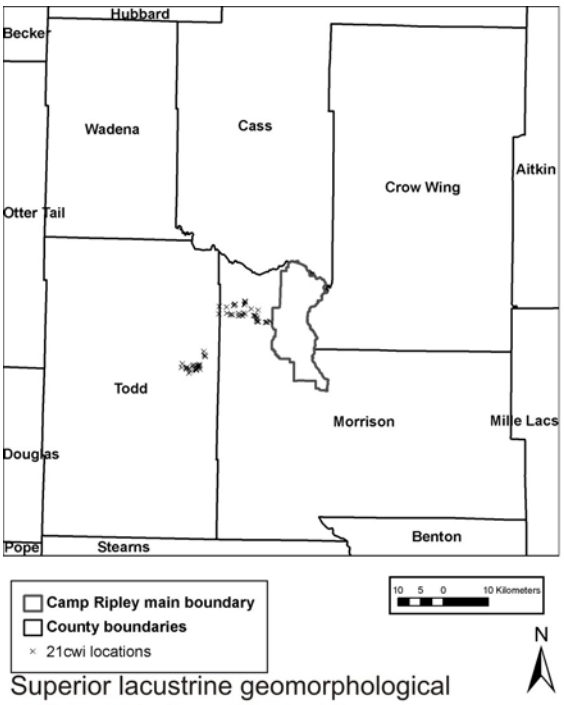

Superior lacustrine geomorphological setting, private well logs only

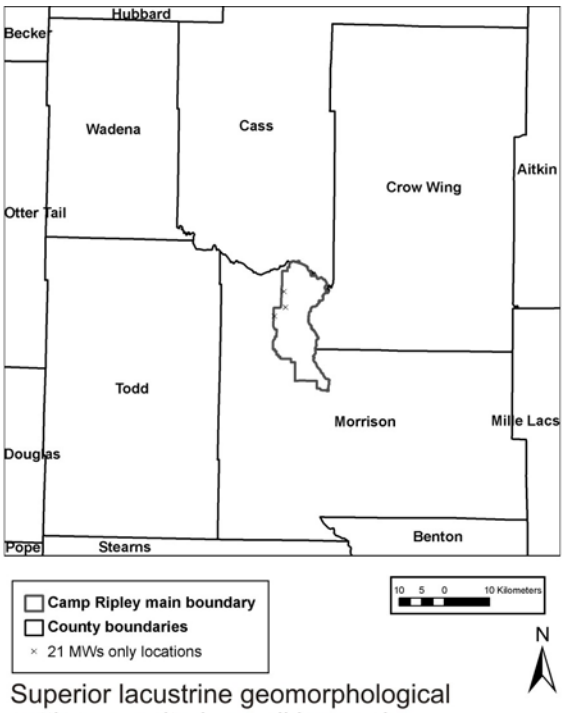

Superior lacustrine geomorphological setting, monitoring well logs only

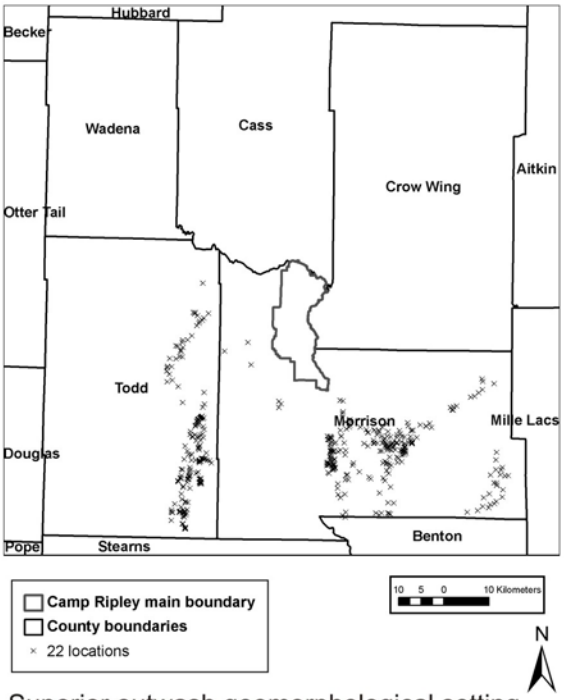

Superior outwash geomorphological setting, private well logs only

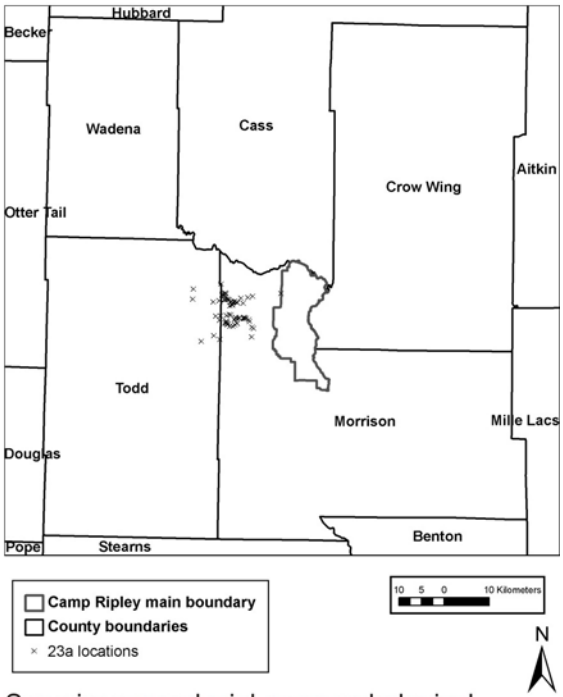

Superior supraglacial geomorphological setting, northern region, private well logs only

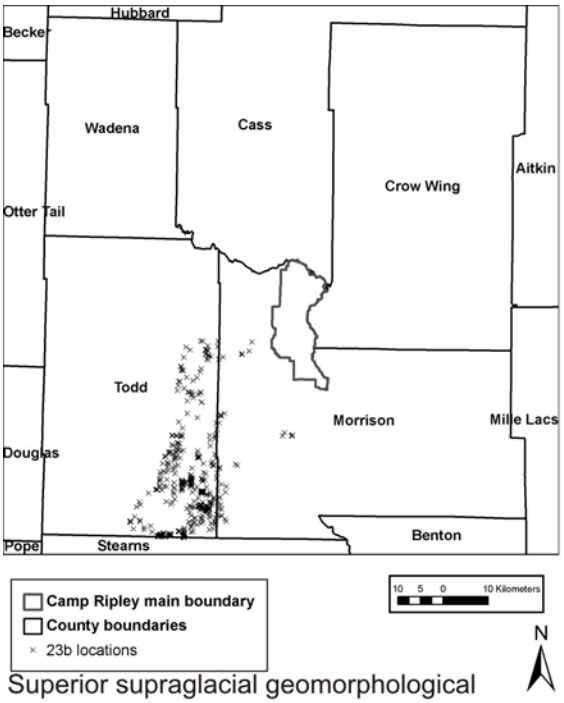

Superior supraglacial geomorphological setting, southern region, private well logs only

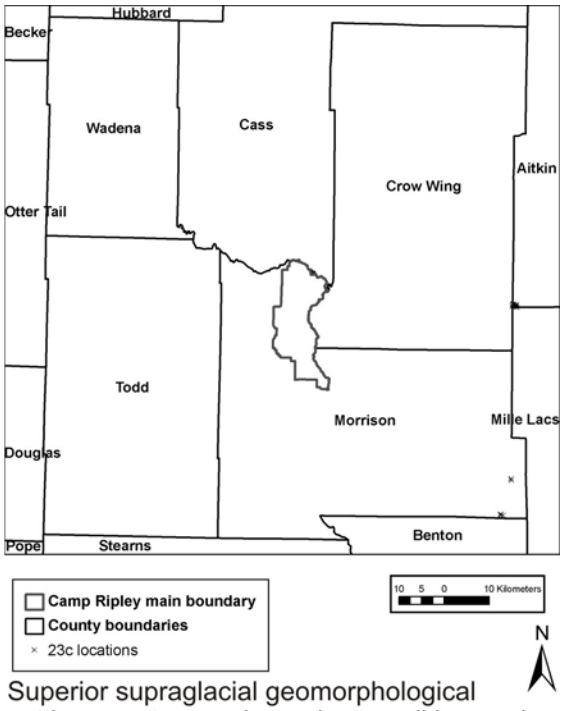

Superior supraglacial geomorphological setting, eastern region, private well logs only

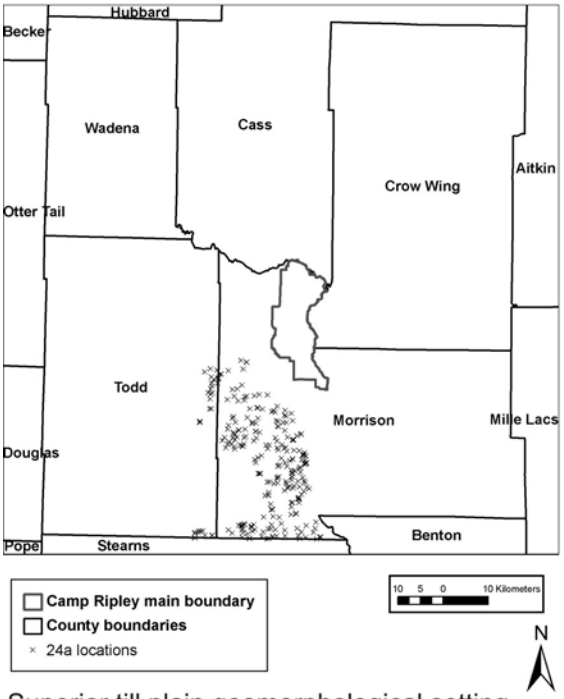

Superior till plain geomorphological setting, eastern region, private well logs only

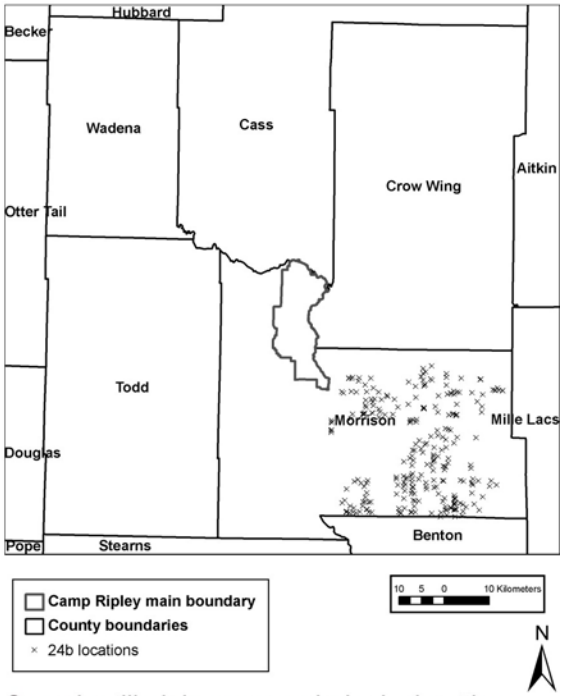

Superior till plain geomorphological setting, western region, private well logs only

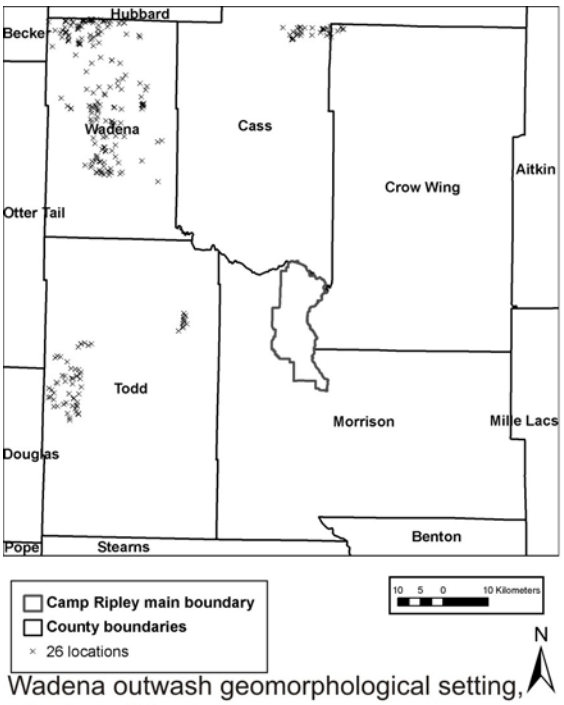

Wadena outwash geomorphological setting, private well logs only

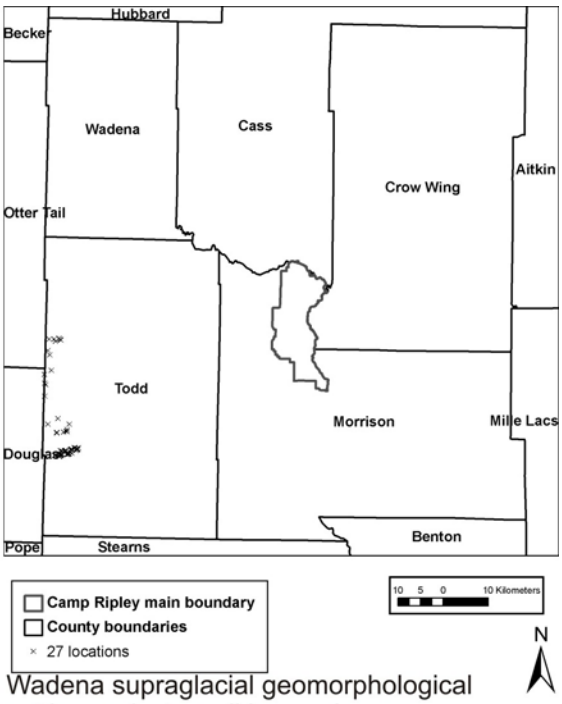

Wadena supraglacial geomorphological setting, private well logs only

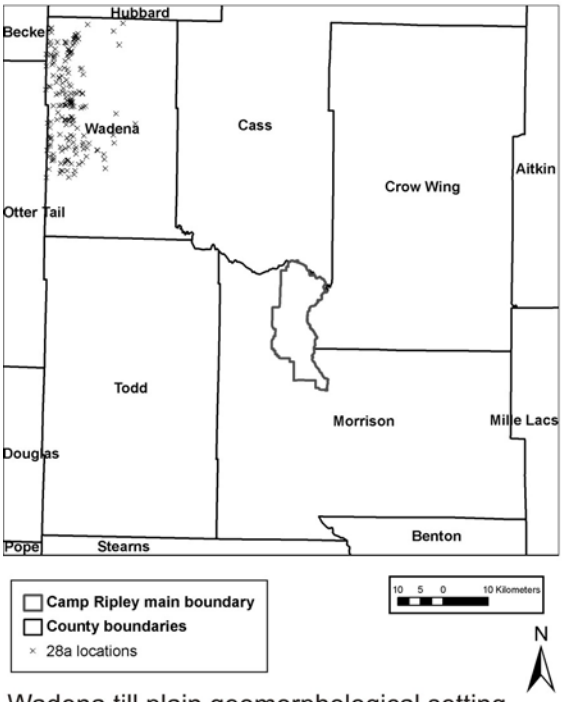

Wadena till plain geomorphological setting, northwestern region, private well logs only

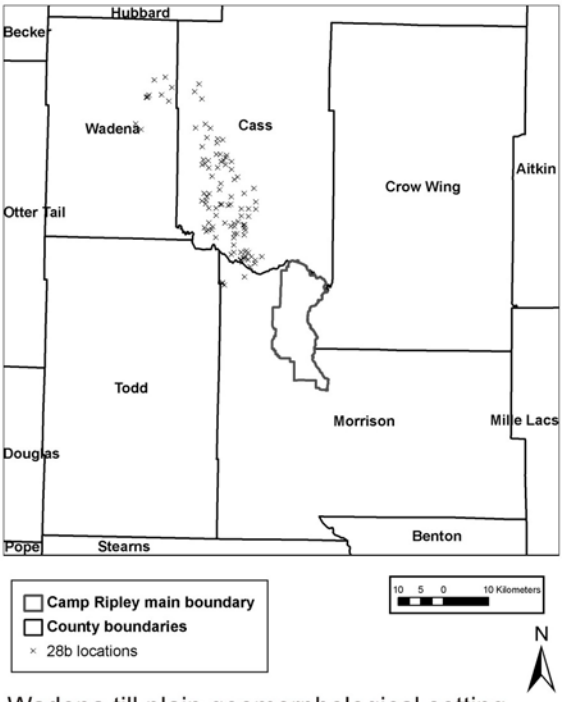

Wadena till plain geomorphological setting, northeastern region, private well logs only

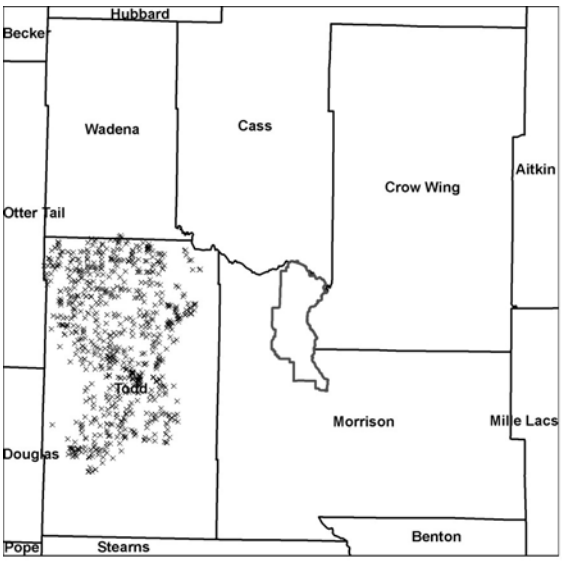

Wadena till plain geomorphological setting, southern region, private well logs only